UNIVERSIDADE ESTADUAL DE CAMPINAS
Faculdade de Engenharia Mecânica

ANDRES FELIPE RODRIGUEZ TORRES

Studies on Thermoelectric Power Generation Consuming Municipal Solid Waste (MSW) and Using Bubbling Fluidized Bed Gasifier

Estudos em Geração Termelétrica a Partir de Resíduos Sólidos Urbanos (RSU) Utilizando Gaseificadores de Leito Fluidizado Borbulhante

CAMPINAS
2016

ANDRES FELIPE RODRIGUEZ TORRES

Studies on Thermoelectric Power Generation Consuming Municipal Solid Waste (MSW) and Using Bubbling Fluidized Bed Gasifier

Estudos em Geração Termelétrica a Partir de Resíduos Sólidos Urbanos (RSU) Utilizando Gaseificadores de Leito Fluidizado Borbulhante

Dissertation presented to the School of Mechanical Engineering of the University of Campinas as partial fulfillment of the requirements for the degree of Master in Mechanical Engineer, in the area of Thermic and Fluids.

Dissertação apresentada à Faculdade de Engenharia Mecânica da Universidade Estadual de Campinas como parte dos requisitos exigidos para a obtenção do título de Mestre em Engenharia Mecânica, na Área de Térmicas e Fluidos.

Orientador: Prof. Dr. Marcio Luiz de Souza-Santos

ESTE EXEMPLAR CORRESPONDE À VERSÃO FINAL DA DISSERTAÇÃO DEFENDIDA PELO ALUNO ANDRES FELIPE RODRIGUEZ TORRES, E ORIENTADA PELO PROF. DR. MARCIO LUIZ DE SOUZA-SANTOS.

ASSINATURA DO ORIENTADOR

CAMPINAS

2016

Agência(s) de fomento e nº(s) de processo(s): CAPES, 33003017

Ficha catalográfica
Universidade Estadual de Campinas
Biblioteca da Área de Engenharia e Arquitetura
Elizangela Aparecida dos Santos Souza - CRB 8/8098

An2s

Rodriguez Torres, Andres Felipe, 1987-
Studies on thermoelectric power generation consuming municipal solid waste (MSW) and using bubbling fluidized bed gasifier / Andres Felipe Rodriguez Torres. – Campinas, SP : [s.n.], 2016.

Orientador: Marcio Luiz de Souza-Santos.
Dissertação (mestrado) – Universidade Estadual de Campinas, Faculdade de Engenharia Mecânica.

1. Gaseificação. 2. Resíduos sólidos. 3. Energia termelétrica. I. Souza-Santos, Marcio Luiz de,1949-. II. Universidade Estadual de Campinas. Faculdade de Engenharia Mecânica. III. Título.

Informações para Biblioteca Digital

Título em outro idioma: Estudos em geração termelétrica a partir de resíduos sólidos urbanos (RSU) utilizando gaseificadores de leito fluidizado borbulhante
Palavras-chave em inglês:
Gasification
Solid Waste
Thermoelectric power
Área de concentração: Térmica e Fluídos
Titulação: Mestre em Engenharia Mecânica
Banca examinadora:
Marcio Luiz de Souza-Santos [Orientador]
Silvio de Oliveira Junior
Joaquim Eugênio Abel Seabra
Data de defesa: 22-02-2016
Programa de Pós-Graduação: Engenharia Mecânica

UNIVERSIDADE ESTADUAL DE CAMPINAS
FACULDADE DE ENGENHARIA MECÂNICA
COMISSÃO DE PÓS-GRADUAÇÃO EM ENGENHARIA MECÂNICA
DEPARTAMENTO DE ENERGIA

DISSERTAÇÃO DE MESTRADO ACADEMICO

Studies on Thermoelectric Power Generation Consuming Municipal Solid Waste (MSW) and Using Bubbling Fluidized Bed Gasifier

Estudos em Geração Termelétrica a Partir de Resíduos Sólidos Urbanos (RSU) Utilizando Gaseificadores de Leito Fluidizado Borbulhante

Autor: Andrés Felipe Rodriguez Torres

Orientador: Marcio Luiz de Souza-Santos

A Banca Examinadora composta pelos membros abaixo aprovou esta Dissertação:

Prof. Dr. Marcio Luiz de Souza-Santos
DE/FEM/UNICAMP

Prof. Dr. Silvio de Oliveira Junior
POLI/USP/SP

Prof. Dr. Joaquim Eugenio Abel Seabra
DE/FEM/UNICAMP

Campinas, 22 de fevereiro de 2016.

Dedicatory

To my parents Herminia, Pedro (and Ana), thank you for the unconditional support, and to my son Jose Gabriel, the fuel of my life.

Resumo

O presente trabalho introduz novos desenvolvimentos da estratégia no conceito *Fuel-Slurry Integrated Gasifier/Gas Turbine* para a geração de potência termoelétrica aplicada ao caso de Resíduos Sólidos Urbanos (RSU). O processo FSIG/GT permite a alimentação do combustível num gaseificador pressurizado utilizando bombas de lama disponíveis no mercado, evitando a necessidade de sistemas de silos em cascata. O gaseificador opera em regime de Leito Fluidizado Borbulhante (*Bubbling Fluidized Bed- BFB*) e adicionalmente dispensa a necessidade de vapor como agente gaseificador simplificado o processo. As principais variáveis de estudo são a pressão operacional de gaseificação e a vazão mássica de ar injetado através do distribuidor. O gás produzido passa pelo sistema de limpeza para atingir os níveis toleráveis de tamanho e conteúdo de partículas, como também a concentração de alcalinos é controlada dentro dos níveis aceitáveis para a injeção na turbina a gás. O trabalho aplica o simulador CeSFaMB© e não considera custos de capital.

Abstract

This work introduces a new optimization of the Fuel-Slurry Integrated Gasifier/Gas Turbine (FSIG/GT) concept for thermoelectric power generation process consuming municipal solid waste (MSW). The FSIG/GT power generation process allows fuel feeding to a power unit based on gasification using commercially available slurry pumps. This dispenses the need of usual sequential or cascade feeding systems. Such fuel is prepared to high dry-solid content and pumped into a dryer, from which the solid particles are fed into a pressurized bubbling fluidized bed gasifier. The produced gas is cleaned to bring the particle content and size, as well as alkaline concentration within the acceptable limits for injections into standard gas turbines. Previous works shows that no steam injection is needed as a gasification agent, thus simplifying the process and decreasing the capital costs. The present work optimizes the operation having the cold efficiency and the exergetic efficiency of the gasifier as objective function. The gasifier operational pressure, its diameter, and the mass flow of injected air into the gasifier are set as main variables. Nevertheless, the present work does not include considerations on the economics of the proposed process. The work applies the comprehensive simulator (CeSFaMB©).

List of Figures

List of Tables

List of Symbols

Latin letters

Symbol	Variable	Unit
A	Cross area	m^2
b	Exergy	kJ/kg
c	Specific Heat	$kJ/(kg\ K)$
d	Particle diameter	mm
D	Equipment diameter	m
d	Chemical availability	kJ/kg
F	Mass flow rate	kg/s
h	Enthalpy	kJ/kg
HHV	Higher Heating Value	kJ/kg
LHV	Lower Heating Value	kJ/kg
m	Mass	kg
M	Molecular mass	$kg/kmol$
n	Number of size levels or sieves	-
P	Pressure	Pa
Q	Heat	kJ
R	Gas universal constant	$kJ/(kmol\ K)$
U	Superficial velocity	m/s
V	Volume	m^3
w	Mass fraction	-
W	Work	kJ
z	Height measured from the base	m

Greek letters

Symbol	Variable	Unit
ρ	Density	kg/m^3
φ	Sphericity	-
η	Efficiency	-
Δ	Difference	-

Subscripts

Symbol	Variable
0	At dead state conditions
1st	First law of thermodynamics
c	Combustion
co	Compressor
exe	Exergetic
f	Formation
gt	Gas turbine
j	Chemical specie or element in the combustible matrix
mf	Minimum fluidization
p,app	Particle, apparent
p,bulk	Particle, bulk
p,real	Particle, real
Pav	Particle average
pu	Pump
s	Average superficial velocity
slurry	MSW fuel slurry
st	Steam turbine
T	Thermal
tr	Turbulent

List of Abbreviations

BIG/GTCC	Biomass Integrated-Gasifier/Gas Turbine Combined Cycle
BFB	Bubbling Fluidized Bed
BFBG	Bubbling Fluidized Bed Gasifier
CeSFaMB	Comprehensive Simulator of Fluidized and Moving Bed Equipment
CEST	Condensing-Extraction Steam Turbine
CHP	Combined Heat and Power
EEA	European Environment Agency
EU	European Union
FSIG/GT	Fuel Slurry Integrated Gasifier/Gas Turbine
GHG	Green House Gases
HCE	Highest Cold Efficiency
HEE	Highest Exergetic Efficiency
IPES	Industrial Plant and Equipment Simulator
ISWA	International Solid Waste Management Association
LWTR	Leather, Wood, Textiles, Rubber.
MSW	Municipal Solid Waste
RE	Renewable Energy
RFD	Refuse Fuel Derived
SCB	Sugar Cane Bagasse
SCR	Selective Catalytic Reducer
TDH	Transport Disengaging Height
WTE	Waste to Energy

Table of Contents

1 INTRODUCTION

1.1 Municipal Solid Waste MSW

Solid wastes are discarded materials. In some cases, some of those can be recovered or recycled as feedstocks. The combustible part of solid wastes is composed by a wide variety of heterogeneous materials. It is possible to classify those residues in the following three categories: MSW, medical and pathological waste, and hazardous waste (TILLMAN, 1991). According to that, the non-dangerous materials discarded in urban areas are considered as MSW. Usually, there are public or private organizations responsible for the collection, transport and final disposal of the solid wastes. However, the world population will continue to grow (CENSUS BUREAU, 2015), thus demanding efficient and sustainable solutions for the waste generated in urban areas. The EPA (U.S. ENVIRONMENTAL PROTECTION AGENCY, 2013) recognizes the MSW as a renewable energy source.

More detailed information about the composition of the MSW can be found in Section 2.6 .

1.2 MSW Management

In order to reduce the huge environmental load of waste discharge, MSW management need to develop and improve systems with energy recovery and conversion techniques (BELGIORNO et al. 2003). Due to the fast industrialization and increasing urban concentration observed in many countries, the environment cannot assimilate the volume of MSW produced.

The amount of MSW produced is growing very fast. The current world production of MSW is around 13 Pg (petagram) per year, and the generation levels are expected to double by 2025 (EUROPEAN ENVIRONMENT AGENCY, 2015).

The waste management among other factors depends on the technological development, the type of waste materials, the availability of large areas for landfills and even the cultural level of the local population (BARBA; BRANDANI; CAPOCELLI, 2015).

There is a wide variety of solid wastes generated by society, therefore MSW cannot be thought of as a single combustible material or fuel. Moreover, the composition of MSW is

constantly changing depending on the location, season and others. Among many possibilities, the main technologies available for MSW management include waste minimization, recycling, landfilling, incineration, and combustion/gasification with energy recovery.

Figure 1.2-1 shows the hierarchy of the solid waste management (FINNVEDEN et al., 2005). There is no single waste management treatment or strategy applicable to all circumstances involving MSW production. The idea of this hierarchy is to obtain the maximum benefits of the products generating the minimum volume of non-recoverable waste (FODOR; KLEMEŠ, 2012).

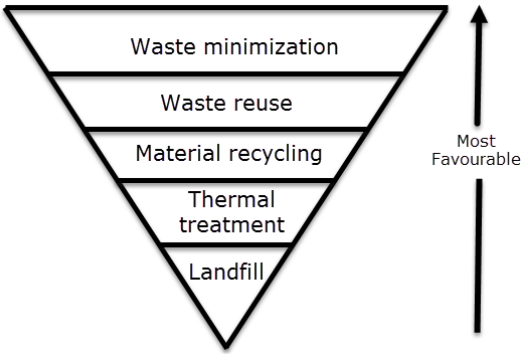

Figure 1.2-1 Hierarchy of solid waste management (FINNVEDEN et al. 2005)

As seen, the most favorable alternatives for waste management are minimization and reuse.

Many energy and natural resources are used to manufacture each product. Therefore, source reduction is also important in manufacturing. Some methods to reduce and reuse residues include donation, less packing, redesign, and many more. However, such methods require the compromise, education, and culture of a society, which are uncertain parameters with some limitations.

After such environmentally friendly methods, waste-to-energy (WTE) processes represent a promising waste management alternative as a renewable energy (RE) source. WTE also minimizes the volume of unusable waste that would end up in a landfill (TAN et al., 2015). WTE processes reduce the solid waste in volume about 80 to 90% and about 70 to 80% in mass (LOMBARDI; CARNEVALE; CORTI, 2014), thus saving or avoiding landfill space, sanitary problems, and environmental damage.

It is important to clarify that thermal treatments, including gasification, do not compete with recycling, just enhance it (GASIFICATION TECHNOLOGIES COUNCIL, 2015). For example, metals and glass cannot be gasified or burned, but they are the main recycled materials. Many plastics cannot be recycled and are good for WTE processes.

Following Figure 1.2-1, landfill disposal is the less favorable alternative in waste management. Unfortunately, the majority of the global waste ends up in landfill sites (TAN et al., 2015). The EEA (EUROPEAN ENVIRONMENT AGENCY, 2009) studies the effectiveness of national policies on diverting total municipal waste from landfill. Such report shows that some EU member countries banned landfill disposal for organic waste and ask for increases in alternative waste management routes such as waste prevention and WTE processes.

Table 1.2-1 (CHENG; HU, 2010) presents the advantages and limitations of the major MSW disposal technology options, such as landfilling, composting, and incineration.

Table 1.2-1 Comparison of the major MSW management technology options: landfilling, composting, and incineration (CHENG and HU 2010)

Technology	Advantages	Disadvantages
Landfilling	An universal solution that provides ultimate waste disposal; Relatively low cost and easy to implement; Complements with other technology options for handling the residual waste; Can derive landfill gas as a byproduct for household and industrial uses; Costs incurred incrementally as landfill expands.	Cost increases significantly with liner, leachate collection and removal system, and stricter regulations; Requires large area of land; Does not achieve the objectives of reducing volume of MSW and converting MSW into reusable resources; May result in secondary pollution problems, including groundwater pollution, air pollution, and soil contamination; May serve as breeding ground for pests and diseases; Long postclosure care obligations and unknowns exist, and sets long-term restrictions on site land use; Site location may be limited by the local geology and natural stability of the underground soil; Due to public acceptance and space limitation, landfills are often far away from the places where waste is generated, necessitating long distance transport of the waste.
Composting	Converts decomposable organic materials into an organic fertilizer; Reduces the amount of waste to be landfilled and integrates well with landfilling and materials recovery/recycling.	Takes up more space than some other waste management technologies; Can be costly to implement and maintain, and has no environmental or economic advantages compared to incineration; Requires waste size reduction and some degree of waste separation/processing; There are issues with public perception, such as odor and bioaerosol emissions during the composting process, and the control of disease producing organisms, weeds, and insects; Quality of the fertilizer produced is low and volume is disproportionately large, resulting in poor market demand; Compost product may cause soil pollution by heavy metals and pathogens.
Incineration	Provides substantial reduction (by 90%) in the total volume of waste requiring disposal in landfill; Requires minimal pre-processing of waste; The bottom ash from incineration is biologically clean and stable, and can be used in road building and the construction industry; A very stable process, and virtually all wastes can be burned and the burning process can be adequately controlled; Heat from combustion can be used as energy source for generation of steam and/or electricity; Incineration facilities can be located near residential areas, thereby reducing costs of transporting MSW to locations of waste disposal; Air emissions can be well controlled; More optimal land use and more efficient integration of resources than landfilling.	High capital and operational and maintenance costs, compared to other, non-incineration options; Significant operator expertise is required; Air pollution control equipment is required to treat the flue gas, and the fly ash needs to be disposed in hazardous waste landfills; More raw material have to be used to replace those that have been incinerated, and it does not save energy in the long run as resources are not recycled; May some time discourage recycling and waste reduction; Public perception is sometimes negative, primarily with dioxins emission.

Gasification of MSW have the same advantages found in the incineration processes, however, as it presented in Section 2.1 , gasification is not incineration because does not lead to the complete oxidation of the fuel. Moreover, high concentration of NO_x in the flue gases are characteristic of elevated temperatures found in combustion chambers of incinerators. Gasification works at lower temperatures, thus leading to lower emissions of NO_x. Additionally, MSW power generation occurs near cities, therefore emissions must satisfy rigorous environmental regulations.

Among the environmental benefits of MSW gasification there is no need for landfill space—or that requirement is drastically reduced—thus avoiding or decreasing organic material decomposition decreasing methane emissions in the landfill. In addition, it eliminates or decreases sanitary problems like ground water contamination and air contamination, and the melted materials after gasification can be used in roadbed construction or roofing materials (GASIFICATION TECHNOLOGIES COUNCIL, 2015).

Nevertheless, the proper and cost-effective disposal of MSW continues to be a problem and there are many of difficulties of applying wastes as fuels for power generation due to their high moisture content, low average heating value and heterogeneous composition (DE SOUZA-SANTOS; CERIBELI, 2013a, 2013b).

Sie Ting (TAN et al. 2015) categorizes the WTE approaches into three types: thermal treatment, biological treatment, and landfill. The options for thermal treatment processes in MSW management are a very attractive method to:

- Recover the renewable energy contained in the waste, producing electricity and heating (BARBA; BRANDANI; CAPOCELLI, 2015).
- Reduce the volume of unusable waste that would end up in a landfill.
- Control pollutant emissions to very low levels, reducing greenhouse gases (GHG) emissions.
- Gain public acceptance of MSW as a relatively clean and renewable source of energy.

The biological approach as anaerobic digestion of MSW produces biogas that can be applied in power generation or chemical processes. It is also fair to say that some landfills are prepared for energy recovery because CH_4 is captured and used in energy power generation. In that case landfilling is considered as a WTE technology as well (TAN et al. 2015). However, those options are not within the scope of the present work.

Thermal treatment of MSW to generate electricity power have minor environmental impacts when compared with other sources of electricity (ARENA, 2012).

Many information on waste management can be found in the literature, as for instance those published by the International Solid Waste Management Association (ISWA, 2015).

1.3 Research Objectives

The main objective of the present work is to continue and improve previous investigations in order to evolve the studies for the FSIG/GT alternative using MSW as energy source (DE SOUZA-SANTOS; CERIBELI, 2013a, 2013b). The adopted assumptions, parameters and methodology are described in chapters 3 y, 4 and 5 respectively.

Based on that and using the software tools for simulation, the present work has the following secondary objectives:

- Optimize the gasification process aiming to achieve the highest exergetic efficiency (HEE) by varying the operational pressure and the mass flow rate of injected air. The highest cold efficiency (HCE) would also be pursed and comparisons between the HEE and HCE options are carried.
- Optimize the entire generation process (FSIG/GT) and maximize the efficiency under the 1st Law of Thermodynamics.
- Optimize the drying process based on the parameters obtained in the objectives above.
- Compare the obtained results with the performances of commercial units of power generation consuming MSW.

1.4 Dissertation Overview

Chapter 2 presents the literature review and introduces the basic concepts about the thermoelectric power generation through MSW gasification. The chapter also justifies the advantages of the adopted alternative.

Chapter 3 describes the basic aspects of the mathematical model and main assumptions behind the applied software (CeSFaMB© and IPES©). Those are applied for simulations and optimizations of the gasifier, dryer, and power generation process.

Chapter 4 presents the parameters and assumptions taken during the present work, including physical and chemical properties of the fuel, dryer and gasifier description, and the detailed description of the power generation process.

Chapter 5 describes the adopted methodology for the simulation and optimization of the thermoelectric power generation process FSIG/GT.

Chapter 6 presents the results and discussion about the various achieved results.

Chapter 7 lists the conclusions.

2 LITERATURE REVIEW

2.1 Gasification

Gasification is the transformation of solid fuel into gases (DE SOUZA-SANTOS, 2010). Usually, gasification burns part of the fuel to provide the energy required by the endothermic gasification reactions. The fuel gas can be applied in power generation processes or goes through further chemical processes to provide syngas, which can be used for the production of fuels, chemical, and fertilizers. However, the present work concentrates not on the production of syngas, but just of fuel gas to be used in power generation.

Prior to enter the gasifier, the solid fuel usually passes through grinding to reach particle sizes compatible with the particular technique to be applied during gasification. In the case of bubbling bed fluidization, such particles must satisfy the maximum particle size diameter as shown in Section 2.6.1, in order to allow good operational fluidization conditions.

A particularly important characteristic of the gasification process is that it operates at lower temperatures than incineration. For example Bubbling Fluidized Bed Gasifiers (BFBG) ensure good efficiencies employing temperatures around 800 and 1000 K (DE SOUZA-SANTOS, 2010) as compared to the minimum 1250 K (ANTHONY, 1995) necessary for MSW incineration technologies. Thus, BFBG leads to lower emissions of NO_x than the levels reached at most processes involving combustions and incinerations. The obtained fuel gas is cleaned to decrease particle and alkaline contents to levels acceptable for injections into commercial turbines or for other applications such as chemical synthesis (GASIFICATION TECHNOLOGIES COUNCIL, 2015).

The gasification is accomplished by many chemical reactions and simultaneous thermal processes. Nevertheless, gasification is not an isolated set of processes. Indeed pyrolysis,

combustion, and gasification reactions occur simultaneously (DE SOUZA-SANTOS, 2010). Combustion is a gasification process where enough oxygen is available for oxidation reactions involving the fuel. The main reaction occurs between carbon and oxygen. Devolatilization or pyrolysis is a very complex process and is part of gasification; their main products released by the volatiles are light gases, tar and char.

Among the many reactions involved in gasification processes, most publications oversimplify the process by considering just the following:

- Carbonaceous solid and water $C + H_2O = CO + H_2$
- Carbonaceous solid and carbon dioxide $C + CO_2 = 2CO$
- Carbonaceous solid and hydrogen $C + 2H_2 = CH_4$
- Shift $CO + H_2O = CO_2 + H_2$

Such a simplification does not take into account other components would be involved as reactant and products, since any usual carbonaceous fuel contains $H, N, O, S,$ etc. Additionally, pyrolysis is also a very important combination of chemical and physical processes that greatly influences the whole process as well the quality of the produced gas (DE SOUZA-SANTOS, 2010).

Gasification needs the supply of an agent (Figure 2.1-1). The literature classifies three types of thermal process to be considered: pyrolysis, direct and indirect gasification(BELGIORNO et al., 2003). Usually, the term pyrolysis is reserved for the process taking place in inert atmospheres, however it can also take place in oxidant ones. In the case of direct gasification, an oxidant gasification agent is used to partially oxidize the carbonaceous fuel, thus providing enough for the endothermic processes. Therefore, such would not require the application of external sources of energy.

Indirect gasification dispenses the use of oxygen as gasification agent using other gases like steam. Nevertheless, it needs an external energy source to heat the gasification agent to high temperatures or to provide energy to the process, such as heating jackets. As shown below in Figure 2.1-1, direct gasification does not need an external energy.

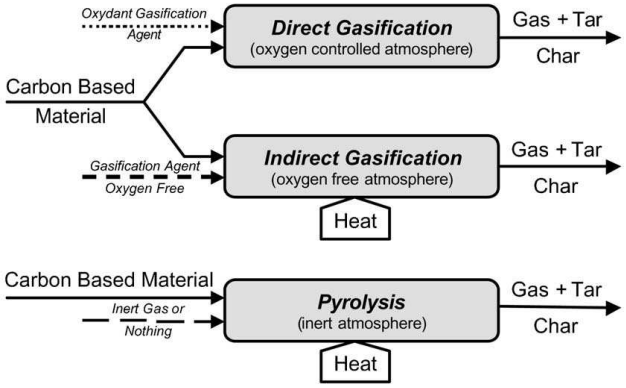

Figure 2.1-1 Gasification and pyrolysis processes (BELGIORNO et al., 2003).

Typically, a gasification process is composed by three main elements or subsystems (BELGIORNO et al. 2003):

1. The gasifier reactor that transforms the solid fuel into gas.
2. The gas clean-up process that decreases alkaline and particle contents in the exiting gas.
3. The processes that uses the chemical potential of the fuel gas to generate power. The present case applies the Fuel-Slurry Integrated Gasifier/Gas Turbine (FSIG/GT) process for power generation (DE SOUZA-SANTOS; BENINCA, 2014).

The gasification technology has been used for a long time. For instance, London was illuminated by gas obtained from coal gasification.

Gasification is among the most commonly used technologies for the thermal treatment of solid fuels and can be considered as an alternative for biomass conversion to energy (BELGIORNO et al., 2003).

The key factor in the revival of the use of gasification processes is the world demand for renewable energy. All around the world more than 800 thermal Waste to Energy (WTE) plants are operating in nearly 40 countries. There are countries more involved in the WTE processes. As an example, Japan has the largest number incineration plants in the world with about 1900 plants, where 10% of them are equipped with power generation facilities. Such plants have the capacity to treat 80% of the total MSW produced there. (TAN et al. 2015).

After proper treatment, the fuel gas produced by gasifiers might be transformed into syngas, which can be applied to produce chemicals and fertilizers. Many industrial units have used gasification processes for more than 75 years to obtain such products. On the other hand, the power generation industry have been using the gasification technologies for at least 35 years (GASIFICATION TECHNOLOGIES COUNCIL, 2015). Nowadays, gasification of MSW is playing an important role as a possible and promising alternative to assist the problem of waste disposal and renewable energy source as well.

Figure 2.1-2 illustrates a scheme of a typical bubbling fluidized-bed equipment. As shown, the oxidant gasification agent (air in the present case) is injected in a plenum located at bottom of the equipment. From there, it passes through the distributor that promotes a uniform flux trough the bed of particles. The bed is composed of two main phases: emulsion and bubbles. The emulsion comprises almost all solid particles in the bed and the part of gas flowing through the bed. The bubbles move upwardly in the bed but are almost free of particles. Above the bed, there is a region called freeboard that provides enough space for the inertial separation between particles and the carrying gas (DE SOUZA-SANTOS, 2010).

A more detailed description of the process, equipment and parameters is presented in Chapter 4 .

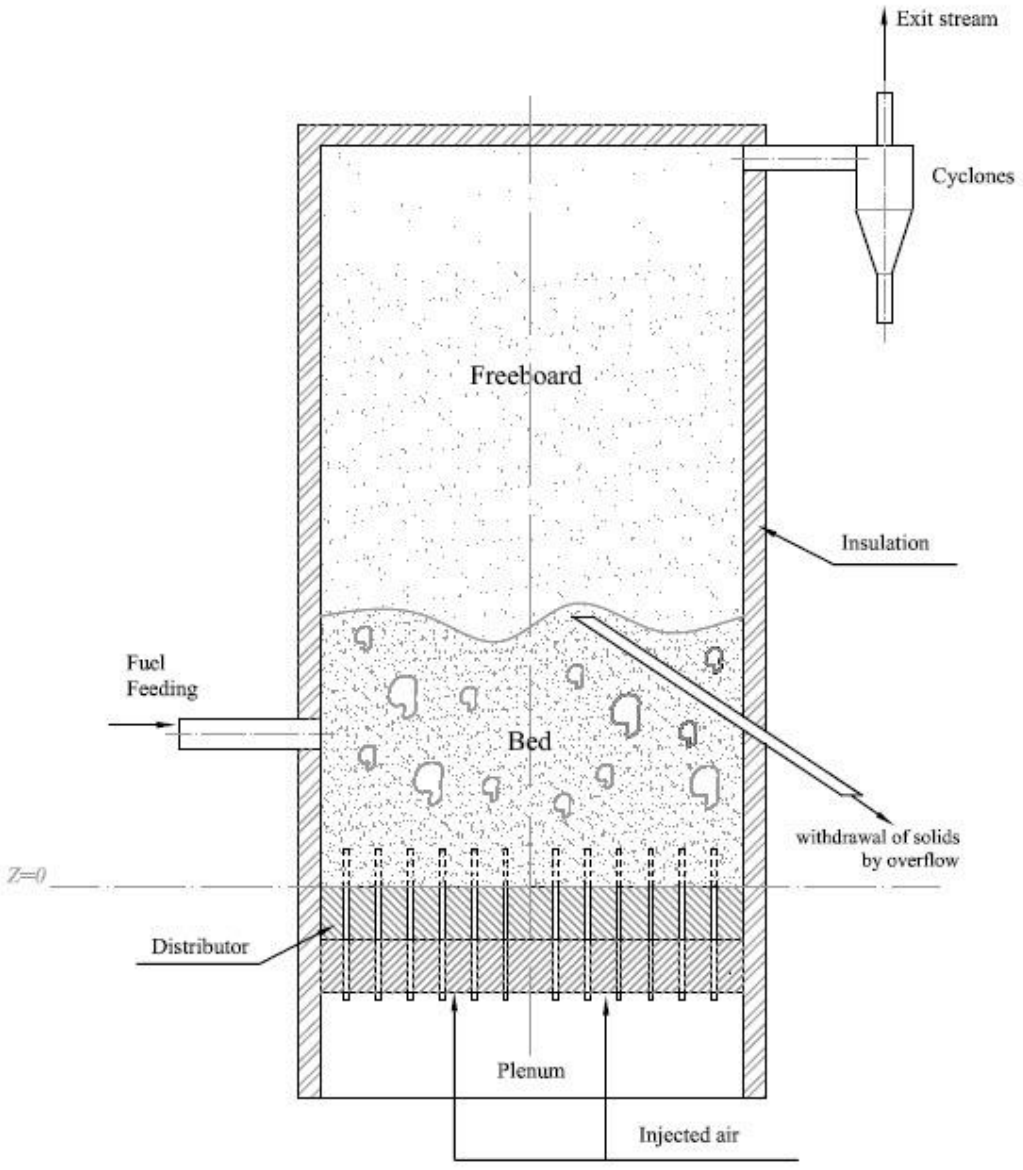

Figure 2.1-2 Basic scheme of bubbling fluidized-bed equipment

2.2 Alternatives for MSW treatment and other gasification processes

Among the alternatives for the MSW treatment the description of some operational installations are presented below.

Figure 2.2-1 shows the flow diagram of a Grate incinerator with SCR (Selective Cathaliyc Reduction) and steam distribution plant installation. The process consists on the following units: waste bunker, the firing system, waste heat boiler, flue-gas cleanning devices, multistage water treatment plant, and steam distribution system. Three incineration lines consumed 196 605 tons of domestic waste from the city of Vienna in the year 2000. The operational pressure of the combustor and the overall efficiency of this process were not available on the publication (EUROPEAN COMMISSION, 2006).

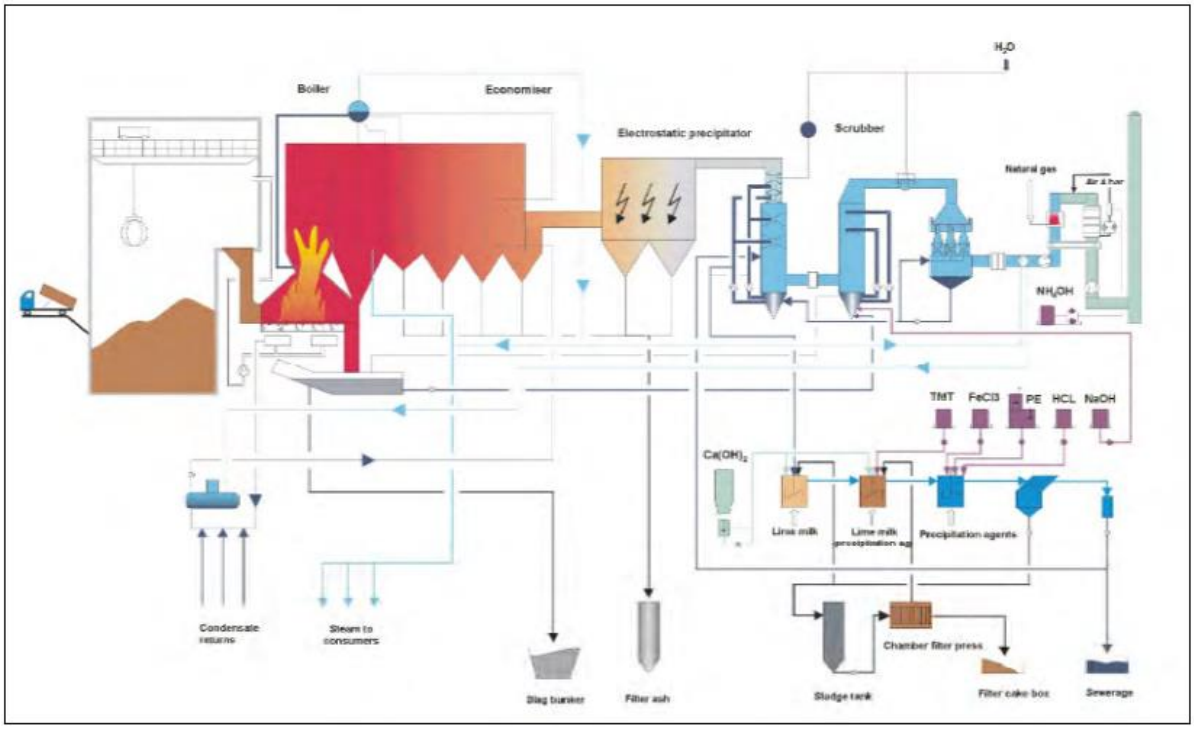

Figure 2.2-1 Process flow scheme of the waste incineration plant Flötzersteig (EUROPEAN COMMISSION, 2006)

The grate incinerator with SCR and CHP system is presented in Figure 2.2-2. The installation is basically composed by the following units: waste bunker, firing system (reciprocating grate), waste heat boiler, flue-gas cleaning system, multistage waste water system, and steam turbine, generator and heat decoupling system. Such plant produces 150 kWh of electricity and 1857 kWh of heat for 1 ton of waste in the year of 2000. The operational pressure of the combustor and the overall efficiency of this process were not available on the publication (EUROPEAN COMMISSION, 2006).

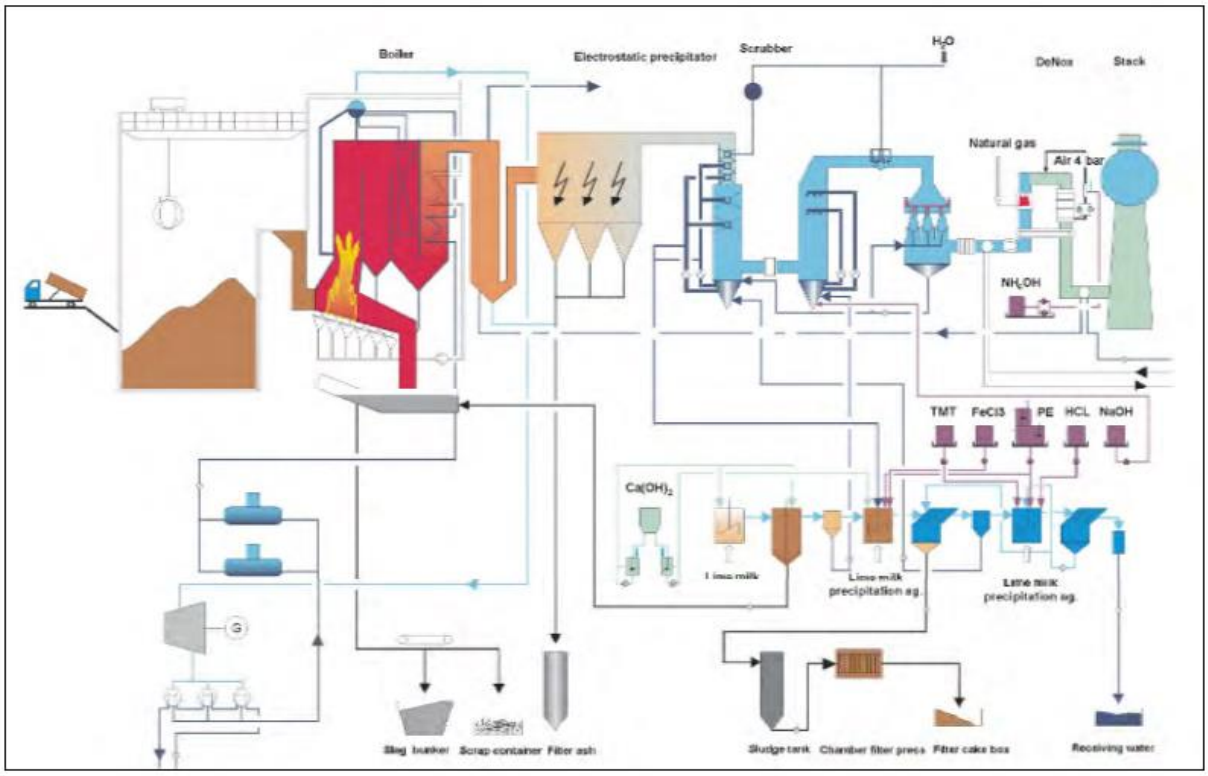

Figure 2.2-2 Process flow scheme of the waste incineration plant Spittelau
(EUROPEAN COMMISSION, 2006)

The diagram flow of the incineration plant of Wels is presented in Figure 2.2-3 below. The installation consists on a grate incinerator with SCR, CHP and bottom ash treatment system. Such process is basically composed by the following units: waste bunker, firing system, waste heat boiler, power generation possibility, flue-gas cleaning devices (including electrostatic precipitator, two-stage wet scrubber, activated coke filter, and catalytic flue-gas cleaning system), residue treatment (include wet chemical/thermal ash treatment, and slag treatment), multistage waste water treatment plant. The steam turbine produces around 600 kWh for 1 ton of waste. The operational pressure of the combustor and the overall efficiency of this process were not available on the publication(EUROPEAN COMMISSION, 2006).

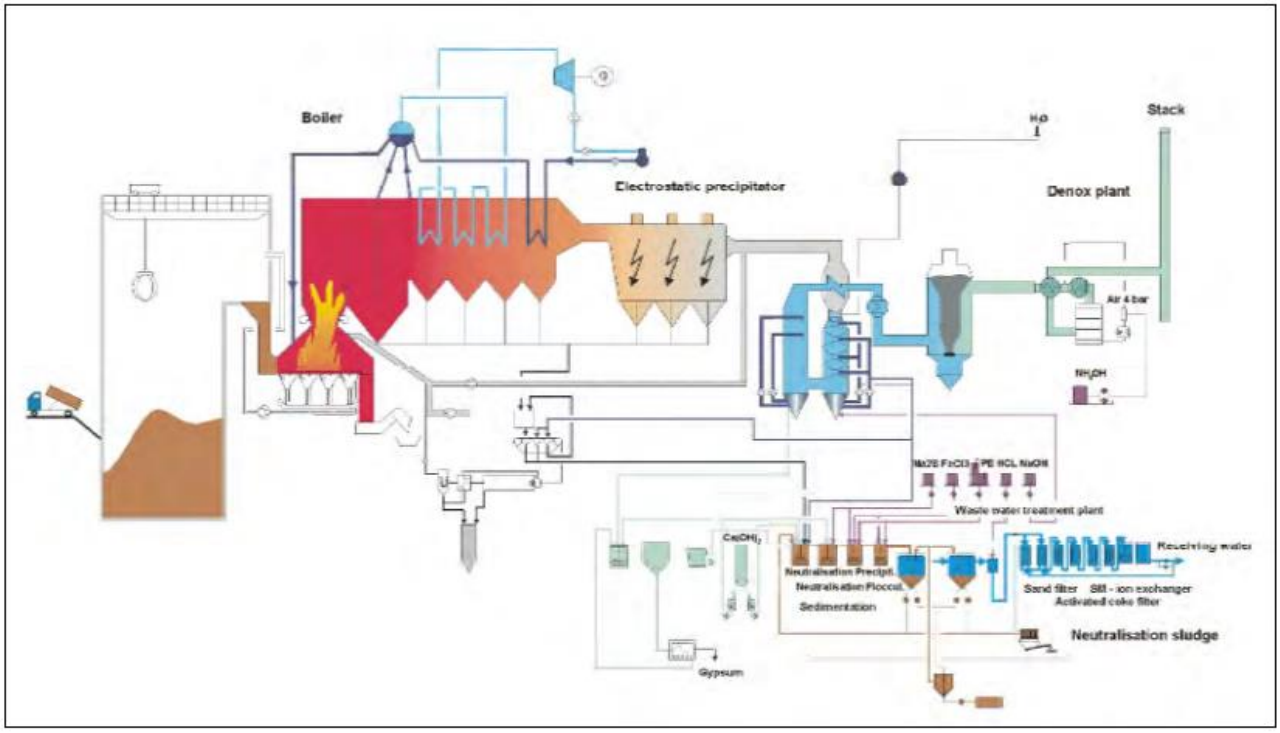

Figure 2.2-3 Process flow scheme of the waste incineration plant Wels – line 1 (EUROPEAN COMMISSION, 2006)

Previous studies (DE SOUZA-SANTOS; CERIBELI, 2013a) have proposed the alternative presented in the Figure 2.2-4. That thermoelectric power generation process consuming MSW applies a BFB boiler with combustion operating under 2 MPa. The flue gases are cleaned and injected into gas turbines. Simultaneously, the steam produced at 10 MPa drives a Rankine Cycle. The plant consumes particulate MSW as slurry pumped into the pressurized combustion chamber by simply commercially slurry pumps. Thus, avoiding costly cascade feeding methods. Despite the relatively low heating value of the MSW, the work demonstrates that when compared with existing power units based on MSW, the proposed alternative achieves relatively high efficiencies, such as 33% based on the 1st law of thermodynamics.

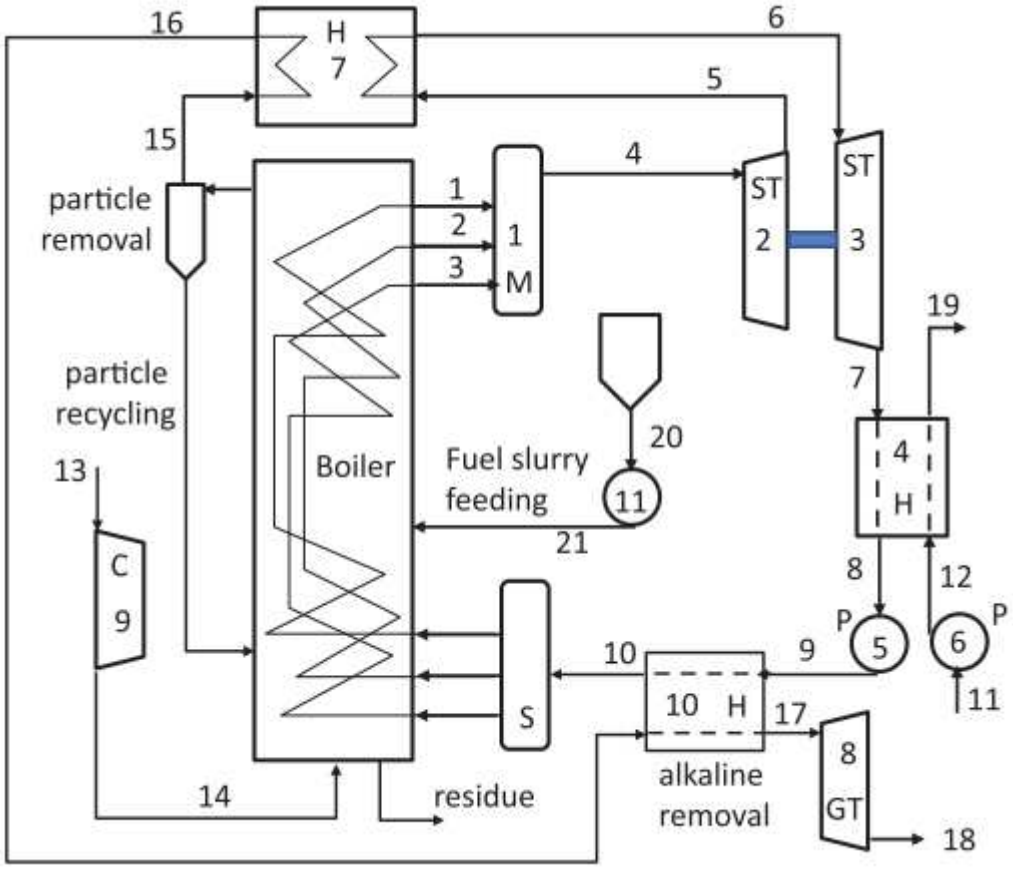

Figure 2.2-4 thermoelectric power generation process consuming municipal solid waste (MSW) (DE SOUZA-SANTOS; CERIBELI, 2013a)

More detailed information for the improvements and operational characteristics of the proposed the FSIG/GT power generation process are presented in section 2.5 .

Among the alternatives for electric or heating power generation using gasification processes, there is the biomass integrated-gasifier/gas turbine combined cycle (BIG/GTCC) consuming sugar cane bagasse (SCB) (LARSON; WILLIAMS; LEAL, 2001), which is illustrated in Figure 2.2-5. In that work, the BIG/GTCC alternative is compared with the most commonly used technology in the field or condensing-extraction steam turbine (CEST). Shown

in Figure 2.2-6. The authors showed that the BIG/GTCC technology achieve higher efficiencies and lower electricity costs than the CEST technology.

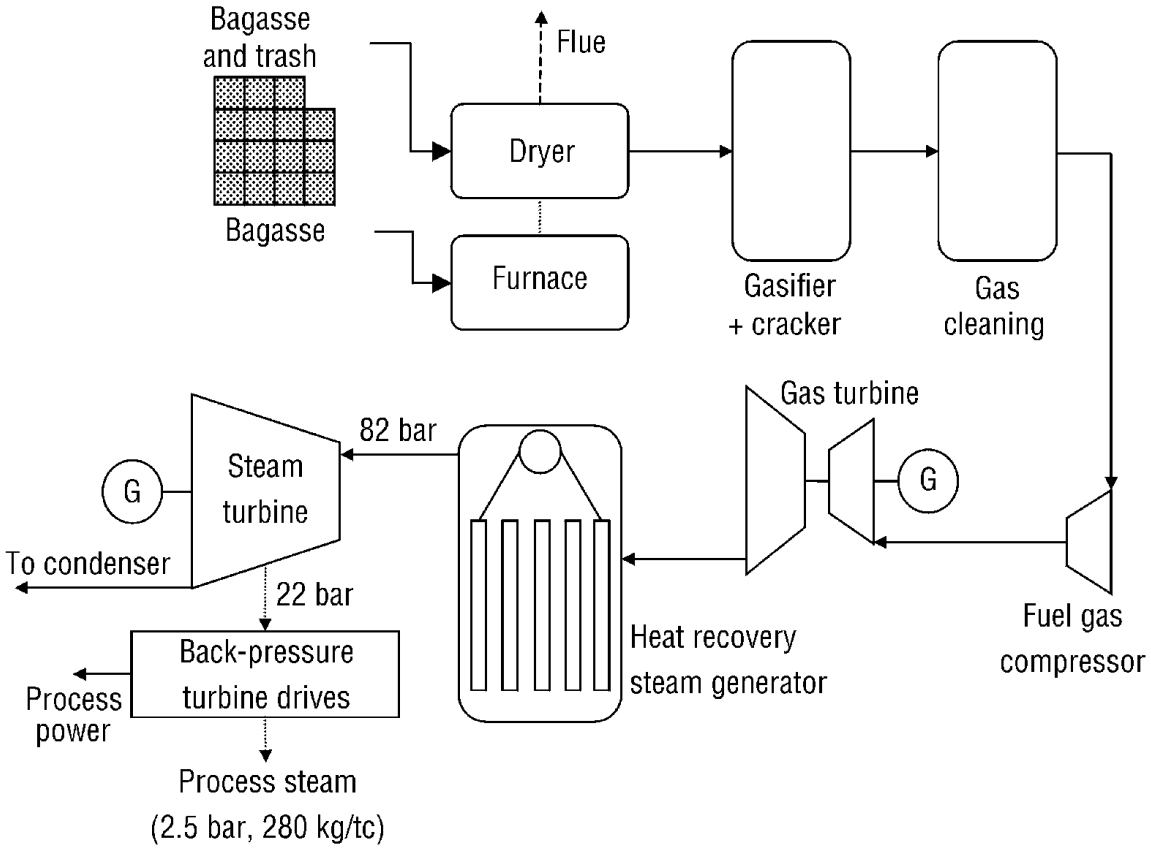

Figure 2.2-5 BIG/GTCC schematic diagram (LARSON; WILLIAMS; LEAL, 2001)

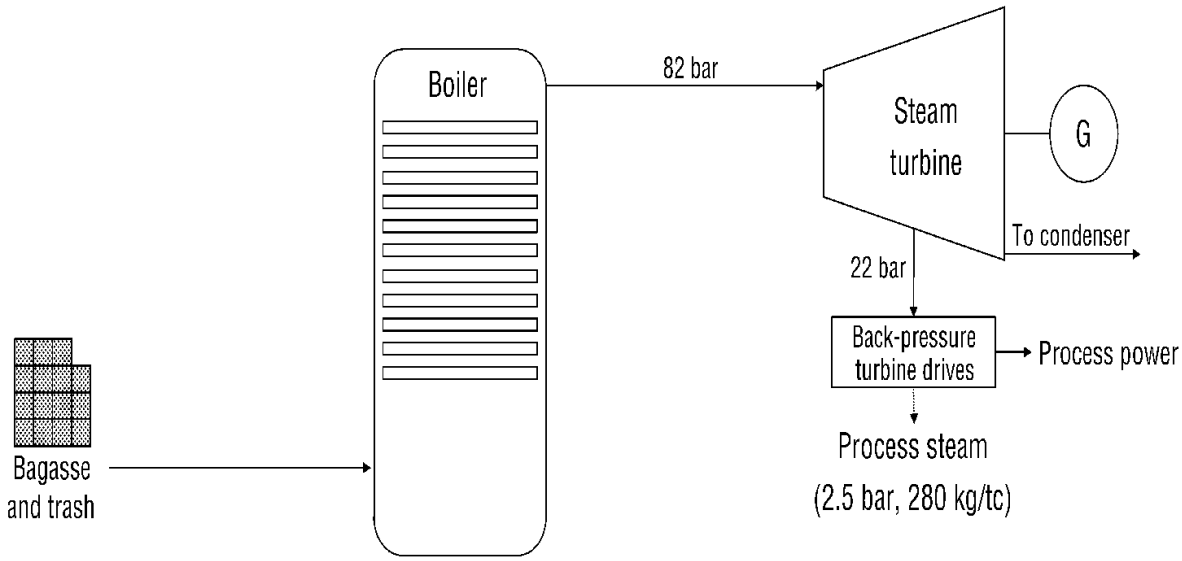

Figure 2.2-6 Condensing-extraction steam turbine (CEST) cogeneration system.
(LARSON; WILLIAMS; LEAL, 2001)

2.3 Advantages of BFB gasification in the case of MSW

In the case of MSW, the bubbling fluidized bed gasification process shows the following advantages (DE SOUZA-SANTOS; CERIBELI, 2013a):

- Wider range of fuel characteristics and sizes are admissible, which is the typical case of MSW. Thus, dispensing special grinding systems found in pulverized combustion.
- Harder and denser materials fed into the reactor fall down into the bottom of the bed and can be removed when properly designed distributors are in place.
- The high degree of contact between gases and particles in the emulsion promotes very uniform temperatures throughout the bed. This simplifies the monitoring and controlling instrumentation.
- Operational average temperatures found in the bed and freeboard are relatively low when compared with those usually measured in combustors, thus saving capital costs of insulation materials, shell, and control systems.
- High degree of controllability, mainly due to the large thermal and dynamic inertia of a bubbling bed as well to the uniform temperatures and high mixing ratio of gases and solids in the bed.
- Low NO_x emissions, due to the relatively low and uniform temperatures when compared to many other techniques.
- If well designed, bubbling fluidized beds might lead to no or very low concentration of tar and oil in the produced gas.

2.4 Feeding systems

Feeding particulates into a pressurized vessel is not trivial and technical barriers are usually found. Feeding screws are commonly used, nevertheless, they would compact the particulate solid fuels into larger and denser blocks. These oversized and high-density blocks would present two main problems:

1. The feeding screw could surpass the maximum torque leading to mechanical failures.
2. Even if it were managed to insert the dense fuel lumps into the gasifier, the superficial gas velocity in the bed would not be enough to maintain those lumps in the midst of the

bubbling fluidized bed. The lumps would fall on the distributor and the intended gasification process would not occur.

An alternative for such problems is the application of cascade feeding systems (VIMALCHAND; PENG; LIU, 2011), which can feed granular or fine particles with moisture content between 1 and 25% and particle diameter in the range up to 6 mm into a gasifier with operational pressure between 0.03 and 6.85 MPa. In such systems Figure 2.4-1, the particulate fuel is fed at the top hopper, which, in turn, feeds another below. Then this second hopper is pressurized with inert gas (usually Nitrogen) to achieve a first level of pressure. The fuel is moved through a rotary valve into a third lock hopper below, initially at the same pressure than the above. The procedure is repeated until the pressure of the destination vessel is reached.

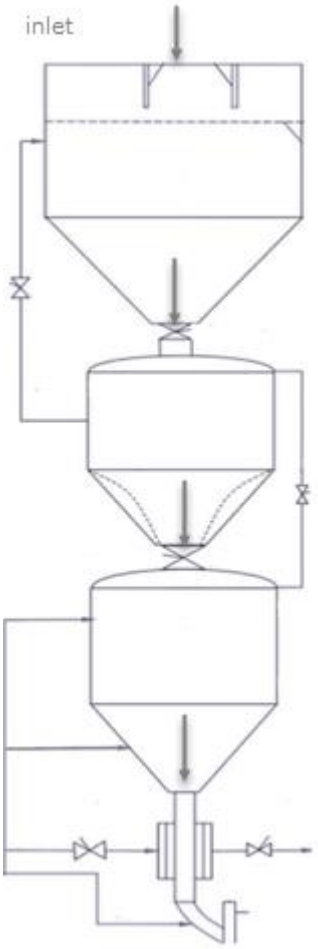

Figure 2.4-1 High pressure feeder (VIMALCHAND; PENG; LIU, 2011)

Of course, the pressure cannot be increased at a single stage without raising the temperature at the hopper, which may lead to partial devolatilization of the fuel. If so, tar would be released, causing the particles to stick together, thus preventing them to proceed or drop into the rotary valve. The final pressure and the maximum gradual compression applied to inert gas injected

into each hopper, without provoking fuel devolatilization, determine the number of steps. Usually, the procedure consumes expensive inert gases and introduces high capital, operational, and maintenance costs to the electricity generation unit, not to mention losses on its overall efficiency due to power diverted to inert gas compressions and cooling. Additionally, it relies on complex sequential operations, which are prompt to failures mainly due to interruptions of continuous flow of fuel downward to the next hopper and respective rotary feeding valve. In case of coals, those problems can be originated by static electricity building-up among particles. In the case of fibrous biomass—such those that are usually found in MSW as well—the problem can be even worsened due to entanglements of neighboring particle extremities (DE SOUZA-SANTOS; CERIBELI, 2013b).

The second alternative is pumping fuel slurries, and has been used for a long time (ANTHONY, 1995). When the moisture content of the fuel is high enough, it behaves as a slurry and can be pumped (ANTHONY, 1995). When compared with cascade systems of hoppers, pumping fuel slurries simplify the feeding process decreasing the operational, maintenance and capital cost (DE SOUZA-SANTOS; CERIBELI, 2013b) (DE SOUZA-SANTOS, BENINCA, 2014).

Nevertheless, drying the original moisture content of the fuel added to the water to prepare such slurries demands energy. Therefore, direct injection of fuel slurries where limited to the use of boilers and incinerators, because the complete combustion of the fuel would be more than enough to vaporize the water. However, this is critical in gasification because the partial combustion of the fuel is not enough to vaporize the water and provide the energy to sustain the endothermic reactions. Either the required gasification temperatures would not be reached or the gasification efficiency would be very low. Extensive simulations confirmed this during previous phases of the present work (DE SOUZA-SANTOS; CHAVEZ, 2012), (DE SOUZA-SANTOS, 2012a), (DE SOUZA-SANTOS, 2012b), (DE SOUZA-SANTOS; CERIBELI, 2013a). Additionally, the literature (BREAULT, 2010) indicates that direct gasification of fuel in feeding slurries would require the use of pure oxygen gasification agent or slurries with hydrocarbons as media to reach ignition of the injected fuel (DE SOUZA-SANTOS; CERIBELI, 2013a).

Based on previous phases of the present work (DE SOUZA-SANTOS; CERIBELI, 2013a), (DE SOUZA-SANTOS; CERIBELI, 2013b), (BERNAL, 2014), (DE SOUZA-SANTOS; BERNAL; RODRIGUEZ-TORRES, 2015) the FSIG/GT process introduces an alternative to solve such problems and is described below.

2.5 The Fuel-Slurry Integrated Gasifier/Gas Turbine (FSIG/GT) process

The present work studies a power generation process based on Fuel-Slurry Integrated Gasifier/Gas Turbine FSIG/GT consuming MSW (Section 2.5). Before the fuel gas is injected into the turbine combustor and then into the turbine itself. Rigorous limits regarding the concentrations of alkaline as well particle sizes and content in the gas stream to be injected into turbines must be satisfied in order to minimize erosion and corrosion of their blades (DE SOUZA-SANTOS, 2010).

The proposed thermoelectric power generation alternative is a product from previous studies and improvements, such as (DE SOUZA-SANTOS; BENINCA, 2014). The feeding system obstacle has been overcome by pumping the fuel as slurry, as described before in the previous section. The authors (DE SOUZA-SANTOS; BENINCA, 2014) introduce three basic alternatives for the FSIG/GT process applied to the case of SCB (Sugar Cane Bagasse). Configurations A (Figure 2.5-1) and B (Figure 2.5-2) use steam or gas with steam as gasification agent, while Configuration C does not use steam.

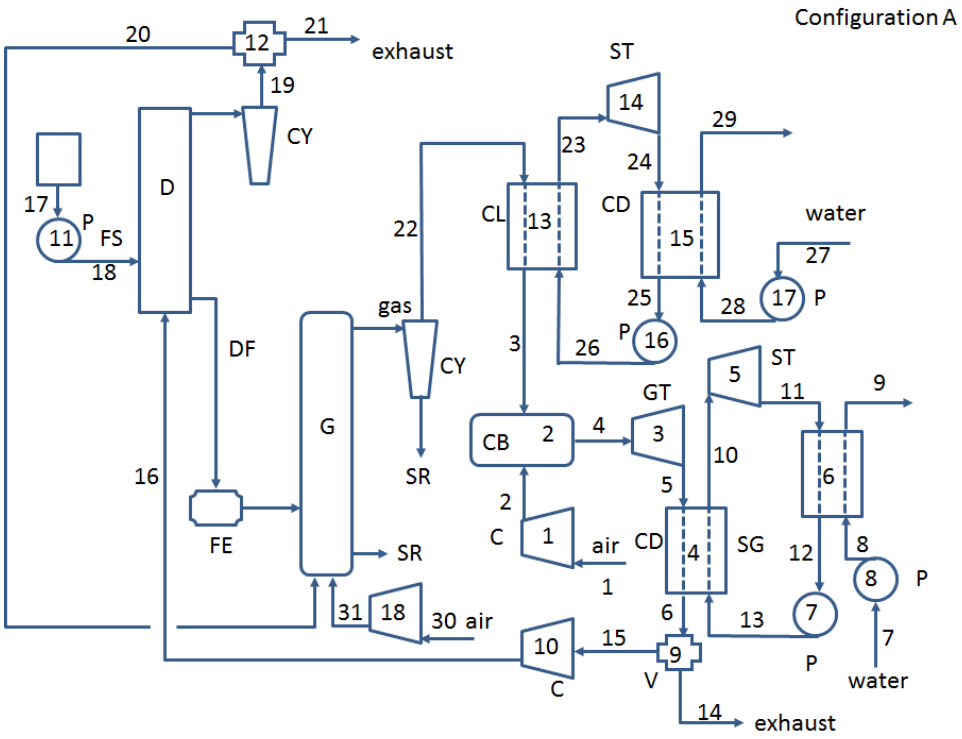

Figure 2.5-1 Configuration A of the proposed FSIG/GT process.

C = compressor, CB = combustor, CD = condenser, CL = cleaning system, CY = cyclone, D = dryer, DF = dried fuel, FE = screw feeding, FS = fuel-slurry pumping, G = gasifier, GT = gas turbine, SG = steam generator, ST = steam turbine, P = water pump, V= valve or splitter (DE SOUZA-SANTOS; BENINCA, 2014).

Configuration A, shown in Figure 2.5-1 above, uses part of the exiting gas from the drying unit (stream 20) as gasification agent. That stream should contain high concentrations of water and might enhance the gasification.

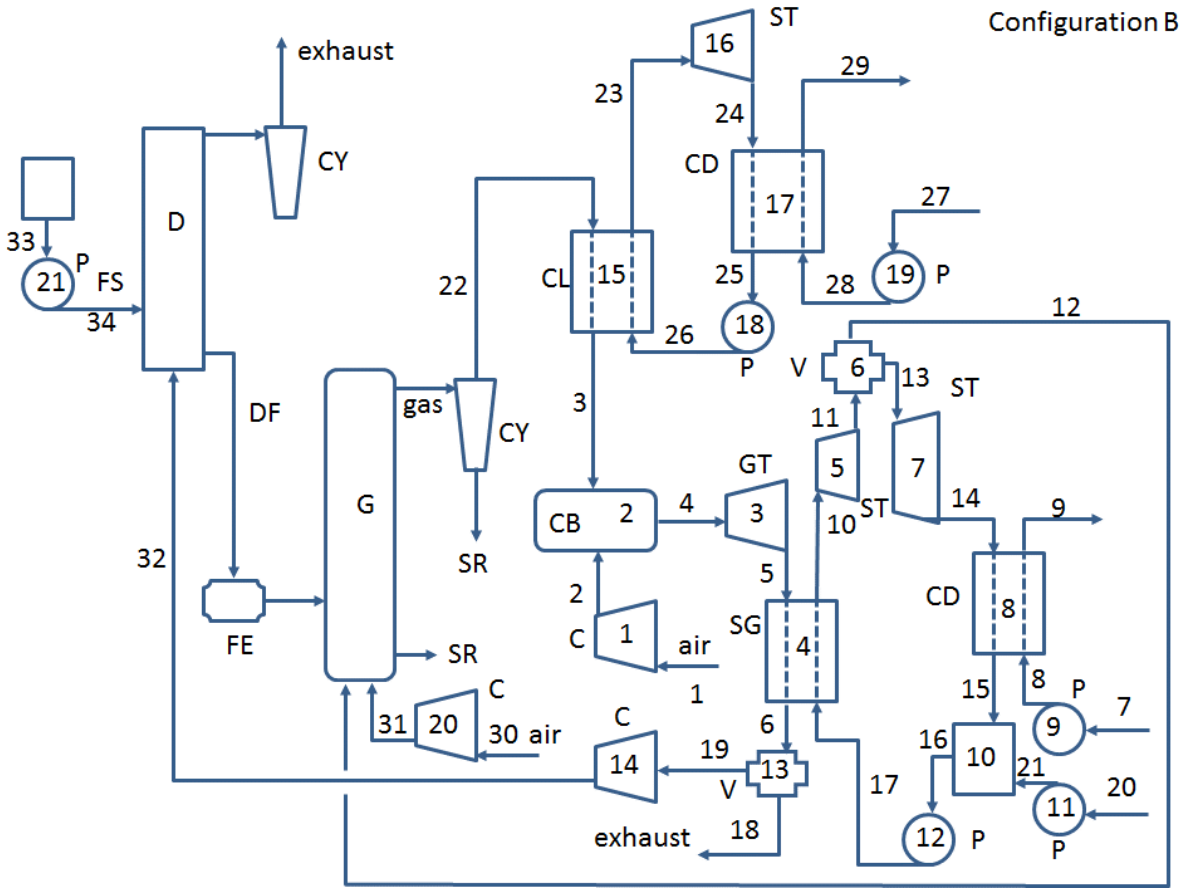

Figure 2.5-2 Configuration B of the proposed FSIG/GT process.

C = compressor, CB = combustor, CD = condenser, CL = cleaning system, CY = cyclone, D = dryer, DF = dried fuel, FE = screw feeding, FS = fuel-slurry pumping, G = gasifier, GT = gas turbine, SG = steam generator, ST = steam turbine, P = water pump, V = valve or splitter (DE SOUZA-SANTOS; BENINCA, 2014)

Configuration B, shown in Figure 2.5-2, proposes an intermediary extraction (stream 12) from the main steam turbine cycle to be injected into the gasifier (G), which provides the steam for gasification.

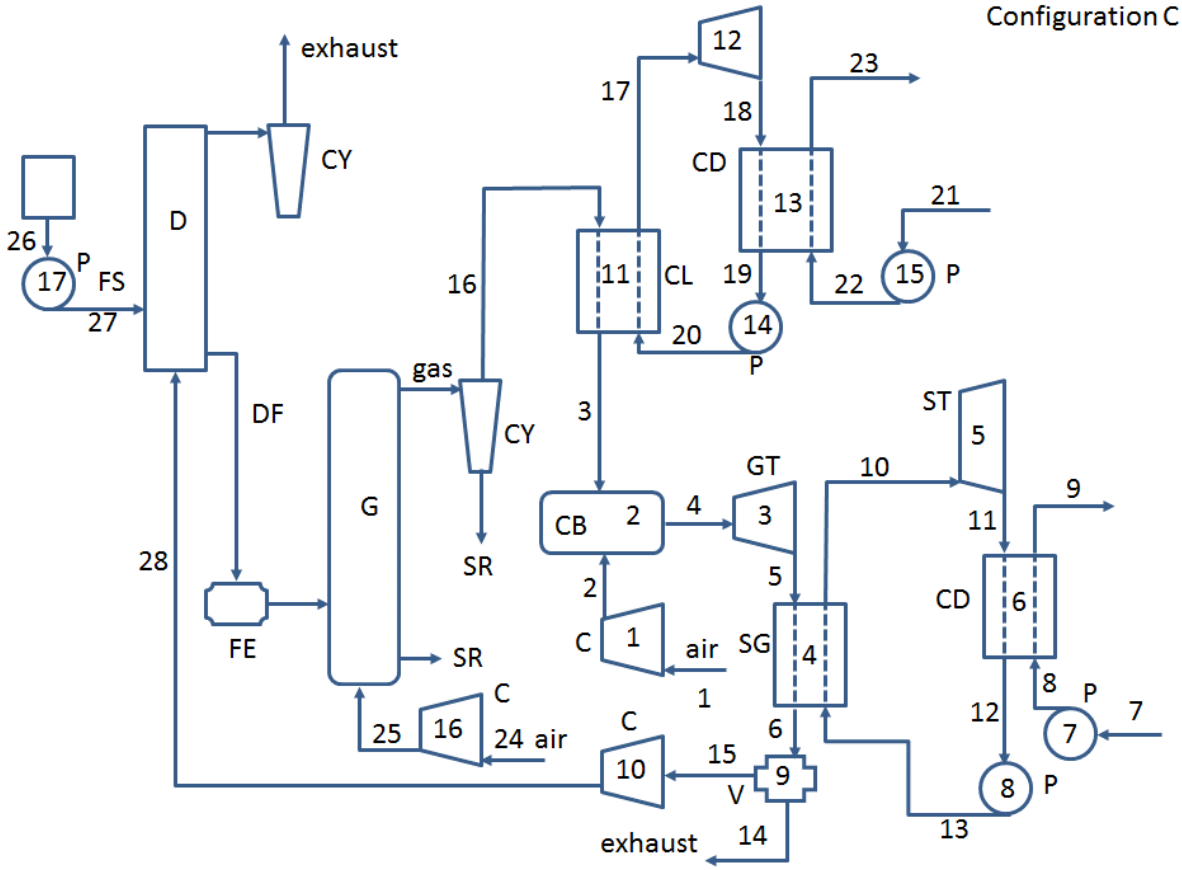

Figure 2.5-3 Configuration C of the proposed FSIG/GT process.

C = compressor, CB = combustor, CD = condenser, CL = cleaning system, CY = cyclone, D = dryer, DF = dried fuel, FE = screw feeding, FS = fuel-slurry pumping, G = gasifier, GT = gas turbine, SG = steam generator, ST = steam turbine, P = water pump, V= valve or splitter (DE SOUZA-SANTOS; BENINCA, 2014).

Figure 2.5-3 illustrates the studied configuration, with no steam injection into the gasifier.

The wet MSW is mixed with water to form the fuel-slurry (Stream 26), which is pumped into the pressurized dryer (D) by a slurry pump (Equipment 17). The pressurized dryer operates at BFB regime with gas injection at Stream 28. The dryer operates at slightly higher pressure than the gasifier does, to ensure that the dried solid fuel will be fed into the gasifier using simple rotary valves and Archimedes screws. The gas used in the drying process is taken from the gas turbine cycle (Equipment 4 to 8). That gas is compressed by Equipment 10 to reach the appropriate temperature for the MSW fuel-slurry drying. The mass flow of gas (Stream 28) that is required for the fuel-slurry drying, is calculated by extensive simulations (as shown in Section 5.3). After drying, the MSW is fed into the gasifier (Equipment 19) using rotary valves and Archimedes screws. Succeeding the gasification process, cyclones and dust collectors clean the fuel gas in order to reach particle diameter values acceptable to be injected into the gas turbine (Equipment 3). The cleaned fuel gas passes through the Equipment 11, decreasing the temperature until 800 K to reach the dew point of the alkaline species. The concentration of

such alkaline species must decrease until values accepted for the injection into the gas turbine (Equipment 3) at Stream 4. Additionally, the energy recovered by the cooling of the fuel-gas at Equipment 11 is used to drive the Steam Rankine Cycle (Equipment 11 to 15) described in the Section 4.6.1. The cooled and cleaned gas then is injected into the gas turbine combustor (Equipment 2) at Stream 3, where it reacts with air (Stream 2) and burn. The burned mixture is injected (Stream 4) into the gas turbine (Equipment 3). The Equipment 4 supply the heat for the second Steam Rankine Cycle composed by the Equipment 4 to 8. Stream 15 is a fraction of the burned flue gas (Stream 6) and is used in the drying stage (Stream 28).

The work of (DE SOUZA-SANTOS; CERIBELI, 2013b) studied FSIG/GT concept for thermoelectric power generation consuming MSW as well. Such work presents two alternatives considering steam injection in one of them. The steam injection might be justified by the presence of water in some of the most important gasification reactions (Section 2.1). Moreover, the heating value of the exiting gas could be increased with additional water. Nevertheless, the results show that the best cold efficiency was achieved for air flow around 15 kg/s with no steam injection. Such result was possible because the MSW structure has enough hydrogen, which once oxidized, provides enough water to promote gasification reactions that need it as reactant (DE SOUZA-SANTOS; CERIBELI, 2013b). The present work starts from that result.

Previous works such as (BERNAL, 2014; DE SOUZA-SANTOS; BERNAL; RODRIGUEZ-TORRES, 2015; DE SOUZA-SANTOS; CERIBELI, 2013b) show that in cases of fuels with significant hydrogen in their composition, no steam is needed as a gasification agent. Simulations of the FSIG/GT process consuming Sugar Cane Bagasse were carried. On that, the injected air and steam flows as well as the gasifier diameter were taken as variables. The results showed that steam injections into the gasifier did not increase its exergetic efficiency significantly when compared with the similar process where only air was used as agent. Indeed, the highest cold efficiency for the whole power generation process was achieved without steam injection into the gasifier. The achieved efficiency was 38.16%, which is above the average range of 20% found in sugar alcohol mills (DEDINI, [s.d.]). Therefore, the process studied in the present work does not apply steam extracted from the Rankine cycles that compose the FSIG/GT process. Such should also lead to savings on capital, operational, and maintenance costs.

More detailed information about the entire power generation process will be shown at Chapter 4 .

2.6 MSW classification

According to publications (TILLMAN, 1991), (GIDARAKOS; HAVAS; NTZAMILIS, 2006) MSW consist mainly of:

- Paper products.
- Polystyrene.
- Polypropylene.
- Polyvinyl chloride.
- Low and high-density polyethylene.
- Wood products.
- Leather and rubber.
- Food waste.
- Yard waste.

Non-combustible materials such as:

- Glass.
- Ferrous metals.
- Aluminum.
- Heavy nonferrous metals.
- Stones.

MSW also includes a variety of products that deserve special consideration including:

- Nickel-cadmium batteries.
- Lead-Acid batteries.
- Lithium batteries.
- Discarded electronics.
- Household cleaners and solvents.
- Paints and thinners.

As mentioned above, MSW is very heterogeneous, and it is important to classify it, to optimize the waste reuse, recycle and WTE treatments. Arafat (ARAFAT; JIJAKLI, 2013) proposes a categorization to separate the waste streams based in their potential treatments as follows:

- Metals.
- Paper.
- Plastics.
- Textiles.
- Wood.
- Food wastes.
- Yard wastes.
- Glass

From those categories, metals and glass are inorganic and cannot be gasified, nevertheless they are the main recycled waste. The remaining categories are organic, therefore can be gasified.

The moisture content in the MSW is an important characteristic that decreases the heating value of the waste. If the moisture content increases, the energy production in the gasification process would decrease. Nevertheless, in this case of study the moisture content of the MSW is not relevant because it will be mixed with water to form the Fuel-Slurry, which will be totally dried before the gasification.

2.6.1. MSW characterization

In the present case, the MSW properties were taken from the work of (GIDARAKOS; HAVAS; NTZAMILIS, 2006) who collected data during one-year survey in the region of Crete. The results of the waste composition analysis for the period 2003–2004 are shown in Figure 2.6.1-1. Three main waste categories can be highlighted: Putrescible, Papers, and Plastics (P3 Dominance), which share about 76% of total MSW. Such P3 waste has a good gasification potential. Putrescible or food waste represents 39%, plastics and paper are second with 17% and 20%, respectively. (GIDARAKOS; HAVAS; NTZAMILIS, 2006).

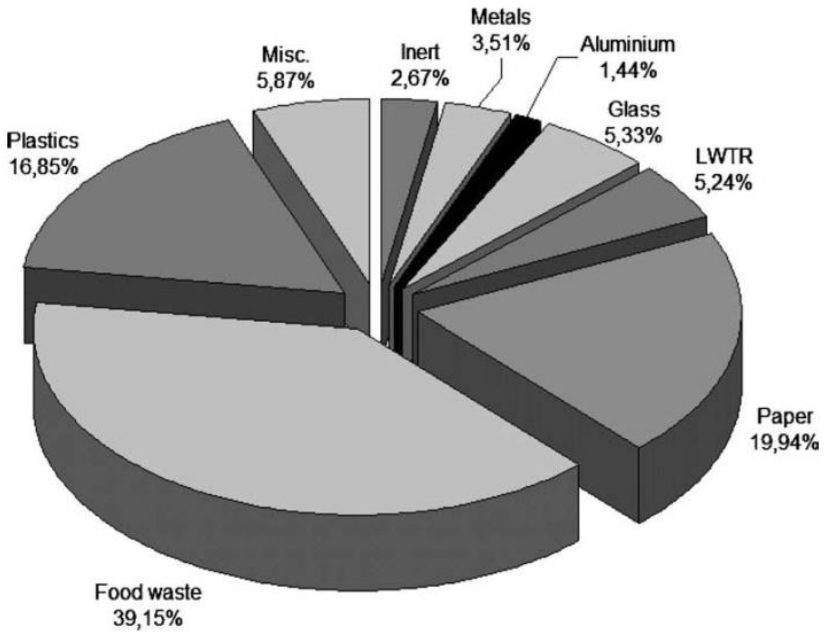

Figure 2.6.1-1 Waste composition analysis (annual), wet weight (GIDARAKOS; HAVAS; NTZAMILIS, 2006)

The fuel ultimate and proximate analyses provide important information regarding its composition and gasification potential. Such analyses are relatively simple and help to determine the basic fractions and composition in a solid fuel. The simpler one is the proximate analysis and determines the moisture, volatile content, the fixed carbon fraction and the ash content in a solid fuel. On the other hand, the ultimate analysis allows determining the mass fractions of chemical species such as carbon, hydrogen, nitrogen, oxygen, sulfur, as well as ash, which is mainly a mixture of oxides. A detailed description of such analysis can be found in several publications (ASTM-INTERNATIONAL, 2015a, 2015b).

The MSW high-heating value (HHV) was computed from the data obtained in the ultimate analysis using known relations described elsewhere (DE SOUZA-SANTOS, 2010). That value agrees with those values reported in the literature (RYU, 2010). Table 4.2.4-1 shows both analyses of the MSW used during the present study. As said before, the MSW is a very heterogeneous source and its properties vary widely. Thus, the results achieved by the present study should be reviewed for specific cases.

Another important characteristic of the MSW is the average particle diameter. The determination of this variable is not a trivial matter because the gasification process involves gas-solid reactions that occur at the surface or in a layer near the surface of the solid fuel particles. The present work uses the following relation to measure the average particle diameter (DE SOUZA-SANTOS, 2010):

$$d_{P_{av}} = \frac{\sum_{i=1}^{n} {d_{P_i}}^3 w_i}{\sum_{i=1}^{n} {d_{P_i}}^2 w_i} \tag{4.1}$$

where w_i is the mass fraction of the particle with diameter d_p and n is the number of size levels or sieves used for determining the particle size distribution. The particle size distribution is obtained by passing the material through a series of sieves with openings of decreasing size based on the US standard sieve series (ASTM-INTERNATIONAL, 2015c). Table 4.2.4-1 also shows the particle size distribution of the consumed MSW, which provides average diameter around 2 mm. That value is proposed after preliminary simulations in order to allow good operational conditions for the dryer and gasifier, while not requiring great expenditures in gridding (DE SOUZA-SANTOS; CERIBELI, 2013).

3 MODELING

Due to the magnitude of the involved phenomena (most thermal systems are fairly complex), the cost-effective implementation of experimental investigations on laboratories or pilot plant scale is not viable. As a consequence, the modeling and simulation approaches are a reliable mathematical tool for the process description, fundamental for the techno-economical evaluation (BARBA; BRANDANI; CAPOCELLI, 2015). Moreover, mathematical models provide information on the behavior of the given system without building a prototype.

This chapter describes the most important aspects of the mathematical models and main assumptions of the used software (CeSFaMB© and IPES©). Such software developed by Professor Dr. Marcio L. de Souza-Santos, were applied during the tasks of modeling, simulation and optimization of the studied processes. The present work follows previous supervised studies by him and intends to amplify the information already achieved on the topic.

3.1 CeSFaMB©

The Comprehensive Simulator of Fluidized and Moving Bed Equipment (previously called CSFB; http://www.csfmb.com/) was applied during the simulation and optimization of the gasifier and dryer operational conditions. The software is prepared to deal with various categories of equipment such as boilers, furnaces or incinerators, gasifiers, dryers, pyrolysers and others; operating under different regimens. It is able to work with a wide range of fuels, including a heterogeneous mixture such as MSW. The present work was developed with the version 59.3 of that software and made available to supervised students in 2014.

CeSFaMB© has been applied in many works to simulate cases of boilers, gasifiers, dryers as well shale retorting consuming or processing a wide range of fuels. The simulation results were compared with real operations in order to verify that they reproduce the experimental measured data -within acceptable levels of deviations. Among the others, the simulator has been validated by the works listed below:

(DE SOUZA-SANTOS, 1987), (DE SOUZA-SANTOS, 1989), (DE SOUZA-SANTOS, 1994a), (DE SOUZA-SANTOS, 1994b), (DE SOUZA-SANTOS; RABI, 2003), (DE SOUZA-SANTOS; RABI, 2004), (RABI; DE SOUZA-SANTOS, 2008), (RABI; DE SOUZA-SANTOS, 2008), (DE SOUZA-SANTOS, 2009), (DE SOUZA-SANTOS, 2010).

The software has also been applied in the works listed below:

(DE SOUZA-SANTOS, 1998), (COSTA; DE SOUZA-SANTOS, 1999), (DE SOUZA-SANTOS, 1999), (VAN DEN ENDEN; LORA, 2004), (BASTOS-NETTO; RIEHL; DE SOUZA-SANTOS, 2010), (SILVA ORITZ; VENTURINI; SILVA LORA, 2011), (ENGELBRECHT et al., 2011), (MOUTSOGLOU, 2012), (DE SOUZA-SANTOS; CERIBELI, 2013b), (DE SOUZA-SANTOS; BENINCA, 2014), (KRZYWANSKI et al., 2015), (DE SOUZA-SANTOS; DE LIMA, 2015), (DE SOUZA-SANTOS; BERNAL; RODRIGUEZ-TORRES, 2015), (DE SOUZA-SANTOS, 2015a).

3.1.1. Mathematical model and assumptions of the simulation process

The Figure 3.1.1-1 illustrates a simplified scheme of the mathematical model behind CeSFaMB©.

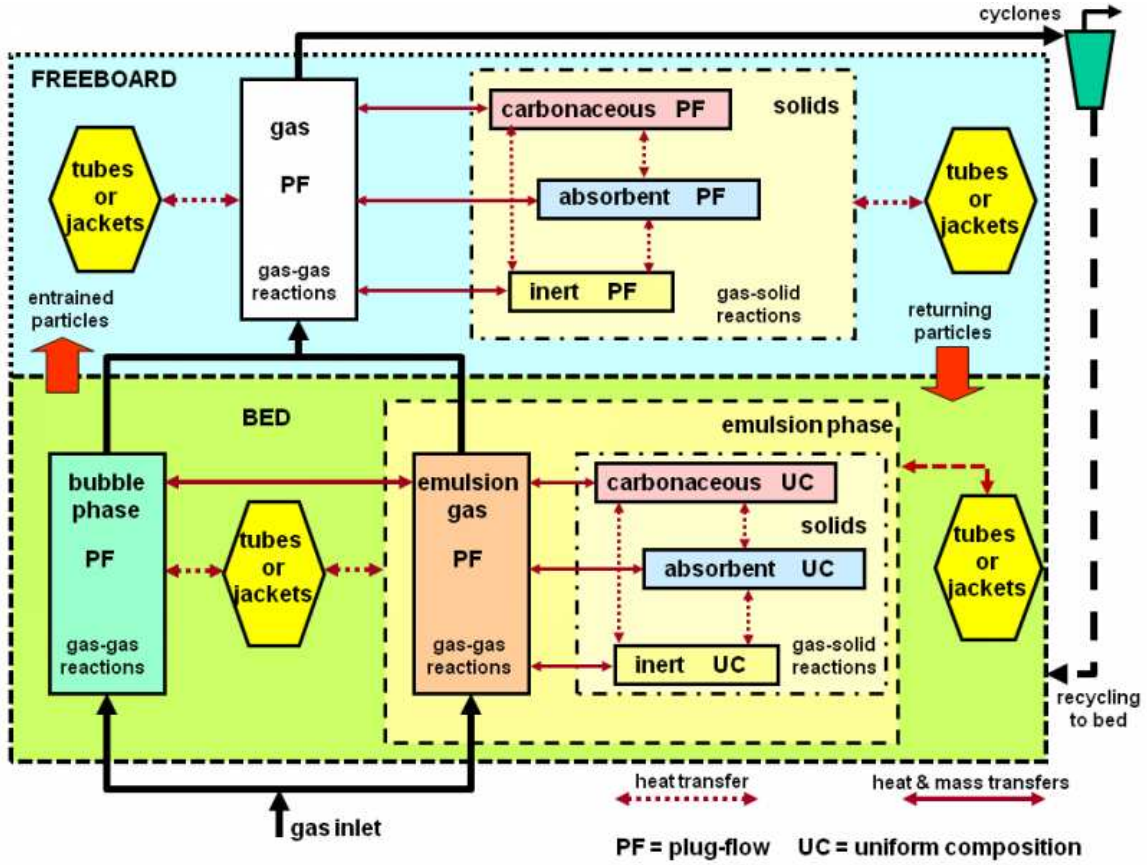

Figure 3.1.1-1 Basic scheme of CeSFaMB© mathematical model (DE SOUZA-SANTOS, 2015b)

The basic assumptions of the model are listed below (DE SOUZA-SANTOS; CERIBELI, 2013b; DE SOUZA-SANTOS, 2010):

The basic assumptions and computational strategy can be summarized as follows:

1) The unit operates in steady-state regime.
2) The equipment is separated in two main regions: dense region (or bed in cases of bubbling condition) and lean region (or freeboard in bubbling processes).
3) The dense or bed region is divided in two main phases: bubble and emulsion.
4) There are three possible solid phases: fuel, inert, and sulphur absorbent such as limestone, dolomite, or mixture of those. Ash, eventually detached from the spent fuel, would constitute part of the inert solid phase.
5) The emulsion is composed by solid particles and percolating gas.
6) Bubbles are assumed free of particles.
7) Emulsion gas is considered inviscid, therefore rises through the bed in a plug-flow regime.

8) The same as above is assumed for the bubble gas. However, dimensions, raising velocity, fraction of bed volume occupied by bubbles, as well other characteristics of bubbles are considered in all calculations regarding that phase.
9) Bubbles and emulsion exchange mass and heat.
10) Mass transfers also occur between particles and emulsion gas.
11) Heat transfers also occur between all phases, including particles.
12) Gases are assumed transparent regarding radiative heat transfers.
13) Emulsion gas exchanges heat with the vessel or reactor walls. Therefore, all heat transfers between the walls and other phases (bubbles and particles) take place indirectly through the emulsion gas.
14) All phases exchange heat with surrounding or eventually immersed surfaces (such as tube banks or jackets) in or around the bed and freeboard.
15) Heat transfers to tube banks or jackets are computed point-by-point between those and bed as well freeboard. Eventual phase changes inside the tubes or jackets are also computed. The present work does not apply immersed tubes or jackets around the equipment.
16) The average composition for each solid particle is computed in the bed or dense region through convergence procedures involving the solutions of differential mass and energy balances are described elsewhere (DE SOUZA-SANTOS, 2010). However, their composition may change in the freeboard. Moreover, particles may exhibit large gradients of temperature and composition in the bed and freeboard.
17) Compositions and temperatures of all gas and solid phases vary in the freeboard and are computed using complete differential and energy balances.
18) Particle size distributions modify due to chemical reactions, attritions between particles themselves, as well due to the entrainment and recirculation processes. Those are also taken into account to compute the size distributions of each solid phase in the bed and freeboard.
19) Heat and mass transfers in the axial or vertical direction within each phase are considered negligible when compared with the respective transfers in the radial or horizontal direction between a phase and neighbouring ones.
20) At each axial position (z), mass transfers between phases result from differences of species average concentrations at each phase. As soon chemical species are consumed or formed by reactions, they are subtracted from or added to the respective phase.

Therefore, these effects appear as sink or source terms in the mass continuity equations for each phase.

21) At each axial position (z), heat transfers between phases result from differences of temperature at each phase. These terms would appear as sinks or sources in the energy conservation equations.
22) At the basis of the dense region (z = 0), the two-phase model is applied to determine the splitting of injected gas stream between emulsion and bubble phases.
23) For points above that (z > 0), the mass flow in each phase is determined by fundamental equations of transport phenomena. Those include mass transfers between the various phase as well homogeneous and heterogeneous reactions. The computation of the chemical species consumption or production rates by heterogeneous reaction include not just the chemical kinetics but also mass transfer resistances due to gas boundary layers around the particle, layers of converted porous solids, and porous reacting nuclei. Unreacted-core or exposed-core can be set as primary models.
24) Boundary conditions for the gas phases concerning temperature, pressure and composition at (z = 0) are given by the values of injected gas stream.
25) At each iteration, boundary conditions at z = 0 for the three possible solid phases (carbonaceous, sulphur absorbent, and inert) are obtained after differential energy balances involving conduction, convection, and radiative heat transfers between the distributor surface and the various phases.
26) The solution of differential equations describing the energy and mass transfers proceed from the distributor (z = 0) to the top of freeboard or lean region ($z = z_F$). The values at the top of the bed or dense region ($z = z_D$) are used as boundary conditions for the bottom of lean one.
27) For the first iteration, a carbon conversion is assumed. After solving the system of coupled non-linear differential equations throughout the equipment, the new carbon conversion is computed. Conversions of all other solid-phases components are computed as well.
28) The cyclone system is simulated and all characteristics of the collected particles are obtained. If those are recycled to the bed, CeSFaMB© includes such a stream into the mass and energy balances during iterations.
29) Steps 25 to 28 are repeated until convergence regarding a weighted overall deviation is achieved. That weighing considers deviations between assumed and computed conversions of chemical species as well between assumed and computed heat transfers

among phases and immersed surfaces in the bed and freeboard. This and the tight coupling of all chemical and physical phenomena involved in the equipment, ensures consistency regarding all mass and energy balances.

Once the simulation is concluded all internal and overall details of the equipment operation such as temperature, concentration, and all other variable profiles throughout the entire equipment, are printed. A graphical interface facilitates the input of data for simulations as well consultation and study of outputs.

3.1.2. Main input data for the simulation process

The basic information necessary for the simulation is listed below (DE SOUZA-SANTOS; CERIBELI, 2013b; DE SOUZA-SANTOS, 2010):

- Type of simulated equipment (boiler, gasifier, reactor, etc.) and the respective fluidization regime.
- Description of the equipment basic geometry including height and hydraulic diameter of the bed and the freeboard (Section 4.2), bed depth, position of main gas withdrawal, etc.
- Conductivities, thickness, and emissivity of the isolated materials of the bed and freeboard shell (Section 4.2.3.).
- Operational pressure of the equipment (variable of study Section 5.1).
- The position of the main gas evacuation (Section 4.2.1).
- Carbonaceous solid fuel characterization (MSW): inlet mass flow rate, inlet temperature, position of carbonaceous fuel feeding, proximate analysis, ultimate analysis, densities of feeding fuels, particle size distribution, etc. (Section 2.6.1).
- Absorbent and inert particles characterization, similar information as mentioned above for the carbonaceous solids must be provided. The software is able to simulate up to five different absorbents and inert solids simultaneously.
- Fuel slurry description: type and content of adopted solvent (Section 4.1.4).
- Dimensions and design details of the gas distributor system (Section 4.2.2).
- Gases injected through the distribution characterization: mass flow, temperature, pressure, and composition.

- Exiting gas and particles cleaning system.
- Tube banks, wall jacket and recycling description (not the case of study).

The Comprehensive Simulator is able to considerate eventual alternatives of the geometric parameters and the process beyond the above possibilities. Those possibilities are outside the scope of the present work.

3.1.3. Main output data of the simulation process

Using the assumptions, parameters and the adopted methodology, CeSFaMB© provides among others, the following results and specific information (DE SOUZA-SANTOS; CERIBELI, 2013b; DE SOUZA-SANTOS, 2010):

- Equipment performance parameters, which include all important overall aspects of the unit operation such as: flow rates of gases and solids leaving the equipment, carbon conversion, mixing rate (allow verification of eventual segregation among solids), residence time of each solid species, TDH, flow rates of tar or oil leaving with gases, etc.
- Devolatilization parameters with all aspects of the volatile release during the operation including rates, composition of released gas (includes amount of tar) and average time for complete pyrolysis.
- Composition, flow rates and thermodynamic, transport phenomena properties, and adiabatic flame temperatures (in the case of gasifiers) of gas streams. These are supplied at each point inside the equipment (including bed and freeboard) as well of those of produced streams under molar and mass basis.
- Composition, particle size distribution, and flow rates of solids or liquids at each point inside the equipment as well of those streams leaving the equipment.
- Overall elemental mass balance verification.
- Temperature profiles of each gas (emulsion and bubbles) and solid (carbonaceous, absorbent, and inert) throughout the entire equipment are provided.
- If tube banks are present, point-by-point profiles of temperature inside the tubes and their walls.

- If the unit is equipped with water or gas jacket, profiles of temperature inside the jacket and walls throughout the entire height.
- If the unit contains tube bank or water jacket, profiles of steam quality throughout each bank and water jacket.
- Process parameters, which includes specific aspects of boilers, gasifiers, dryers, shale retorts, pyrolysers, or any other type of simulated equipment.
- Rates and parameters related to heat transfer to ambiance and internals with detailed account of heat transfer rates.
- Rates of erosion at tube bank walls and the respective mean-life times.
- General warnings to the user related to possible operational problems as well a list of various aspects that might interest the user is presented. Among the most critical, there is the possibility of slugging flow, surpassing solid particle softening temperatures, excessive elutriation rates, low cyclone efficiencies, etc.
- Point-by-point information related to the dynamics of fluidization, such as: diameter and rising velocity of bubbles in the bed, void fractions and particle size distributions of all solid species throughout the bed and freeboard, superficial velocities, circulation rates of particles in the bed, and fluxes of solids in throughout the freeboard.
- Composition profiles of each chemical species (18 possible components) throughout the entire equipment and at each phase (emulsion, bubbles, gas in the freeboard).
- Rate profiles for each reaction at each phase throughout the entire equipment.
- Main pressure losses at various points or sections of the equipment.
- Overall exergy analysis of the unit operation.
- If sulphur absorbent is fed into the unit, several efficiency-related parameters to sulphur capture.

These results provide a complete picture of the internal process and most are presented in graphs or tables.

3.2 IPES©

The Industrial Plant and Equipment Simulator is based on mass and energy balances according to the 1st and 2nd Law of thermodynamics. The software developed by Professor Marcio L. de Souza-Santos predicts the operational conditions of a single equipment (control

volume) or an entire thermal power plant. Among the equipment that the software is able to simulate there are: combustors, compressors, chemical reactors, heat exchangers, mixers, pumps, reformers, splitters, turbines, and valves. The wide range of processes covered by the simulator makes the software an ideal and helpful tool to simulate, analyze and optimize the studied cycle. The program can deal with a mixture of gases, liquids and solids. It also contains a large data bank to estimate physical and chemical properties of the involved species (DE SOUZA-SANTOS, 2014).

Each equipment might have one or several inlet and outlet streams. The properties of such streams may be known or not, or may be imposed conditions (e.g., exhaust gas temperature). Those parameters combined with zero-order energy and mass balances (including 2nd Law of thermodynamics and exergy analysis) allow setting the system of equations around each unit. The software forms a square matrix, where the number of variables equals the number of equations. After solving the matrix, the program provides the temperature, pressure, composition, mass flow, enthalpy, entropy, density and other important properties of all streams. Besides this, the overall 1st and 2nd Law efficiencies, related to simulated process, are provided.

IPES© has been applied in previous works. The most recent are: (BERNAL, 2014; DE SOUZA-SANTOS; BENINCA, 2014; DE SOUZA-SANTOS; BERNAL; RODRIGUEZ-TORRES, 2015; DE SOUZA-SANTOS; CERIBELI, 2013a, 2013b; DE SOUZA-SANTOS; CHAVEZ, 2012; DE SOUZA-SANTOS; DE LIMA, 2015; HE; PARK; NORBECK, 2009). Additional R&D projects where the program has been applied can be found on www.desouzasantos.info.

4 PROJECT PARAMETERS AND ASSUMPTIONS

4.1 Dryer

The size of the equipment was optimized in previous works (DE SOUZA-SANTOS; BENINCA, 2014; DE SOUZA-SANTOS; BERNAL; RODRIGUEZ-TORRES, 2015; DE SOUZA-SANTOS; CERIBELI, 2013a; DE SOUZA-SANTOS; CHAVEZ, 2012) to guarantee

enough residence time for the complete drying of the fuel-slurry. The freeboard height is also above the TDH, thus avoiding considerable particle loses by the solid elutriation. The adopted geometry and the operational conditions minimize the carbonaceous material loses due to possible pyrolysis reactions in the drying process.

4.1.1. Dryer geometry

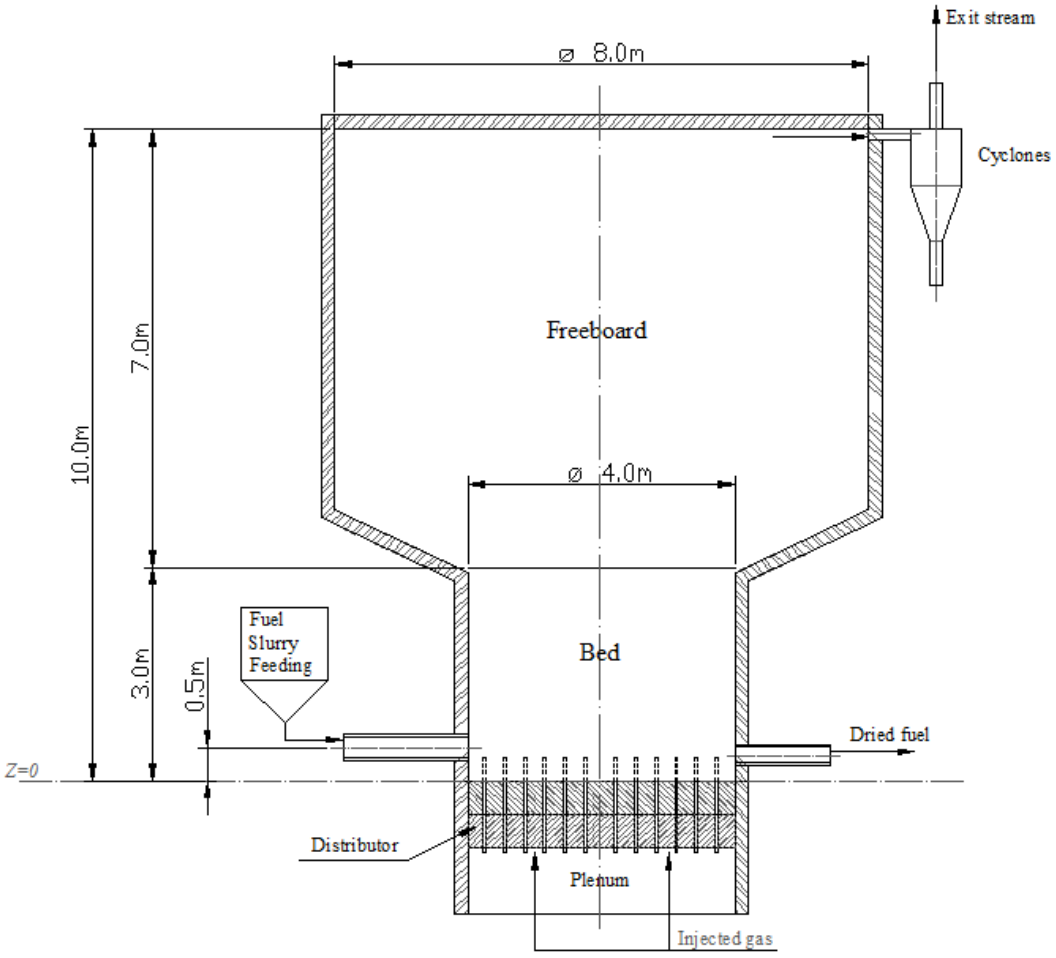

Figure 4.1.1-1 Dryer geometry (simplified scheme)

4.1.2. Dryer distributor

The injected gas used to dry the slurry passes through the distributor. Such component is an injection system that allows a uniform distribution of the gas minimizing the pressure losses. Generally speaking, the distributor is a plate with perforated tubes or flutes as shown in the scheme below:

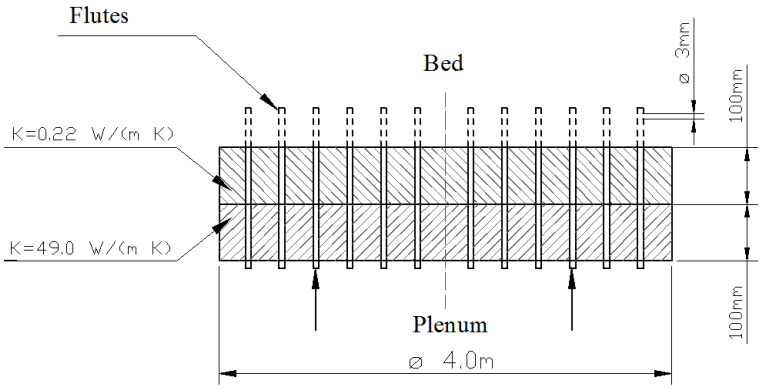

Figure 4.1.2-1- Distributor geometry (simplified scheme).

The complete characteristics of the distributor are listed below:

- $50x10^3$ flutes are distributed uniformly on the cross section.
- Flute internal diameter: 12.7 mm
- Flute external diameter: 13.2 mm
- Number of orifices of each flute: 10
- Orifices diameter: 3 mm
- Thermal insulation layer thickness: 100 mm
- Thermal insulation conductivity: 0.22 W/(m K)
- Carbon steel plate: 100 mm
- Steel conductivity: 49 W/(m K)

4.1.3. Dryer shell and insulation

The dryer reactor insulation consists of two layers of different materials, with a metallic shell (steel) between them. Each material provides specific properties, such as, mechanical resistance to the stress generated by the internal vessel pressure, and thermal insulation to protect the dryer from considerable heat exchanges with the surroundings. Figure 4.1.3-1 shows a cross-section of the equipment wall.

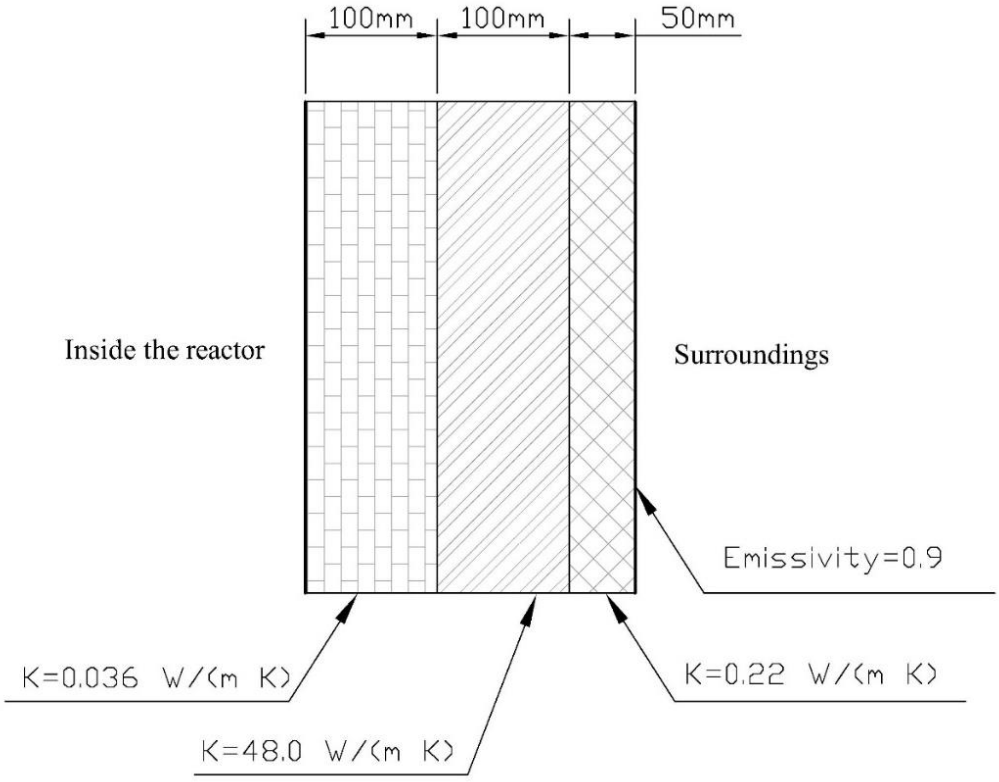

Figure 4.1.3-1Freeboard and bed insulation and shell layers

CeSFaMB© computes the minimum required steel thickness for each situation. The value described in the above figure is just an example and the thickness includes safety factors. However, variations on that thickness would not significantly affect the simulation results for the dryer operational parameters. The simulator also verifies if the temperatures on the metal surfaces are within the range that maintain its mechanical integrity.

4.1.4. MSW Fuel-Slurry feeding into the dryer

The fuel slurry is prepared by mixing the water and MSW. The fraction of water present in the slurry define the pumping characteristics. In the present work, the mass fraction of dry solid in the slurry has been set at 44.29%, which according to the literature, can be pumped by commercially available equipment (HE; PARK; NORBECK, 2009). The same values was adopted in previous investigations (DE SOUZA-SANTOS; CERIBELI, 2013a, 2013b).

The consumption rate of MSW has been set at 28.45 kg/s wet or 18 kg/s (dry basis). That corresponds to the waste generated by cities with around 1.3 million inhabitants that produce around 700 kg per capita/year of MSW (THE CONFERENCE BOARD OF CANADA, 2013).

Table 4.1.4-1 presents the basic characteristics of the injected slurry (DE SOUZA-SANTOS; CERIBELI, 2013a, 2013b).

Table 4.1.4-1 Main characteristics of the injected fuel into the dryer

Fuel Slurry characteristics	Value	
Higher heating value (dry basis)	22.30	MJ/kg
Mass flow rate of MSW (wet basis)	28.445	kg/s
Mass flow rate of MSW (dry basis)	18.00	kg/s
Mass flow of added water	12.191	kg/s
Total mass flow of slurry	40.636	kg/s
Feeding temperature	290	K
Global or bulk density*	200	kg/m^3
Particle apparent density**	720	kg/m^3
Real or skeletal density ***	1394	kg/m^3
Sphericity****	0.3	
proximate analysis (wet basis)		
moisture	36.72	%
volatile	52.64	%
fixed carbon	6.02	%
ash	4.62	%
ultimate analysis (dry basis)		
C	53.00	%
H	7.32	%
N	1.32	%
O	30.96	%
S	0.10	%
ash	7.3	%
solid fuel particle size distribution		
sieve opening (mm)	retained mass	%
10	1	%
5	2	%
3	3	%
2	91	%
1	2	%
0.5	1	%

*see Equation 4.3 , **see Equation 4.1, ***see Equation 4.2, ****see Equation 4.4

The densities of solid particles are defined below (DE SOUZA-SANTOS, 2010).

- Apparent density

$$\rho_{p,app} = \frac{m_p}{V} \tag{4.1}$$

where m_p is the mass of the particle, and V is the total particle volume.

- Real or skeletal density

$$\rho_{p,real} = \frac{m_p}{V_p - V_{pores}} \tag{4.2}$$

where V_{pores} is the volume taken by the pores inside the particle.

- Global or bulk density

$$\rho_{p,bulk} = \frac{m}{v} \tag{4.3}$$

where m is the total mass of the bed, and v its volume.

The sphericity is defined by

$$\varphi_p = \frac{Surface\ area\ of\ spherical\ particle}{Surface\ area\ of\ particle\ with\ the\ same\ volume\ of\ the\ spherical\ one} \tag{4.4}$$

4.2 Gasifier

4.2.1. Gasifier geometry

The proposed gasifier has a circular cross section with constant internal diameter. However, and as explained in the next section, the internal diameter of the equipment varies in order to maintain similar gas superficial equipment operation at different pressures. This allows comparing the results achieved here with previous ones (DE SOUZA-SANTOS; CERIBELI, 2013b).

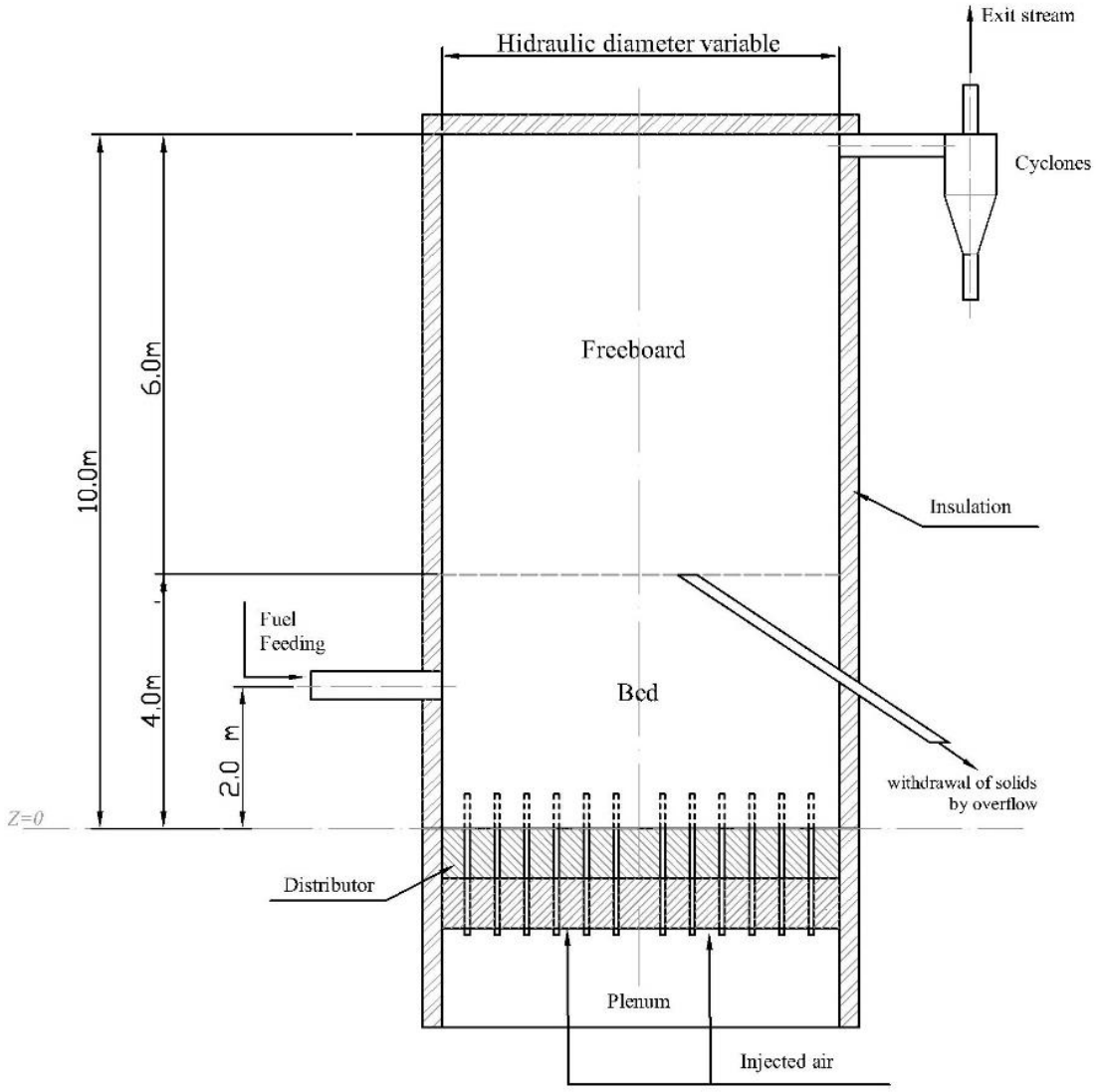

Figure 4.2.1-1 Gasifier geometry (simplified scheme)

The height of the equipment is above the TDH, which guarantees minimal amount of solid particles carried with the gas stream to cyclones.

The equipment does not apply recycling of particles collected by cyclones.

4.2.1.1. Gasifier diameter

Departing from a previous optimization of a gasifier operating at 2.0 MPa (DE SOUZA-SANTOS; CERIBELI, 2013b), its internal hydraulic diameter has been set as a function of the operational pressure. If the air injected into the gasifier could be maintained at the same

temperature, such would allow similar gas superficial velocities at the basis of the bed equipment.

According to that, using the equation of continuity, the following relation maintains the gas flow as a function of the cross area.

$$P_1 A_1 = P_2 A_2 \tag{4.5}$$

where P is the operational pressure and A is the cross sectional area. Thus:

$$P_1 {D_1}^2 = P_2 {D_2}^2 \tag{4.6}$$

Based on that relation, the obtained diameters in function of the operational pressure of the gasifier are listed below.

Table 4.2.1.1-1Hydraulic diameter in function of the operational pressure

$\boldsymbol{P_2}$ $[Mpa]$	0.5	1.0	1.5	2.0	2.5	3.0	3.5	4.0	4.5	5.0
$\boldsymbol{D_2}$ $[m]$	7.7	5.7	4.7	4.1	3.7	3.4	3.1	2.9	2.8	2.6

4.2.2. Gasifier distributor

The injected air to promote fluidization conditions and oxidant passes throughout the distributor. Such device allows uniform distribution of the gas. As said before, the distributor is a plate with perforated tubes or flutes as shown in the scheme below.

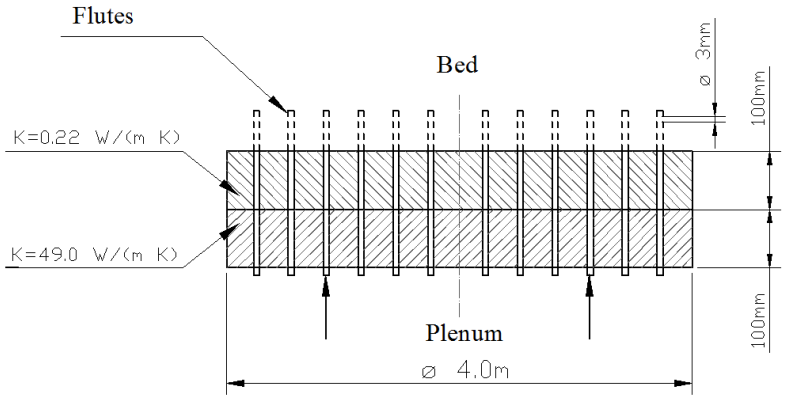

Figure 4.2.2-1 Distributor geometry (simplified scheme)

The complete characteristics of the distributor are listed below:

- Flute internal diameter: $12.7mm$

- Flute external diameter: $13.2mm$
- Number of orifices of each flute: 10
- Orifices diameter: $3\ mm$
- Thermal insulation thickness: $100\ mm$
- Thermal insulation conductivity: 0.22 W/(m K)
- Carbon steel plate: 100 mm
- Steel conductivity: 49 W/(m K)

The number of flutes varies because the available cross-area of the distributor depends on the hydraulic diameter of the equipment. The values are presented below:

Table 4.2.2-1 Number of flutes in the distributor in function of the hydraulic diameter

D2 [m]	7.7	5.7	4.7	4.1	3.7	3.4	3.1	2.9	2.8	2.6
Flutes	183 333	100 000	68 750	52 381	42 308	35 484	30 556	26 829	23 913	21 569

4.2.3. Gasifier shell and insulation

Two insulating materials and one steel shell composes the reactor wall, as shown in Figure 4.2.3-1. Their properties are thermal insulation and mechanical resistance to the stress generated by the operational pressure, even at the maximum values of such variable. Again, CeSFaMB© computes the minimum required steel thickness for each situation. The value described below is just an example and the thickness includes safety factors. However, variations on that thickness would not significantly affect the simulation results for the gasifier operational parameters. The simulator also verifies if the temperatures on the metal surfaces are within the range that maintain its mechanical integrity.

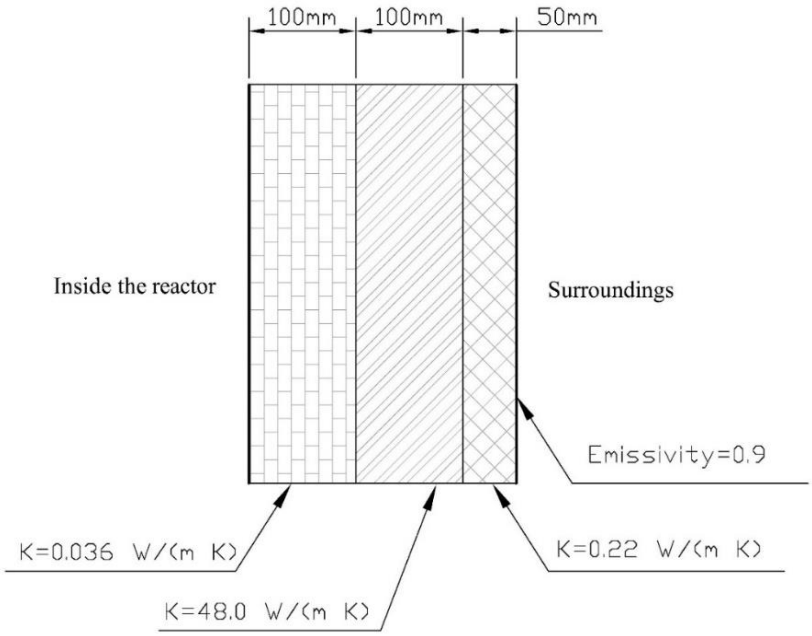

Figure 4.2.3-1 Gasifier (bed and freeboard) insulation (simplified scheme)

There is no double wall or jacket in the gasifier.

4.2.4. Injected fuel into the gasifier

After drying, the MSW is fed into the gasifier using simple rotary valves and Archimedes screws. The adopted characteristics of the injected fuel for the simulations using CeSFaMB© are listed below.

The dryer operates 0.1 MPa above the operational pressure of the gasifier in order to guarantee the fuel feeding and no gas returning to the interior of the gasifier. The mass flow of injected fuel is based on the flow coming from the dryer.

Table 4.2.4-1 Main characteristics of the fuel injected into the gasifier
(DE SOUZA-SANTOS; CERIBELI, 2013b; DE SOUZA-SANTOS; CHAVEZ, 2012)

Fuel characteristics	Value	
Mass flow rate	18	kg/s
Feeding temperature	290	K
Global or bulk density*	100	kg/m^3
Particle apparent density**	360	kg/m^3
Real or skeletal density ***	1394	kg/m^3
Sphericity****	0.3	
Shape	Cylinder/Needle	
proximate analysis (wet basis)		
moisture	0.00	%
volatile	83.19	%
fixed carbon	9.51	%
ash	7.30	%
ultimate analysis (dry basis)		
C	53.00	%
H	7.32	%
N	1.32	%
O	30.96	%
S	0.1	%
ash	7.3	%
particle size distribution		
sieve opening (mm)	retained mass	%
10	1	%
5	2	%
3	3	%
2	91	%
1	2	%
0.5	1	%

* see Equation 4.3 , ** see Equation 4.1, *** see Equation 4.3, **** see Equation 4.4

4.3 Turbines, pumps, and compressors

Thermodynamic balances on the control volumes evaluate the pumps, turbines, and compressor operational conditions.

The following efficiencies are adopted for each equipment assuming isentropic conditions.

- Pumps: $\eta_{pu} = 90\%$ (VERES, 1994)
- Compressors: $\eta_{co} = 87\%$ (GRESH; SASSOS; WASTON, [s.d.])
- Steam turbines: $\eta_{st} = 80\%$ (U.S. ENVIRONMENTAL PROTECTION AGENCY; COMBINED HEAT PARTNERSHIP, 2015)
- Gas turbines: $\eta_{gt} = 87\%$ (GRESH; SASSOS; WASTON, [s.d.])

A temperature of 1700 K is set as the maximum temperature of the injected gas into the gas turbine.

4.3.1. Air compressor

The high operational pressure in the equipment (maximum value of 5.0 MPa), cause considerable stress on the impeller and induce elevated working temperatures. Some investigations (ZHENG et al., 2012) show that the stress caused by the loads is dominant, and the effect of aerodynamic and thermal loads can be ignored even at high operational pressures. Moreover, the proportion of impeller stress caused by aerodynamic and thermal loads ($2\%\ and\ 0.25\%$ respectively) does not increase with the increase of the pressure ratio. Nevertheless, the material properties of the compressor blades may deteriorate at high pressure ratios (ZHENG et al., 2012). Using IPES©, the maximum temperature of the injected air was calculated at around $976\,K$ for 5.0 MPa. According to (BOYCE, [s.d.]) the maximum compressor blade working temperatures are around $950\,K\ (1250\,°F)$ for compressor blades made of martensitic high temperature stainless steel. It should be noticed that the present work tries not to involve intercooling, which would be required when the compressor temperature surpasses the limiting value of 950 K. The calculated temperature is 2.7% above the limit; nevertheless, the present study intends to explore such limits without the application of intercooling.

4.4 Heat exchangers

Thermodynamic balances on the control volume evaluate the heat exchanger performances. The minimum temperature difference of $10\,K$ has been adopted between exchanging heat streams (DE SOUZA-SANTOS; BENINCA, 2014; DE SOUZA-SANTOS; BERNAL; RODRIGUEZ-TORRES, 2015; DE SOUZA-SANTOS; CERIBELI, 2013b; DE SOUZA-SANTOS; DE LIMA, 2015). Temperature differences below that lead to very large surface areas and are not commonly found in commercial units, probably because it would not be cost-effective. The thermal efficiency has been set as $\eta_T = 98\%$. Therefore, the heat loss between the equipment and the surroundings is 2%.

These conditions are commonly found in industrial equipment. The main conclusions of the present work do not change drastically if such conditions were slightly modified.

4.5 Gas cleaning systems

The gas from fluidized-bed combustors and gasifiers contains alkaline species and particles, and is relatively free of tar. Before the injection into the turbines rigorous conditions must be met to protect such equipment, and the tolerances as well recommended values can be found elsewhere (BROWN; BAKER; MUDGE, 1987; COHN, 1985; DE SOUZA-SANTOS, 2010; MEADOWCROFT; STRINGER, 1987). The particulate may cause erosion on the surfaces of the turbine blades, while the corrosion of blades is provoked mainly by the presence of alkaline species. Moreover, such deteriorating processes may combine synergistically leading to a threefold increase in the rate of material loss from the turbine blades (MEADOWCROFT; STRINGER, 1987). The cleaning systems are described below:

- Cyclones: remove the particulates from the gas stream through vortex separation. The efficiency depends on the cyclone geometry and size of the removed particles. The drying and gasification systems have 20 cyclones with the geometry presented in Figure 4.5-1.

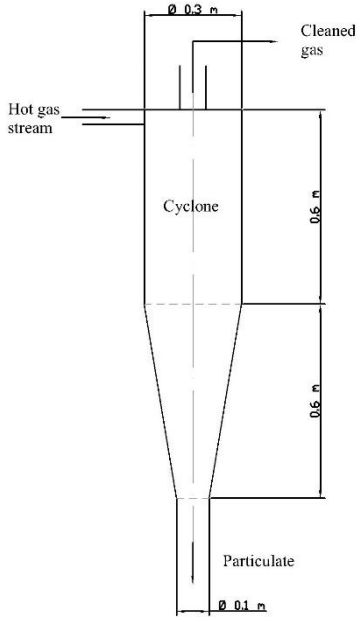

Figure 4.5-1 Cyclone basic geometry

- Filters: Depending on the sizes of particles retained by the cyclones, these accessories are selected to guarantee the permissible level of particulate material in the gases.
- Alkaline condensers: when the temperature decrease until values between $920\ to\ 800\ K$, the dew points of the alkaline species are achieved. The present work set a temperature of $800\ K$ to guarantee such a condition. The removed material is deposited in the internal surfaces of the equipment. Equipment 11 represents this equipment in Figure 2.5-3. It takes the Stream 16 and uses the heat exchanged to drive the steam Rankine cycle (Equipment 11 to 15).

4.6 Thermodynamic power generation processes configuration

As mentioned before (section 2.5), Configuration C for the FSIG/GT Figure 2.5-3 process has been used in the present study.

4.6.1. Steam Rankine Cycles

The need to reduce the temperature of the fuel gases obtained from the gasifier to condense the alkaline implies on losses to the generation system efficiencies. The configuration adopted uses the energy alkaline condensations to drive a steam power generation cycle is shown in Figure 4.6.1-1.

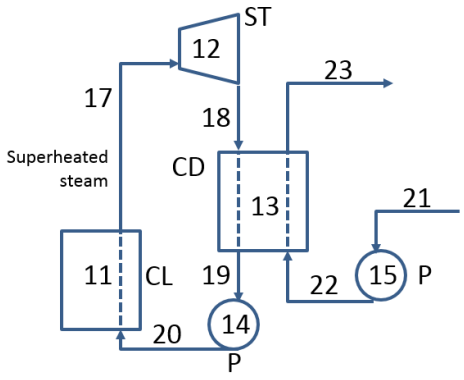

Figure 4.6.1-1 Steam Rankine cycle Equipment 11 to 15

(CD=condenser, CL=cleaning system, P=water pump, ST=steam turbine)

Superheated steam (Stream 17) leaves the Equipment 11. Then, it is expanded through the steam turbine (Equipment 12). The turbine exit is condensed in heat exchanger 13 using cooling water Stream 22.

Figure 4.6.1-2 shows the second Steam Rankine Cycle that is based on the same principles of the process described above. The main difference between both cycles is that this second one is driven by the flue-gas of the gas turbine at Equipment 4. Therefore, the operational conditions of both cycles are different.

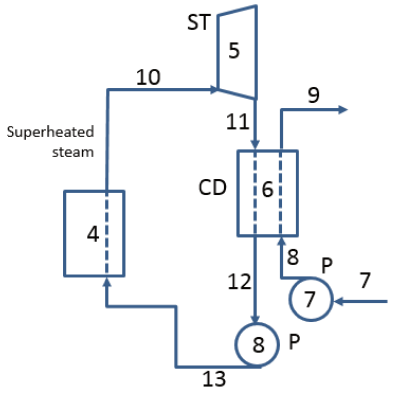

Figure 4.6.1-2 Steam Rankine cycle Equipment 4 to 8
(CD=condenser, CL=cleaning system, P=water pump, ST=steam turbine)

5 METHODOLOGY

The present work demands extensive simulations and optimizations of the gasification and drying processes, as well the projected thermodynamic system. The main objective function was to maximize the overall process efficiency according to the 1st Law of Thermodynamics.

The process design started establishing the overall geometry and configuration of the system, including all components or subsystems and how they interact. Physical parameters and initial values of the variables were established based on the information given in the literature and previous works (BERNAL, 2014; DE SOUZA-SANTOS; BENINCA, 2014; DE SOUZA-SANTOS; BERNAL; RODRIGUEZ-TORRES, 2015; DE SOUZA-SANTOS; CERIBELI, 2013b; DE SOUZA-SANTOS, 2010).

The adopted optimization objective function depends on the studied equipment or process as described in the sections below. The present gasifier optimization seeks to maximize the exergetic and cold efficiencies. The objective for the dryer optimization was to minimize the

mass flow of injected gas and the exergy carried by the exiting gas. The entire power generation process analysis seeks to maximize the efficiency under the 1st Law of Thermodynamics.

Figure 5-1 shows the steps that have been followed in the optimization strategy, such as:

1. Gasification optimization (CeSFaMB©).
2. 1st FSIG/GT process optimization. Using the results of step 1 and seek the highest 1st Law efficiency for the whole process (IPES©).
3. Dryer optimization (CeSFaMB©).
4. 2nd process optimization. Repeat step 2 using the results from step 3.
5. Verification if streams conditions are feasible for operation of real equipment. If not return to step 1.
6. End when all conditions have been satisfied.

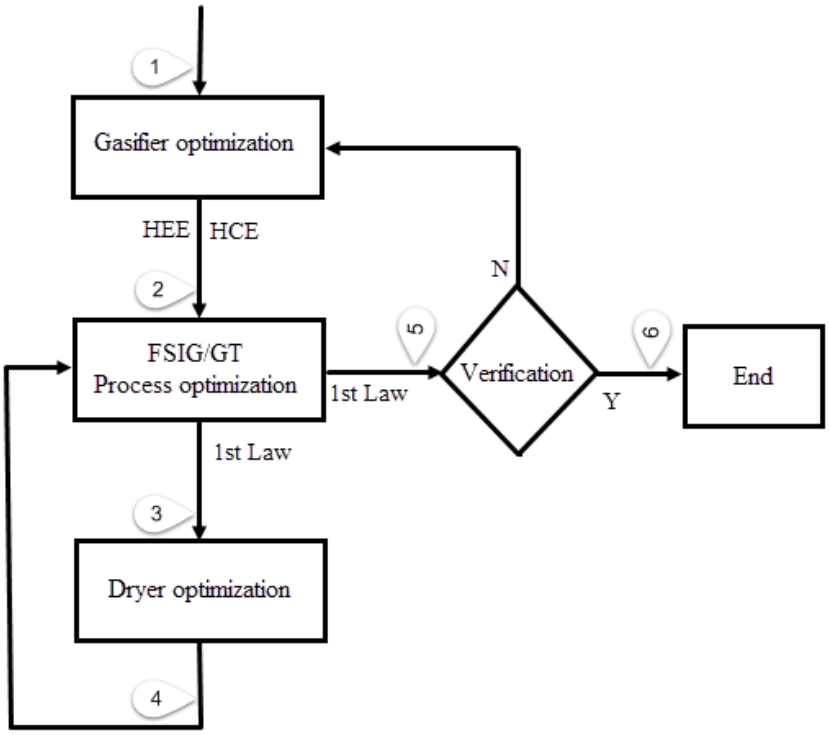

Figure 5-1 Steps of the adopted optimization strategy

The details of optimizations and respective objective functions are described in sections 5.1 , 5.2 and 5.3 ahead.

It is important to clarify that the best operational conditions for one component of the cycle may not lead to the highest efficiency for the entire power generation process. Moreover, in

some cases such operational conditions lead to system operations outside the possible for real equipment. That is why an iterative strategy is adopted.

5.1 Gasifier optimization

CeSFaMB© was applied for the gasifier optimization. It seeks to maximize two objective functions: Exergy Efficiency (HEE) and Cold Efficiency (HCE). Of course, each optimization function might lead to different gasification operations. If those optimizations lead to different results, the present work verifies the effect of each optimization on the overall power generation process.

The software verifies if the fluidization conditions of the bubbling fluidized bed gasifier (BFBG) are within the appropriate range of operation. Such parameters can be found elsewhere (DE SOUZA-SANTOS, 2010). CeSFaMB© also check if the superficial velocities are above the minimum fluidization one and below the second turbulent limit at each position in the bed. The software also verifies conditions that might lead to temperatures above the ash-melting for the carbonaceous particles that would lead to agglomeration and further bed collapsing. Additionally, CeSFaMB© computes the total carbon conversion, the composition and temperature of produced gas, the temperature and composition of all phases as well the rates of homogeneous and heterogeneous reaction rates throughout the equipment, and verifies if the complete devolatilization and tar destruction inside the bed is accomplished (DE SOUZA-SANTOS, 2010)(DE SOUZA-SANTOS; CERIBELI, 2013a)(DE SOUZA-SANTOS; BERNAL; RODRIGUEZ-TORRES, 2015). Such parameters among the others were analyzed to estimate the proper operation of the equipment and process. Some of those limitations are described in section 6.1 .

The simulation variables can be classified in two categories: independent and dependent. Among the independent variables there are the ***operational pressure*** and the ***mass flow of injected air***. In the present work, the dependent variables are the temperature of injected air and the gasifier diameter. Both depend on the ***operational pressure***.

- ***Operational pressure*** was covered the range between $0.5 - 5.0\ MPa$ with $0.5\ MPa$ steps. The maximum adopted value $(5.0 MPa)$ regarding the state of art in the field of the materials of the air compressors blades (BOYCE, [s.d.]).

- ***Mass flow of injected air*** covering the range between $10\ and\ 18kg/s$ with 1 kg/s steps. Previous works (BERNAL, 2014; DE SOUZA-SANTOS; BERNAL; RODRIGUEZ-TORRES, 2015; DE SOUZA-SANTOS; CERIBELI, 2013b) have been simulating similar configurations of the process. The initial values of present work are based on those studies. The pressurized airflow allows the fluidization of the particulate and provide the oxidant agent for the exothermic reactions. Moreover, it plays an important role in the transport phenomena (heat transfer, mass, and momentum).

- *Temperature of injected air*. In order to overcome the pressure losses in the reactor, the injected air must be pressurized $100kPa$ above the gasifier operational pressure. According to that, the air temperature increases as well. The respective values of such temperatures (Stream 24-Figure 2.5-3) were calculated using IPES© and are presented in Table 5.1-1

Table 5.1-1 Temperature of the injected air as a function of the injected air pressure

$\boldsymbol{P_{air}}$ $[Mpa]$	0,6	1,1	1,6	2,1	2,6	3,1	3,6	4,1	4,6	5,1
$\boldsymbol{T_{air}}$ $[K]$	515	622	697	756	805	847	891	917	948	976

- *Gasifier diameter* is here computed as a function of the operational pressure of the gasifier (Section 4.2.1.1). The table below shows the values against the operational pressure.

Table 5.1-2 Gasifier diameter in function of the operational pressure

$\boldsymbol{P_{operational}}$ $[Mpa]$	0,5	1,0	1,5	2,0	2,5	3,0	3,5	4,0	4,5	5,0
$\boldsymbol{D_{gasifier}}$ $[m]$	7,7	5,7	4,7	4,1	3,7	3,4	3,1	2,9	2,8	2,6

It should be stressed that the superficial gas velocity at the bed basis also varies with the mass flow of injected gas and it is temperature. The above values for bed diameter were taken if those were kept constant, which is not the case. Therefore, the present work is just a first study on the influence of pressures on the gasifier efficiency as well overall power generation efficiency.

It is also important to clarify that the variation of the gasifier diameter implies the variation of the distributor dimensions as well. Therefore, the number of flutes of the distributor was adjusted in function of the gasifier/distributor diameter Section 4.2.2.

5.1.1. Exergy Analysis

The exergy analysis is a method that combines the 2nd Law of Thermodynamics with the principles of energy and mass conservation. Such method enables the location, type, and magnitudes of the losses (irreversibilities), with the aim of obtaining the most efficient resource use (MORAN; SHAPIRO, 2006). This information may be used in the optimization of the thermal system reducing the sources of inefficiency.

Exergy (sometimes-called availability) is the potential energy of a system expressed as the maximum theoretical work that could be done by a system until the equilibrium with the environment is achieved. Among the possibilities, irreversibilities may be caused by heat transfer with the surroundings, lost work, physical and chemical losses, and thermodynamic phenomena in the gasification process.

Real processes are irreversible. Therefore, it is possible to evaluate the efficiency of the energy source use by comparisons to know how well the fuel is consumed (DE SOUZA-SANTOS, 2010). As the leaving gases (fuel gas) will be used in the power generation process, the exergetic efficiency of the gasification system is given by

$$\eta_{exe} = \frac{exergy\ of\ exiting\ gas\ (flue\ gas)}{total\ exergy\ of\ streams\ \ enter\ the\ gasifier\ (gaseous\ or\ solids)} \tag{5.1}$$

where the exergy of each stream is represented by the product between the mass flow and the specific exergy. The streams that enter the gasifier are the dried MSW and the injected pressurized air. The exergy of the exiting gas represents the useful mechanical power output because it will drive the power generation processes.

From now on, the conditions that provide the gasifier highest exergetic efficiency will be called HEE.

5.1.2. Cold efficiency analysis

Despite the exergy analysis being very useful, the cold efficiency seems to be more appropriated as the objective function for the gasification process because the fuel gas requires cooling in order to condensate alkaline before the injection into the gas turbine incinerator (DE SOUZA-SANTOS; BERNAL; RODRIGUEZ-TORRES, 2015).

The cold efficiency is given by

$$\eta_{cold} = \frac{enthalpy\ of\ exiting\ gas\ \ at\ 298K}{total\ enthalpy\ of\ streams\ \ entering\ the\ gasifier\ (gaseous\ and\ solids)} \quad (5.2)$$

where the enthalpy of each stream is represented by the product between the mass flow and the specific enthalpy, which includes its combustion enthalpy. The fuel gas combustion enthalpy is computed at $298\ K$ (LHV) a dry and tar-free gas.

From now on, the conditions that led to the highest cold efficiency will be called HCE.

5.2 Dryer optimization

The optimization of the drying process was undertaken using CeSFaMB© (Section 3.1) as a computational tool for the simulation the equipment in each of the assumed cases. The objective was to reach the convergence of the following operational conditions:

- The process must be conducted until almost complete drying of the injected slurry in the dryer. In other words, the original and the added moisture must be vaporized.
- The process must require the minimum mass flow of hot injected gas. Thus, in order to improve the global efficiency of the overall generation process because of the power consumed by the compressor (Equipment 10–Figure 2.5-3) varies in function of the mass flow.
- The operational pressure of the dryer must be at slightly higher pressure than the gasifier operational pressure, to ensure that the dried solid fuel will be fed into the gasifier using simple rotary valves and Archimedes screws. According to that, the dryer operates $100\ kPa$ above the gasifier operation.
- The freeboard effluent gases must carry the minimum exergy, in order to minimize the chemical reaction rates of the fuel inside the dryer.

5.3 Power generation process optimization

The simulation of the overall power generation process was possible using IPES© (Section 3.2). The software generates a matrix with the temperatures, pressures, and composition of each stream (Figure 2.5-3) and solves the system of equations (mass, heat and momentum balances). That allows determining the various properties of each stream as well overall parameters including among the others, the exergetic and cold efficiencies.

The capacities of each individual component of the whole system were analyzed and each equipment of the process was characterized depending on their specific working conditions and assumptions (Chapter 4) in order to reach the best performance of the entire power generation process.

As said before the overall power generation process was divided into subsystems. First, extensive simulations of the gasifier were made using CeSFaMB© to find its operational conditions and geometries leading to the best efficiencies (HEE and HCE). Important properties of the exiting gas stream (Stream 16-Figure 2.5-3 were obtained, such as composition, temperature, and pressure for each alternative HEE and HCE). The obtained data are taken as inputs for the simulation of the overall power generation process using IPES©. The simulations aimed the maximization of the overall power generation efficiency using either the HCE and HEE gasifier operational conditions. Additionally, some streams of the steam cycles were adjusted to comply with good operational practices. For instance, the temperature of the released water at Stream 23 and Stream 9-Figure 2.5-3 must be above $40°C$. It was also ensured that the temperature of the Stream 4-Figure 2.5-3 was not above $1700\ K$, which has been taken as the limit for injections into gas turbines.

The entire process of optimization aims the maximization of its $1^{st}\ law\ efficiency$. Variations of water flow rates through both steam Rankine cycles were tested. Multiple tests were performed using the gas from the hee and hce gasification operations. Then, the drying process was optimized and the whole process was simulated and adjusted again.

6 RESULTS AND DISCUSSION

This chapter presents the data obtained from the simulation, analysis and optimization of the FSIG/GT alternative for power generation process consuming MSW.

The chapter is divided into 6 sections. Section 6.1 present the simulation and optimization of the BFB gasifier based in two objective functions: Highest Exergy Efficiency (HEE) and Highest Cold Efficiency (HCE). The section 6.2 presents the simulation and optimization of the entire power generation process FSIG/GT applied to the HEE and HCE operational conditions achieved at section 6.1. At this point, limitations on the temperature of gas exiting axial compressors were found. In view of that, new rounds of simulations and optimizations were performed and are presented in section 6.3. The most important operational parameters and fluidization conditions of the selected gasifier are presented in section 6.4. Section 6.5 describes the dryer operational conditions, after the optimization aimed to minimize the mass flow of the injected gas into that equipment. Finally, section 6.6 presents the characteristic of each stream involved in the power generation process and the thermodynamic analysis for the gas and the steam cycles.

6.1 BFB Gasifier optimization

The CeSFaMB© software was applied for the gasifier optimization. The optimization seeks to maximize two objective functions: Exergy Efficiency (HEE) and Cold Efficiency (HCE) having the operational pressure, the mass flow and temperature of the injected air, and the hydraulic diameter of the gasifier as variables. Detailed information about those variables was presented in section 5.1.

Many variations on the operational pressure and mass flow of injected air have been tried as shown in Table 6.1-1 and Table 6.1-2.

One should have in mind that the operational pressure is somewhat linked with the gasifier diameter as well with the temperature of the injected air. Viable bubbling bed operations are only possible for values of air mass flow rates between the ranges presented here. Values leading to very low gasification efficiency or outside the feasible operational ranges are not presented in Figure 6.1-1 and Figure 6.1-2, but are presented in Table 6.1-1 and Table 6.1-2. Unfeasible conditions occur when one or various of the following situations take place:

- Conditions that would result in operations outside the range of bubbling fluidization such as superficial velocities below the minimum fluidization one at any point of the bed or velocities above the 2nd turbulent limit.
- Temperature beyond the ash-melting limit, which would lead to particle agglomerations followed by bed collapsing.

- Segregation of one solid particulate species from the average in the bed. If the fluidization is not vigorous enough, lighter particles tend to float or concentrate near the bed surface. This would prevent the fuel particles to be well-mixed and maintain a good contact with the gases involved in heterogeneous reactions. In addition, those fuel particles near the top of the bed would go through pyrolysis and the released tar may pass through the freeboard and leave the equipment with the produced gas stream. That would cause serious problems to the gas cleaning process. Moreover, the tar would not be cracked or cooked inside the bed, thus not contributing for the production of valuable fuel gases. The recent CeSFaMB© versions include the computations that verify if segregation is taking place and prints a warning.
- Impossibility of achieving steady-state operation. For instance, in many bubbling operation, the bed height is usually kept constant by continuous or batch withdrawals of solid particles using overflow pipes. However, at given the rates of fuel feeding and conversion, if the rate of particle elutriation is too high the bed height might drop below the position where the top of the overflow pipe is situated. Therefore, the bed height cannot be maintained constant.

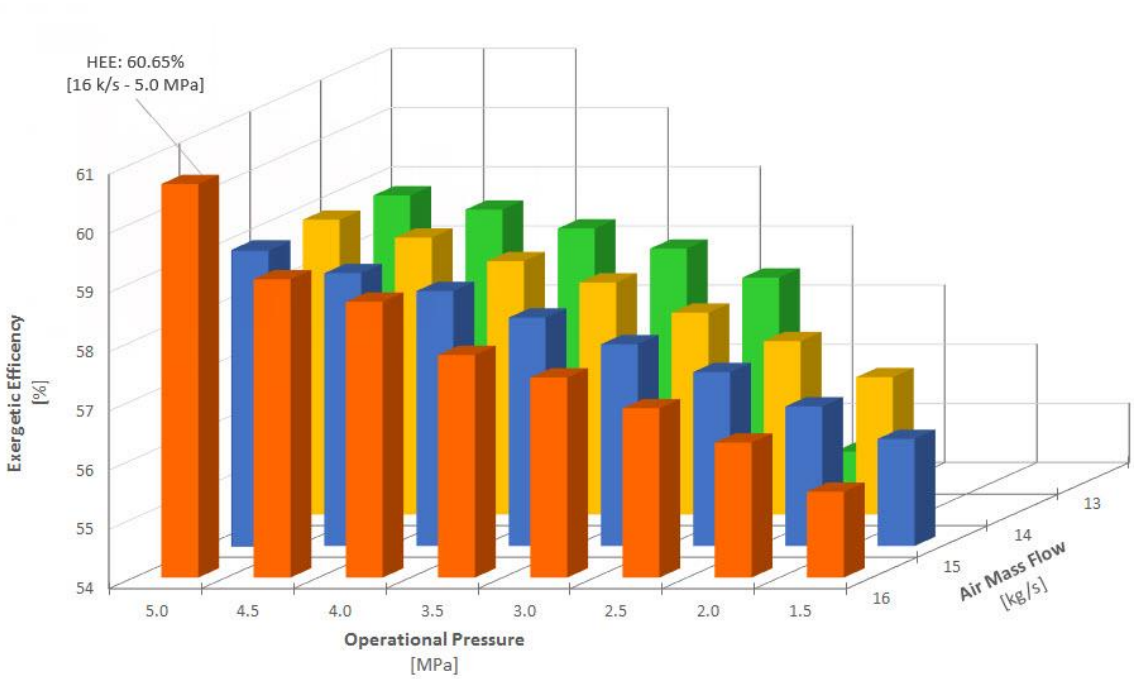

Figure 6.1-1 Exergetic efficiencies for gasification processes

Table 6.1-1 Exergetic efficiencies for the gasification process for different combinations of operational pressure and mass flow of injected air

		OPERATIONAL PRESSURE [MPa]									
		0.5	**1**	**1.5**	**2**	**2.5**	**3**	**3.5**	**4**	**4.5**	**5**
MASS FLOW OF INJECTED AIR [kg/s]	**10**	-	-	-	-	-	-	-	-	-	-
	12	-	-	-	-	-	-	-	-	-	-
	13	-	-	-	-	54.53	57.47	57.96	58.3	58.62	58.86
	14	-	-	-	56.32	56.93	57.41	57.92	58.28	58.68	58.98
	15	-	-	55.81	56.36	56.94	57.41	57.86	58.31	58.61	59
	16	-	-	55.45	56.28	56.86	57.38	57.76	58.66	59.04	60.65
	18	-	-	-	-	-	-	-	-	-	-
		EXERGETIC EFFICIENCY [%]									

Figure 6.1-1 and Figure 6.1-2 illustrate the gasifier efficiencies having the operational pressure and the mass flow of injected air as variables. The obtained data are presented in Table 6.1-1 and Table 6.1-2 as well.

Here, the covered range of air flow was between 13 and 16 kg/s, while the range of pressure stayed between 1.5 and 5.0 MPa. As said before (Section 4.2.1.1) the bed internal diameter varies as well between 4.6 and 2.6 m.

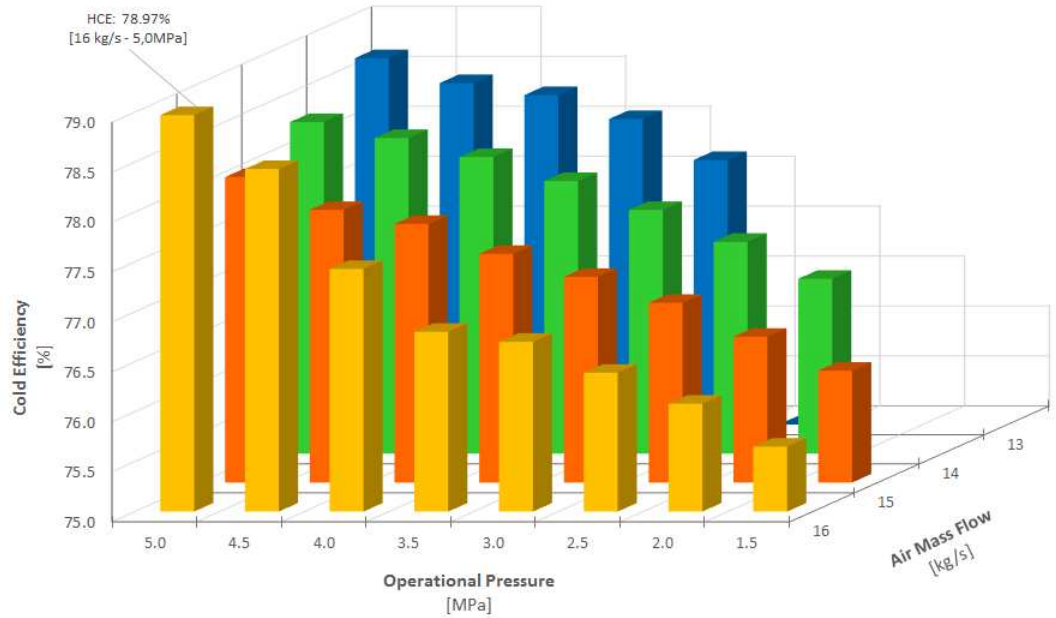

Figure 6.1-2 Cold efficiencies for the gasification processes

Table 6.1-2 Cold efficiencies for the gasification process for different combinations of operational pressure and mass flow of injected air

		OPERATIONAL PRESSURE [MPa]									
		0.5	**1**	**1.5**	**2**	**2.5**	**3**	**3.5**	**4**	**4.5**	**5**
MASS FLOW OF INJECTED AIR [kg/s]	**10**	-	-	-	-	-	-	-	-	-	-
	12	-	-	-	-	-	-	-	-	-	-
	13	-	-	-	-	0.01	77.65	78.06	78.3	78.42	78.67
	14	-	-	-	76.75	77.12	77.44	77.73	77.97	78.16	78.32
	15	-	-	76.12	76.46	76.8	77.06	77.29	77.59	77.73	78.06
	16	-	-	75.65	76.08	76.39	76.7	76.8	77.43	78.43	78.97
	18	-	-	-	-	-	-	-	-	-	-
		COLD EFFICIENCY [%]									

As seen, higher efficiencies are achieved for higher operational pressures. Those have also led to higher temperatures inside the reactor, which, in turn, promote fast devolatilization, gasification, and combustion reactions. Both efficiencies (HEE and HCE) occur at 5.0 MPa and for airflow injection rate around 16 kg/s. The relatively high hydrogen content of the MSW provides all the water for the gasification reactions, thus dispensing the use of steam injection (DE SOUZA-SANTOS; BERNAL; RODRIGUEZ-TORRES, 2015; DE SOUZA-SANTOS; CERIBELI, 2013b).

More refined optimizations grids might be applied in coming works, but such should not significantly change the results and conclusions obtained at the present work.

The main gasifier geometric characteristics as well as the most important input and output parameters of operating condition are summarized in Table 6.1-3 and Table 6.1-4 below.

Table 6.1-3 Gasifier main inputs and operational conditions operating under HEE and HCE conditions

Main input condition or parameters	Value
Bed internal diameter [m]	2.6
Bed height [m]	4.0
Freeboard internal diameter [m]	2.6
Freeboard height	6.0
Insulation thickness around the bed and freeboard [mm]	100
Number of flutes in the distributor	2.1×10^4
Number of orifices per flute	10
Diameter of orifices [mm]	3.0
Fuel feeding position (above the distributor) [m]	2.0
Mass flow of feeding fuel (dry) [kg/s]	18.0
Mass flow of injected air [kg/s]	16
Temperature of injected air [K]	976
Mass flow of injected steam [kg/s]	0.0
Average pressure inside the equipment [MPa]	5.0

Table 6.1-4 Gasifier main parameters and operational conditions operating under HEE and HCE conditions

Main output condition or parameters	Value
Mass flow of gas leaving the equipment [kg/s]	33.04
Fluidization voidage (bed middle)	0.80
Minimum fluidization velocity (bed middle) [m/s]	0.01
Transport velocity (bed middle) [m/s]	0.58
Fluidization superficial velocity (bed middle) [m/s]	0.19
Carbon conversion [%]	85.64
Average carbonaceous particle diameter in the bed [mm]	0.52
Average temperature at the middle of the bed [K]	1034.50
Average temperature at the top of the freeboard [K]	1045.51
Pressure loss at the distributor [kPa]	0.01
Pressure loss in the bed [kPa]	14.38
TDH – transport disengaging height [m]	4.93
Rate of energy input by fuel to the equipment [MW]	379.27
Total rate of energy input to the equipment [MW]	390.94
Rate of energy output by the hot gas[a] [MW]	346.79
Rate of energy output by the cold gas[b] [MW]	308.71
Combustion enthalpy of cold gas [MJ/kg]	9.68
Hot efficiency [%]	88.70
Cold efficiency [%]	78.97
Exergy flow brought with the dry fuel [MW]	566.80
Exergy flow brought with the injected gas [MW]	11.54
Total entering exergy flow[c] [MW]	578.30
Exergy flow leaving with the gas [MW]	347.42
Total exiting exergy[d] [MW]	350.70
Ratio between total leaving and entering exergy flows [%]	60.65
Ratio between the exergy leaving with produced gas and the total entering exergy [%]	60.08

[a] "Hot gas" refers to the temperature, pressure, and composition as found at the exiting point from the gasifier. [b] "Cold gas" refers to the gas properties if at 298 K, 101.325 kPa, dry and tar free. [c] Sum of exergies brought by gases, liquids, or solids injected or fed into the gasifier. [d] Sum of exergies carried by gases, liquids, or solids leaving the gasifier.

It is important to notice that the value for TDH is 4.925 m, which is well below the position of 10 m set for the main gas withdrawal.

Table 6.1-5 shows the produced gas composition obtained at that operation. The concentration of H_2 is relatively high for operations using just air as gasifying agent. Once again, this shows that steam is not needed as gasifying agent because the amount of hydrogen in the average MSW composition is more than enough to provide all the water needed for the main gasification reactions involving such a chemical species as found in previous publication (DE SOUZA-SANTOS; CERIBELI, 2013b).

Table 6.1-5 Composition of the Gas leaving the gasifier under operation at HEE and HCE

Chemical species	Mass percentage	Molar percentage	Chemical species	Mass percentage	Molar percentage
H2	1.4483	16.6251	CO	32.9820	27.2496
H2O	3.4765	4.4658	CO2	15.6386	8.2232
H2S	0.0480	0.0326	HCN	0.0638	0.0546
NH3	0.7363	1.0005	CH4	7.7851	11.2299
NO	0.0000	0.0000	C2H4	0.1940	0.1601
NO2	0.0000	0.0000	C2H6	0.1617	0.1244
N2	37.2343	30.7595	C3H6	0.0108	0.0059
N2O	0.0000	0.0000	C3H8	0.0108	0.0057
O2	0.0000	0.0000	C6H6	0.1940	0.0575
SO2	0.0157	0.0057	Tar	0.0000	0.0000

The obtained results are part of the input data for the FSIG/GT simulation and optimization using IPES. Such input data include the mass flow, temperature, and pressure of the exiting gas stream (Table 6.1-4 and Table 6.1-5).

6.2 FSIG/GT simulation and optimization under HEE and HCE gasifier operation

The selected configuration and parameters applied for the simulation of the entire power generation process is presented below. The simulations were carried using IPES© and allows finding and selecting the best operational conditions involving the subsystems. Those would permit to find the conditions that provide the best efficiency for the power generation process.

Figure 6.2-1 shows the adopted control volume for the analysis of the power generation process.

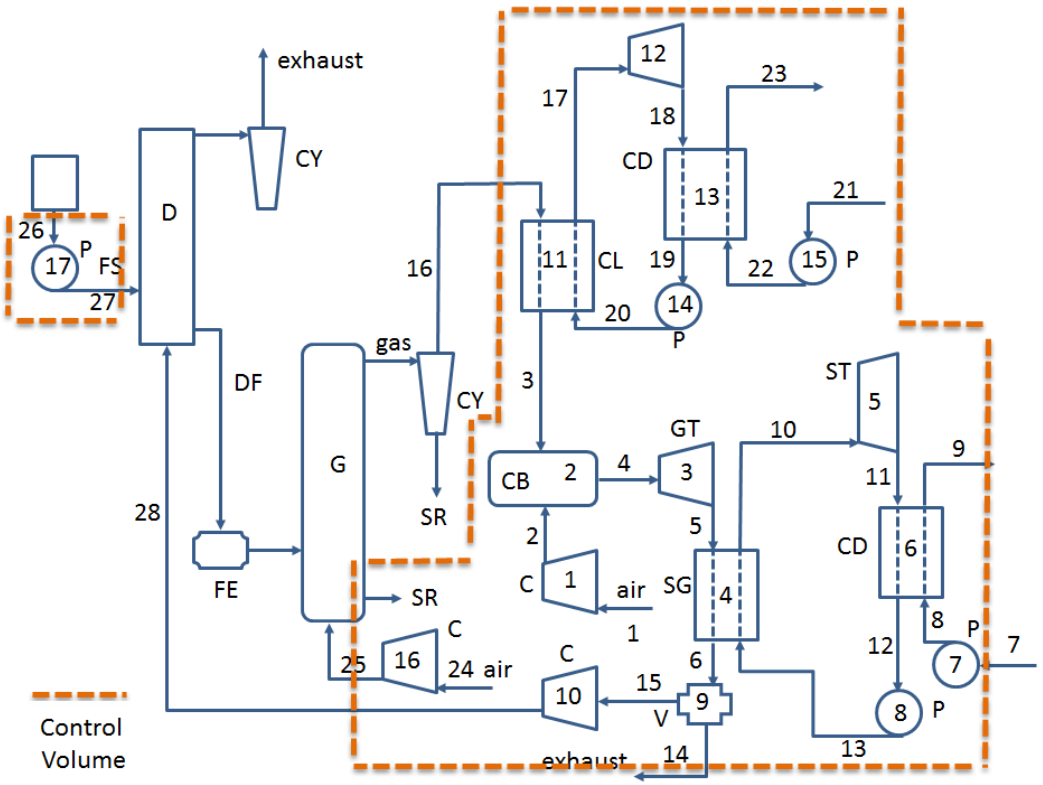

Figure 6.2-1 Control Volume of the entire power generation process

C = compressor, CB = combustor, CD= condenser, CL = cleaning system, CY = cyclone, D = dryer, DF = dried fuel, FE = screw feeding, FS= fuel-slurry pumping, G = gasifier, GT = gas turbine, SG = steam generator, ST = steam turbine, SR= solid residue, P = water pump, V= valve or splitter

Variations of water flowrates in both steam Rankine cycles were tested with the aim of obtain the maximum overall efficiency. The energy removed from the expanded gas (Stream 5) drives the main Rankine cycle (equipment 4 to 8). The mass flow of water running through the Rankine cycle was optimized in order to use the most of the energy in the flue-gas. The secondary Rankine cycle, composed by Equipment 11 to 14, is driven by the heat exchange required to cool stream 16 until the alkaline dew point at 800 K.

Table 6.2-1 presents the temperatures, pressures and mass flows of each stream of the power generation process operating at the best performance through the simulations.

Table 6.2-1 Description of conditions at each Stream of the FSIG/GT power generation process under HEE and HCE gasifier operation

Stream	Fluid nature	Temp. [K]	Pressure [kPa]	Mass Flow [kg/s]	Stream	Fluid nature	Temp. [K]	Pressure [kPa]	Mass Flow [kg/s]
1	Air	298.0	101.3	300.0	**15**	Gas	492.0	108.0	60.0
2	Air	992.7	5000.0	300.0	**16**	Gas[c]	1045.5	5010.0	33.0
3	Gas[a]	800.0	5000.0	33.0	**17**	Steam	1030.9	10000.0	3.9
4	Gas	1694.5	4990.0	333.0	**18**	Steam	573.3	475.8	3.9
5	Gas	835.3	120.0	333.0	**19**	Water	422.0	465.8	3.9
6	Gas	492.1	110.0	333.0	**20**	Water	422.1	10010.0	3.9
7	Water[b]	298.0	110.0	1200.0	**21**	Water	298.0	110.0	150.0
8	Water	298.0	130.0	1200.0	**22**	Water	298.0	130.0	150.0
9	Water	315.3	110.0	1200.0	**23**	Water	313.2	110.0	150.0
10	Steam	825.0	10000.0	40.0	**24**	Air	298.0	110.0	16.0
11	Steam	325.9	123.0	40.0	**25**	Air	975.6	5100.0	16.0
12	Water	370.0	120.0	40.0	**26**	Slurry	298.0	110.0	40.6
13	Water	370.1	10100.0	40.0	**27**	Slurry	298.0	5100.0	40.6
14	Gas	492.0	108.0	273.0	**28**	Gas	1464.8	5200.0	60.0

[a]After cleaning set alkaline concentration within acceptable levels. [b]Water= liquid water. [c]After cleaning to set particle size and content within acceptable levels.

However, the above results should be analyzed to verify their feasibility.

As said before, part of Stream 15 must be pressurized to allow it to be injected into the pressurized dryer. According to that, the Equipment 10 compresses the gas to 5.2 MPa, achieving a temperature around 1464.8 K. That value surpasses the maximum of 950 K allowed for axial compression exiting streams (BOYCE, [s.d.]). Therefore, this poses an impossibility. Consequently, despite the fact that the higher efficiencies of the gasifier were found operating at 5.0 MPa, it is necessary to find the limiting pressure for the present power generation process operating at the current equipment technologies.

The sections below will present few consideration regarding the viable pressure limits for the process architecture as shown in Figure 6.2-1. On the other hand, at chapter 7 will present few alternatives to improve the architecture of the entire power generation process and allow the system to operate at elevated pressures.

6.3 FSIG/GT optimization seeking the conditions to operate with temperature of Stream 28 below 950 K

Extensive simulations of the entire FSIG/GT process were conducted in order to find the adequate operational conditions that could meet the limiting temperature of 950 K imposed for stream 28 (Figure 2.5-3). To avoid such limitation, an intercooling would be required between the compression of stream 15 to stream 28. However, that is not within the scope of the present study and might be included in future works.

Having that in mind, the simulation included the range between 4.0 MPa and 2.0 MPa. The results are presented at Appendix B and show that the temperature limitation of 950 K is only met for gasifications at 2.0 MPa or below it.

The main geometric characteristics, as well as the most important input parameters of the gasifier operating at 2.0 MPa are summarized below.

Table 6.3-1 Gasifier main inputs and operational conditions operating at 2.0 MPa

Main input condition or parameters	Value
Bed internal diameter [m]	4.1
Bed height [m]	4.0
Freeboard internal diameter [m]	4.1
Freeboard height	6.0
Insulation thickness around the bed and freeboard [mm]	100
Number of flutes in the distributor	5.2×10^4
Number of orifices per flute	10
Diameter of orifices [mm]	3.0
Fuel feeding position (above the distributor) [m]	2.0
Mass flow of feeding fuel (dry) [kg/s]	18.0
Mass flow of injected air [kg/s]	15
Temperature of injected air [K]	756
Mass flow of injected steam [kg/s]	0.0
Average pressure inside the equipment [MPa]	2.0

The mass flow, temperature, composition and pressure of the gas leaving the gasifier operating at 2.0 MPa were obtained using CeSFaMB©. Such information is used as an input data for the optimization of the entire power generation process in IPES and is presented below.

Table 6.3-2 Composition of gas leaving the gasifier under operation at 2.0 MPa

Composition of gas leaving the equipment			
Chemical Species	**Molar percentage**	**Chemical Species**	**Molar percentage**
H2	26.5208	CO	28.7045
H2O	4.1154	CO2	7.0948
H2S	0.0308	HCN	0.0370
NH3	0.9725	CH4	5.0152
NO	0.0000	C2H4	0.1509
NO2	0.0000	C2H6	0.1173
N2	27.1708	C3H6	0.0056
N2O	0.0000	C3H8	0.0053
O2	0.0000	C6H6	0.0542
SO2	0.0050	Tar	0.0000
Output condition or parameter			**Value**
Mass flow of gas leaving the equipment [kg/s]			32.06
Temperature of gas leaving the equipment [K]			961.6

The optimization of the FSIG/GT process using IPES was made and the table below presents some of the obtained results.

Table 6.3-3 Description of conditions of each Stream of the FSIG/GT power generation process under gasifier operation at 2.0 MPa

Stream	Fluid nature	Temp. [K]	Pressure [kPa]	Mass Flow [kg/s]	Stream	Fluid nature	Temp. [K]	Pressure [kPa]	Mass Flow [kg/s]
1	Air	298	101	205	**15**	Gas	389	108	55
2	Air	763	2000	205	**16**	Gas[c]	962	2010	32
3	Gas[a]	800	2000	32	**17**	Steam	943	10000	2.67
4	Gas	1701	1990	237	**18**	Steam	515	475	2.67
5	Gas	1047	120	237	**19**	Water	422	465	2.67
6	Gas	389	110	237	**20**	Water	422	10010	2.67
7	Water[b]	298	110	500	**21**	Water	298	110	100
8	Water	298	130	500	**22**	Water	298	130	100
9	Water	353	110	500	**23**	Water	313	110	100
10	Steam	1037	10000	49	**24**	Air	298	110	15
11	Steam	440	130	49	**25**	Air	766	2200	15
12	Water	376	120	49	**26**	Slurry	298	110	41
13	Water	376	10100	49	**27**	Slurry	298	2200	41
14	Gas	389	108	182	**28**	Gas	941	2200	55

[a]After cleaning set alkaline concentration within acceptable levels. [b]Water= liquid water. [c]After cleaning to set particle size and content within acceptable levels.

As seen above, the value for stream 28 is now below the limiting value of 950 K. More detailed information about the conditions of each stream of the process is presented at Appendix B.

6.4 Gasifier parameters and conditions operating under 2.0 MPa

The main output parameters and conditions of the gasifier operating under 2.0 MPa are summarized in below.

Table 6.4-1 Gasifier main characteristics and parameters operating at 2.0 MPa

Main output condition or parameters	Value
Mass flow of gas leaving the equipment [kg/s]	32.06
Fluidization voidage (bed middle)	0.75
Minimum fluidization velocity (bed middle) [m/s]	0.09
Transport velocity (bed middle) [m/s]	0.32
Fluidization superficial velocity (bed middle) [m/s]	0.14
Carbon conversion [%]	79.51
Average carbonaceous particle diameter in the bed [mm]	0.96
Average temperature at the middle of the bed [K]	967.38
Average temperature at the top of the freeboard [K]	966.65
Pressure loss at the distributor [kPa]	0.01
Pressure loss in the bed [kPa]	29.92
TDH – transport disengaging height [m]	4.32
Rate of energy input by fuel to the equipment [MW]	376.93
Total rate of energy input to the equipment [MW]	384.14
Rate of energy output by the hot gas[a] [MW]	327.49
Rate of energy output by the cold gas[b] [MW]	293.71
Combustion enthalpy of cold gas [MJ/kg]	9.49
Hot efficiency [%]	85.25
Cold efficiency [%]	76.46
Exergy flow brought with the dry fuel [MW]	566.70
Exergy flow brought with the injected gas [MW]	7.22
Total entering exergy flow[c] [MW]	574.00
Exergy flow leaving with the gas [MW]	322.67
Total exiting exergy[d] [MW]	323.50
Ratio between total leaving and entering exergy flows [%]	56.36
Ratio between the exergy leaving with produced gas and the total entering exergy [%]	56.22

[a] "Hot gas" refers to the temperature, pressure, and composition as found at the exiting point from the gasifier. [b] "Cold gas" refers to the gas properties if at 298 K, 101.325 kPa, dry and tar free. [c] Sum of exergies brought by gases, liquids, or solids injected or fed into the gasifier. [d] Sum of exergies carried by gases, liquids, or solids leaving the gasifier.

According to the composition of the gas leaving the equipment (Table 6.3-2) high concentration of H_2 has been achieved, despite the lack of steam injection in the gasifier. This is only possible due to the high concentration of hydrogen in the MSW average composition.

In addition to the information shown above, CeSFaMB© provides the temperature and concentration profiles throughout the bed and freeboard. Such profiles are plotted through a graphical interface and are presented below.

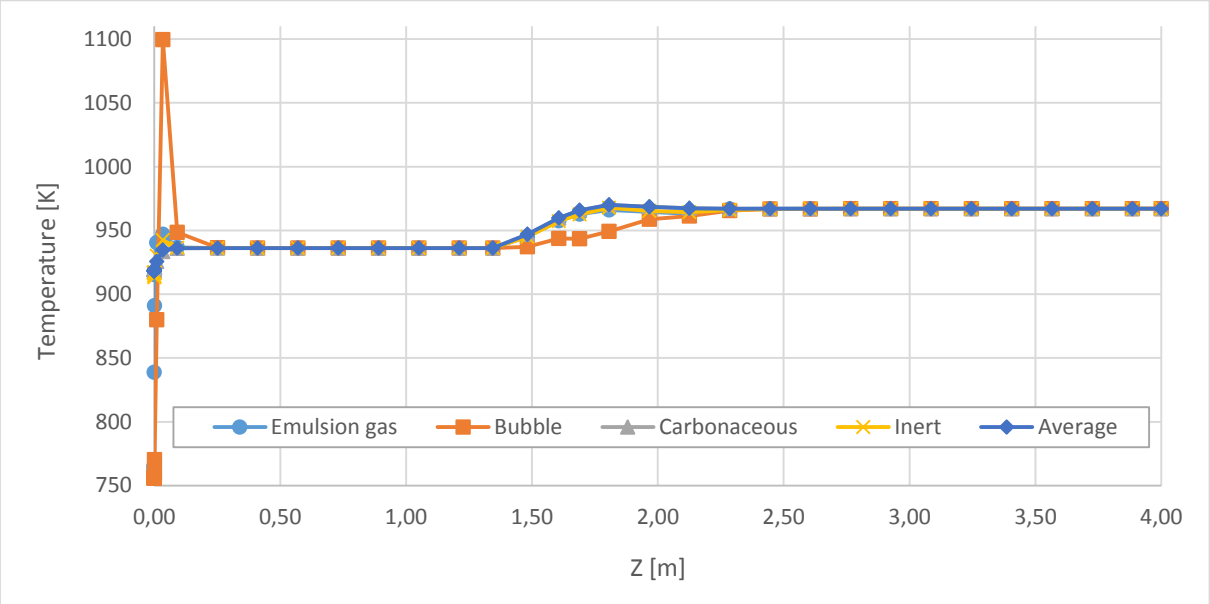

Figure 6.4-1 Temperature profiles at the bed gasifier region

EMULS.GAS= gas in the emulsion phase; BUBBLE= gas in the bubble phase; CARBONAC.= solid carbonaceous particles; INERT= inert solid particles or ashes detached from the original fuel; AVERAGE= average among all phases

Figure 6.4-1 shows the temperature profiles for the different phases in the bed. Coordinate z represents the position above the distributor surface. At several positions, the temperature profiles of various phases coincide throughout the bed. It is possible to identify differences of temperatures between the carbonaceous and gas phases (bubbles and emulsion) in two different regions or peaks. The first one, near the distributor with a quick increase of temperature due to the swift oxidation of the fuel, and the second one correspond to the region near the fuel feeding position (z = 2m). The peak of temperatures near the fuel feeding position is mainly due to the destruction of tar released by the fuel pyrolysis, which in many situations can be seen as an overall slightly exothermic process.

It is important to feed the fuel near the distributor to allow enough residence time for tar cracking and cooking into the bed region. Otherwise, it might be present in the leaving gas stream and provoke various operational and maintenance problems to the cleaning system.

The average temperature throughout the bed, as confirmed in experimental observations (DE SOUZA-SANTOS, 2010) does not present significant variations.

Although there is a false impression that all gas and solid phases inside fluidized beds have the same temperature. Figure 6.4-2 shows the temperature profiles for the different phases in the bed in a logarithmic scale, to clearly illustrate the profiles near the distributor surface (z=0).

The injected air flow splits between the bubble and the emulsion phases. The fraction in the emulsion experiences a faster increase in their temperature, because is in direct contact with the hot particles in the fluidized bed. The oxygen is rapidly consumed near the distributor (Figure 6.4-6), due to the close contact between the emulsion gas and the solid fuel particles. Besides that, there is a relative low rate of heat transfer between the bubbles phase and the emulsion phase, which lead the bubbles at relatively low temperatures.

After certain height in the bed, almost all the oxygen in the emulsion is consumed and is possible to find fuel gases. Such gases tend to migrate and accumulate into the bubbles. Then, fast combustion takes place inside the bubbles, leading to a sudden increase in their temperature (Figure 6.4-2). The value has even surpassed the average in the bed during a brief interval. That phenomenon may occur not just in gasification, but in BFB combustion as well (DE SOUZA-SANTOS, 2010). As seen in the figure below, the temperatures of fuel and detached ashes (inert) are below the ash-softening limit throughout the entire bed.

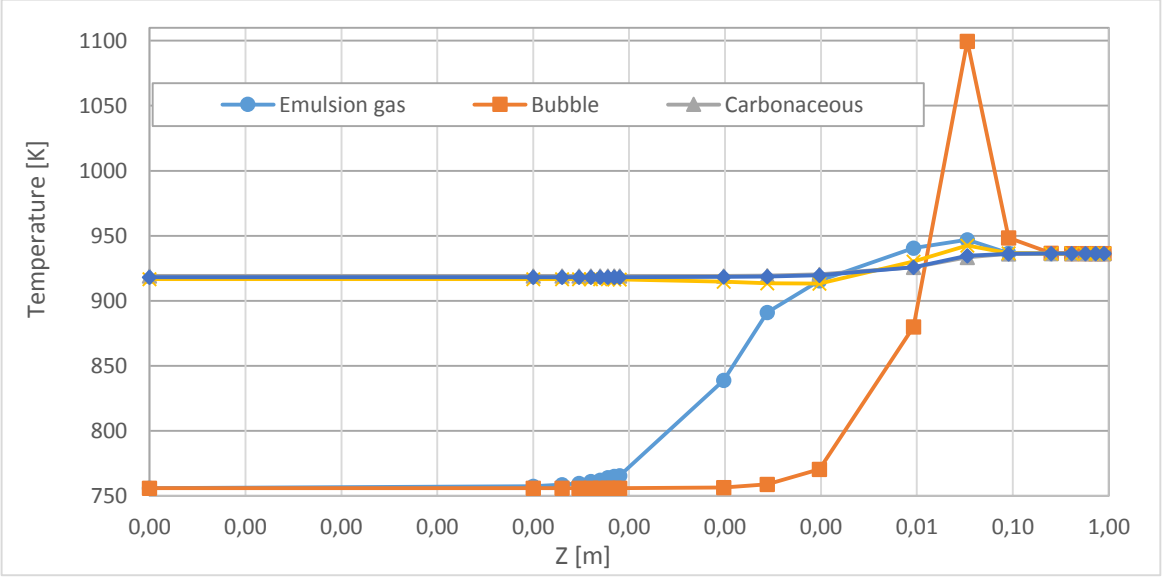

Figure 6.4-2 Temperature profiles at the gasifier bed region in logarithmic scale

EMULS.GAS= gas in the emulsion phase; BUBBLE= gas in the bubble phase; CARBONAC.= solid carbonaceous particles; INERT= inert solid particles or ashes detached from the original fuel; AVERAGE= average among all phases.

Figure 6.4-3 shows the temperature profiles throughout the freeboard. The ash segregated from the solid fuel particles becomes part of the inert solid phase.

As seen relatively small variations in the temperature are found in the freeboard.

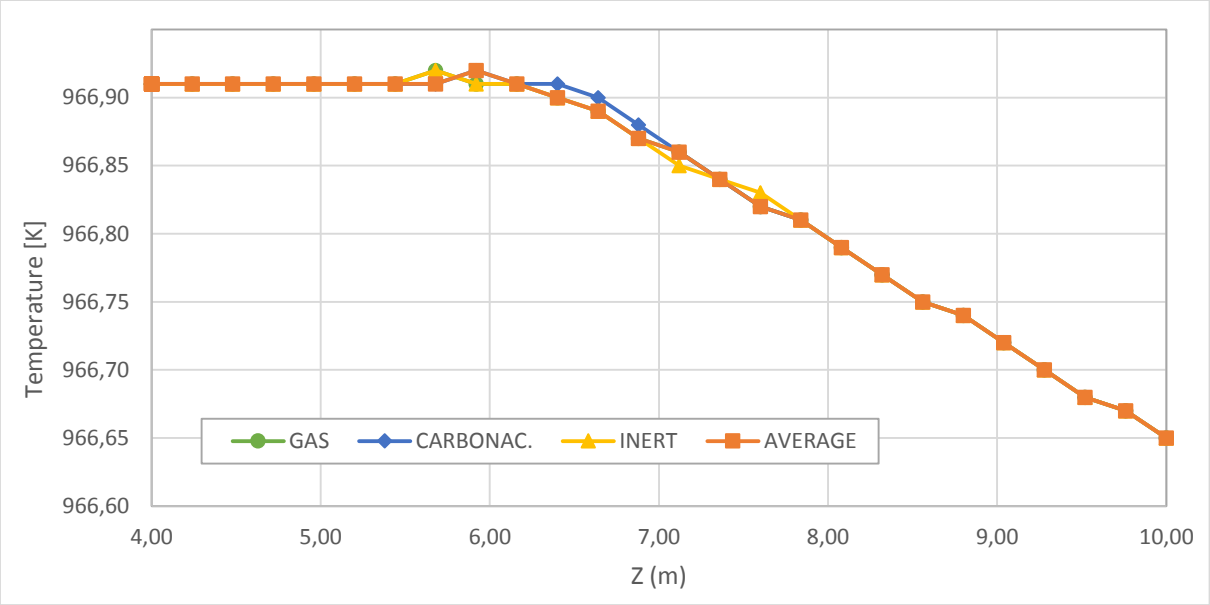

Figure 6.4-3 Temperature profiles in the freeboard region of the gasifier operating at 2.0 MPa. Notation: GAS = gas in the freeboard, CARBONAC. = carbonaceous fuel particles, INERT = inert or as particles, AVERAGE = average among all phases.

Figure 6.4-4 shows that there are no large bubbles inside the bed, avoiding risk of a slugging-flow operation.

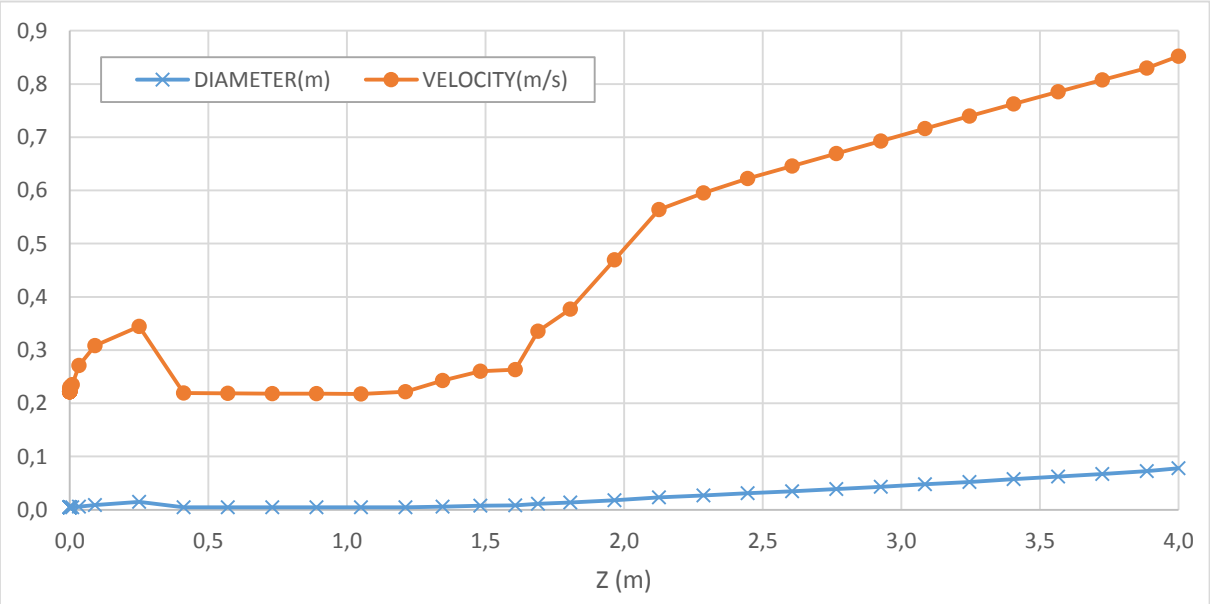

Figure 6.4-4 Bubble sizes and raising velocities through the bed

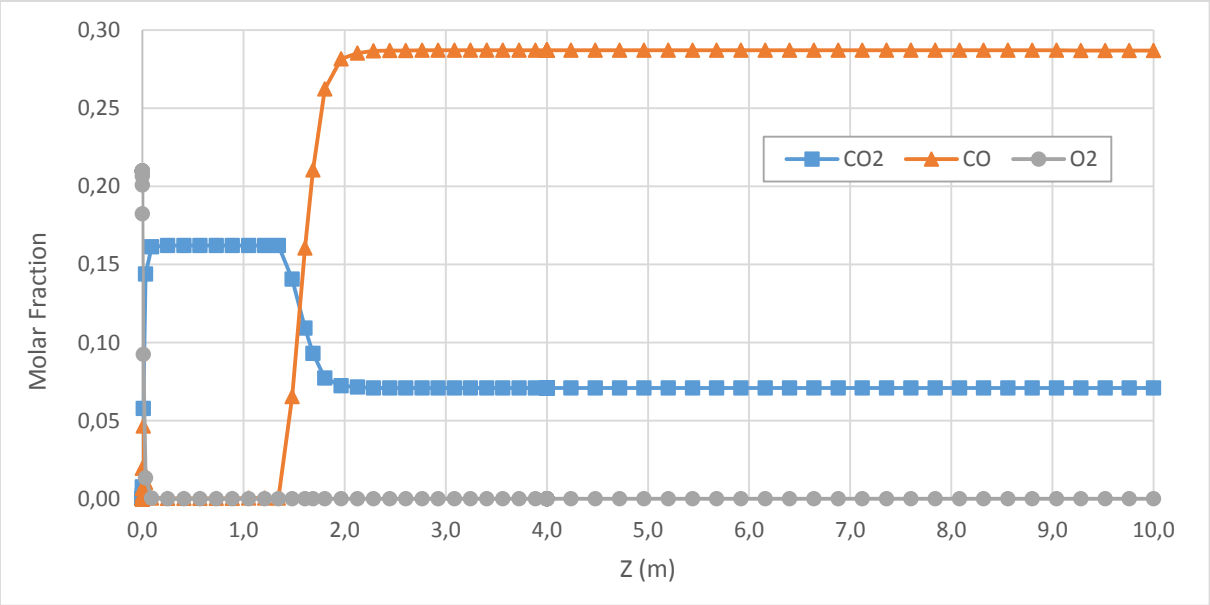

Figure 6.4-5 Concentration profiles of CO, CO_2 and O_2 throughout the equipment

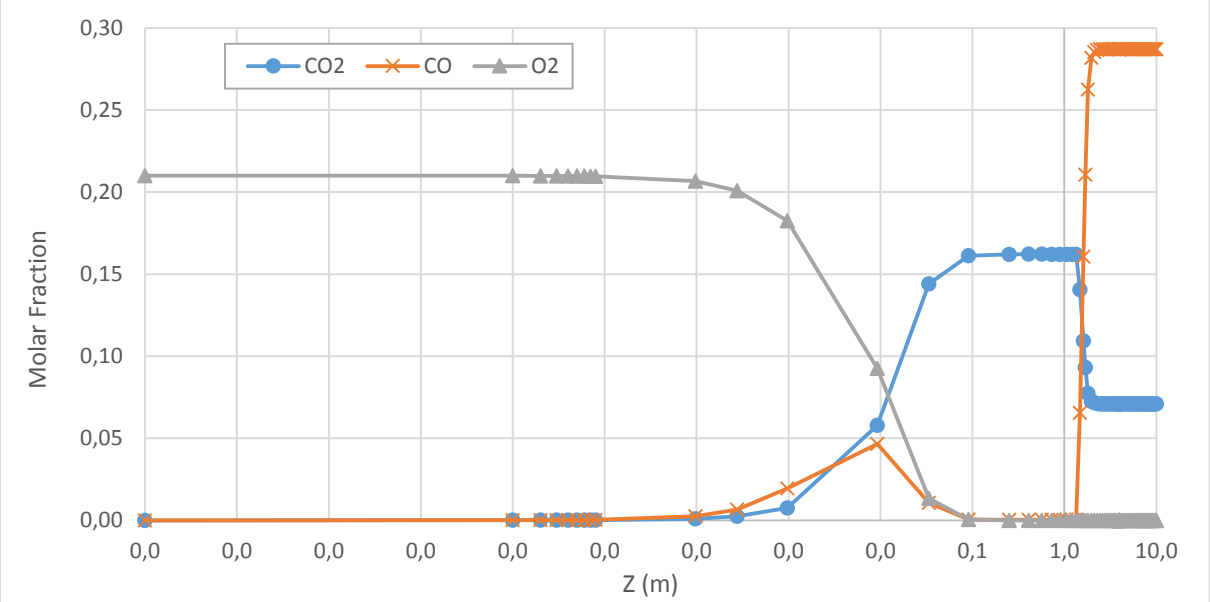

Figure 6.4-6 Concentration profiles of CO, CO_2 and O_2 throughout the equipment, plotted in logarithmic scale

Figure 6.4-5 and Figure 6.4-6 (the last one in logarithmic scale) shows how the swift oxidation of the solid fuel consume the oxygen rapidly. The combustion of the solid fuel near the distributor (z=0) lead to the production of CO and CO_2. The produced CO_2 reacts with carbon and produce more CO. However, CO accumulation is only possible after the complete consumption of O_2.

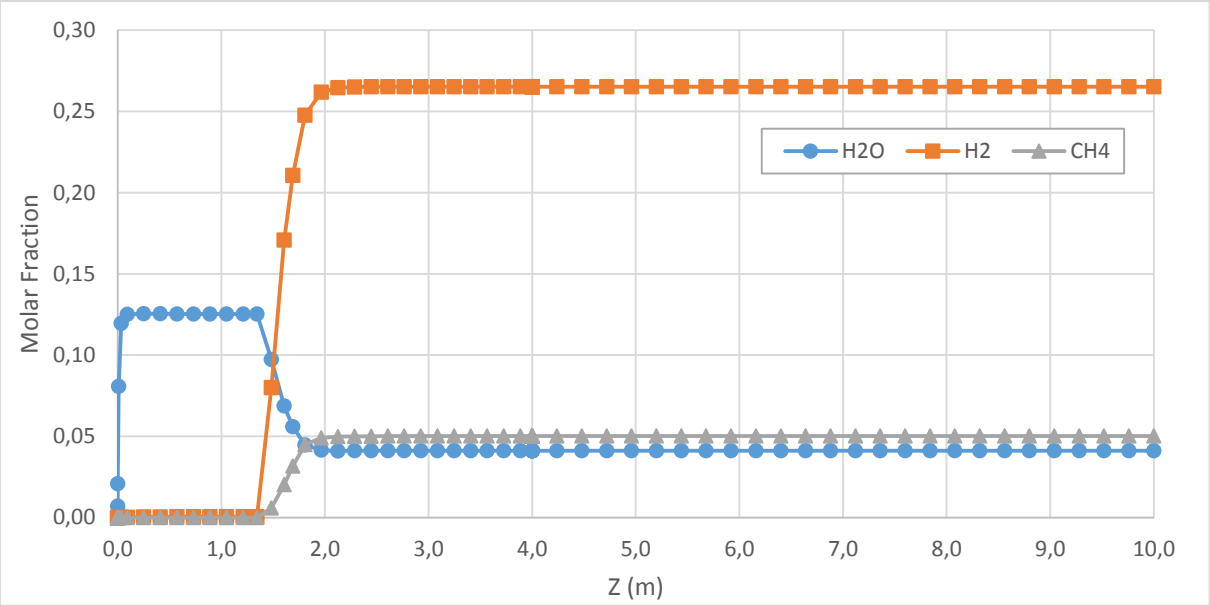

Figure 6.4-7 Concentration profiles of H_2O, H_2 and CH_4 throughout the gasifier

Figure 6.4-7 illustrates the evolution of other important gases inside the reactor. The concentration of those gases varies significantly when the oxygen is consumed allowing the accumulation of fuel gases. Moreover, hydrogen is produced around 2 m above the distributor, due to the pyrolysis of the fuel near the feeding position. The water is mainly produced near the distributor (z = 0) and is mostly formed by the oxidation of the hydrogen present in the fuel. Several other reactions takes place in the gasifier, the complete list of the reactions considered by CeSFaMB© can be found in the literature (DE SOUZA-SANTOS, 2010).

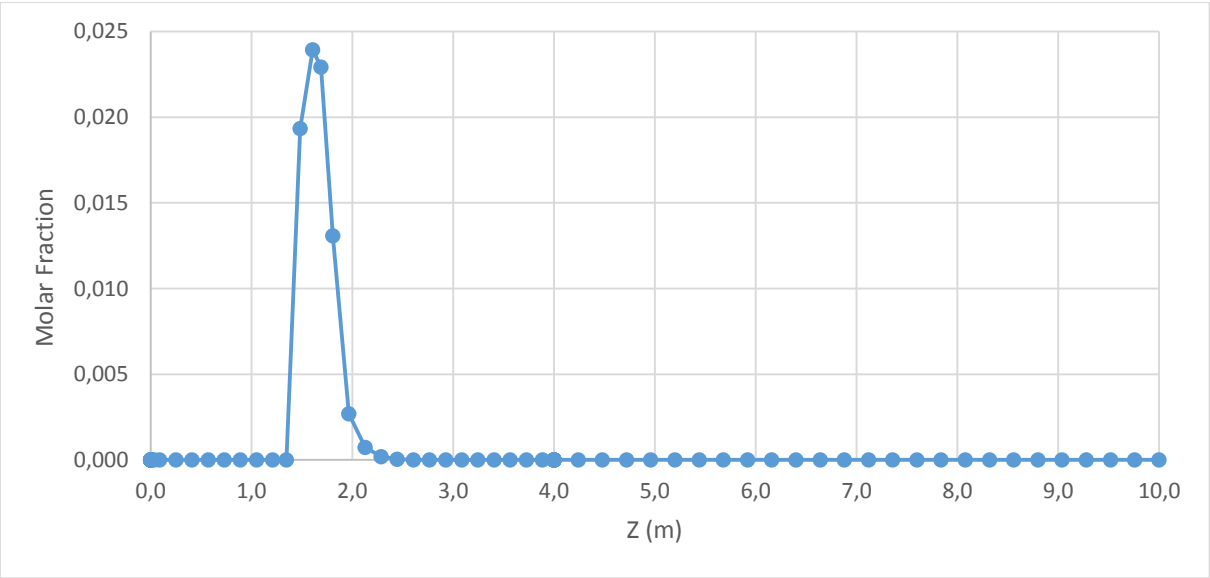

Figure 6.4-8 Concentration profile of tar throughout the equipment.

Figure 6.4-8 illustrates the fast release of tar near the MSW feeding position and its destruction due to cracking and cooking in the region above. This is an important characteristic of fluidized beds and avoid the presence of tar in the gases leaving the reactor.

The particle size distributions in the bed is presented in Table 6.4-2.

Table 6.4-2 Particle size distributions in the bed and the freeboard top

Diameter (m)	**Mass-frac. (bed)**	**Mass-frac. (top-freeb.)**
0.00E+00	0.00E+00	0.00E+00
2.50E-05	4.61E-03	7.60E-01
2.50E-05	4.61E-05	7.59E-03
9.83E-05	3.61E-03	2.33E-01
1.50E-04	2.86E-04	3.30E-09
2.50E-04	1.30E-02	1.50E-07
4.00E-04	4.29E-04	4.95E-09
5.90E-04	2.21E-02	2.55E-07
7.50E-04	2.86E-04	3.30E-09
9.83E-04	8.98E-01	1.04E-05
1.00E-03	1.43E-04	1.65E-09
1.57E-03	2.91E-02	3.36E-07
2.95E-03	1.92E-02	2.21E-07
3.93E-03	9.31E-03	1.07E-07

6.5 Dryer optimization

The optimization of the dryer was carried assuming the constant geometry described in Section 4.1.1. The objective was the minimization of injected gas flow through the distributor.

The flue gas temperature and composition of the Stream 28 were obtained through simulations of the entire power generation process in IPES© (Table 6.5-1).

Table 6.5-1 Composition of the injected gas into the dryer

Chemical species	Mass fraction	Molar fraction	Chemical species	Mass fraction	Molar fraction
H2	0.000000	0.000000	CO	0.00000	0.00000
H2O	0.048663	0.078035	CO2	0.11538	0.07574
H2S	0.000000	0.000000	HCN	0.00000	0.00000
NH3	0.000000	0.000000	CH4	0.00000	0.00000
NO	0.001825	0.001757	C2H4	0.00000	0.00000
NO2	0.000000	0.000000	C2H6	0.00000	0.00000
N2	0.712150	0.734410	C3H6	0.00000	0.00000
N2O	0.000000	0.000000	C3H8	0.00000	0.00000
O2	0.121840	0.109990	C6H6	0.00000	0.00000
SO2	0.000146	0.000066	Tar	0.0000	0.0000

After extensive simulations using CeSFaMB©, the minimum required mass flow of injected gas into the dryer, to achieve complete fuel drying, was 51.7 kg/s.

The specific operational parameters of the selected dryer are shown in Table 6.5-2.

Table 6.5-2 Operational parameters of the selected dryer operating at 2.0 MPa

Main output condition or parameters	Value
Mass flow of gas leaving the equipment	74.35 kg/s
Temperature of gas leaving the equipment	449.69 K
Mass flow of gas injected through the distributor	51.7 kg/s
Temperature of the gas injected through the distributor	947.00 K
Mass flow of solids leaving the dryer	17.96 kg/s
Concentration of water in the solids discharged from the bed	0.00 %
Minimum fluidization velocity at the middle of the bed (U_{mf})	0.12 m/s
Superficial velocity at the middle of the bed (U_s)	0.40 m/s
Transport velocity at the middle of the bed (U_{tr})	0.81 m/s
Bed volume	37.70 m^3
Mass flow of tar at the freeboard top	0.00 kg/s
Pressure loss across the distributor	0.07 kPa
Pressure loss across the bed	2.29 kPa
Total carbon conversion	0.09 %
Rate of energy input to the system due to fuel	362.64 MW
Total rate of energy input to the system	400.33 MW
Rate of energy transferred to the gas leaving the dryer	26.71 MW
Temperature of the gas leaving the equipment	449.59 K
Exergy flow brought by the fuel	576.2 MW
Exergy flow brought by the distributor injected gas	36.74 MW
Total exergy flow into the equipment	613.0 MW
Exergy flow leaving the equipment	384.8 MW
Exergy flow carried by the main exiting gas stream	41.72 MW
Ratio between exergy of exiting gas and total exergy leaving the equipment	6.81 %
Ratio between exergy of the exiting gas and total exergy entering the equipment	10.84 %
Percentage of pyrolysis products released from the feeding fuel	0.00 %

Based in the information presented in Table 6.5-2 some aspects of the equipment could be analyzed:

- The three average superficial velocities indicated for the bed satisfy the following relation:

$$U_{mf} < U_s < U_{tr}$$

  therefore the dryer operates in bubbling fluidized bed regime (DE SOUZA-SANTOS, 2010).
- The process guarantees the complete drying of the fuel slurry without substantial pyrolysis products released.
- The mass flow of injected air was minimized in order to minimize the power consumed by the compressor (Equipment 10).
- The exiting gas stream carries relatively low exergy of the amount entering with the fuel slurry.

The composition of the gases leaving the dryer is shown in Table 6.5-3.

Table 6.5-3 Composition of the exiting gas leaving the dryer

Chemical species	**Mass percentage**	**Molar percentage**	**Chemical species**	**Mass percentage**	**Molar percentage**
H2	0.000000	0.000000	CO	0.00000	0.00000
H2O	33.843300	45.846500	CO2	8.06510	4.47230
H2S	0.000000	0.000000	HCN	0.00000	0.00000
NH3	0.000200	0.000200	CH4	0.00000	0.00000
NO	0.126900	0.103200	C2H4	0.00000	0.00000
NO2	0.000500	0.000300	C2H6	0.00000	0.00000
N2	49.519200	43.140700	C3H6	0.00000	0.00000
N2O	0.000000	0.000000	C3H8	0.00000	0.00000
O2	8.434700	6.432900	C6H6	0.00000	0.00000
SO2	0.010200	0.003900	Tar	0.0000	0.0000

In addition to the information provided above, CeSFaMB© provides the temperature and concentration profiles throughout the bed and freeboard. Such profiles are plotted in a graphical interface and are presented below.

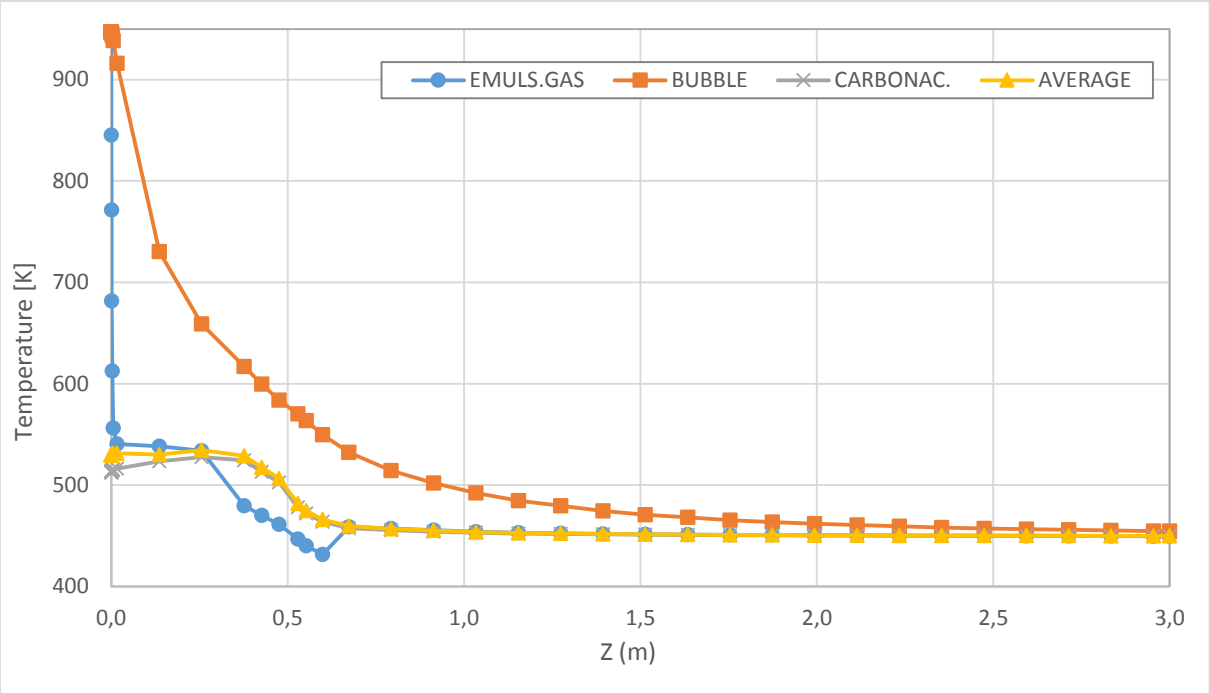

Figure 6.5-1 Temperature profiles at the bed dryer region

EMULS.GAS= gas in the emulsion phase; BUBBLE= gas in the bubble phase; CARBONAC.= solid carbonaceous particles; INERT= inert solid particles or ashes detached from the original fuel; AVERAGE= average among all phase.

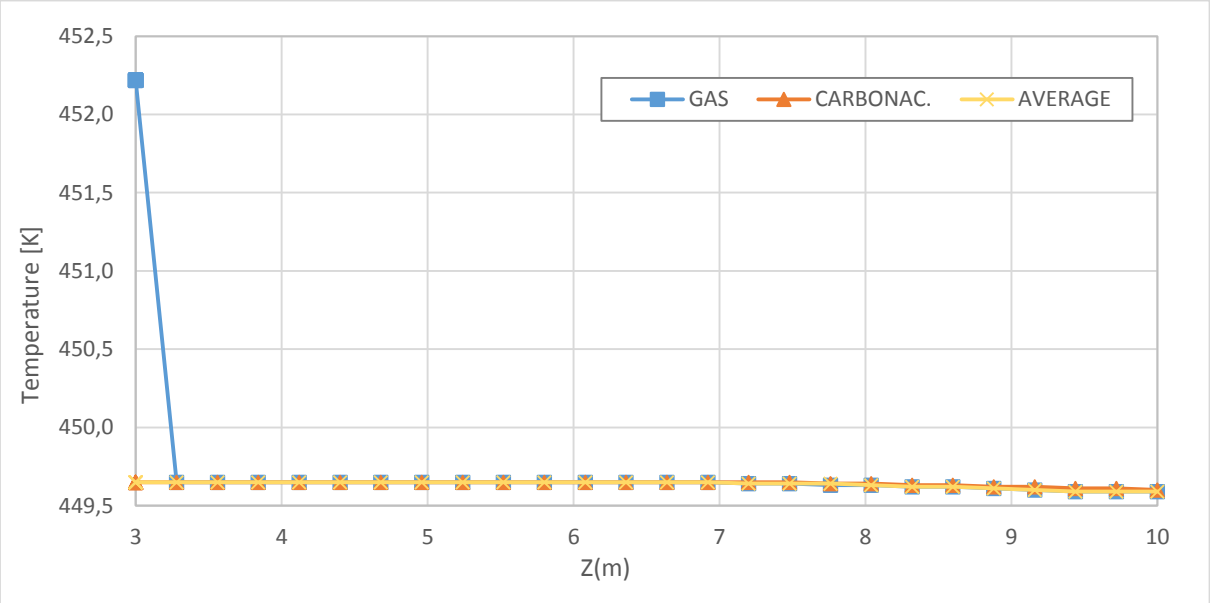

Figure 6.5-2 Temperature profiles in the freeboard region of the dryer operating at 2.1 MPa.

Notation: GAS = gas in the freeboard, CARBONAC. = carbonaceous fuel particles, INERT = inert or as particles, AVERAGE = average among all phases

As seen in Figure 6.5-1 and Figure 6.5-2, the temperature remains almost constant from z = 2m to the top of the equipment at z = 10m, and relatively small variations in the temperature are found in the freeboard of the dryer.

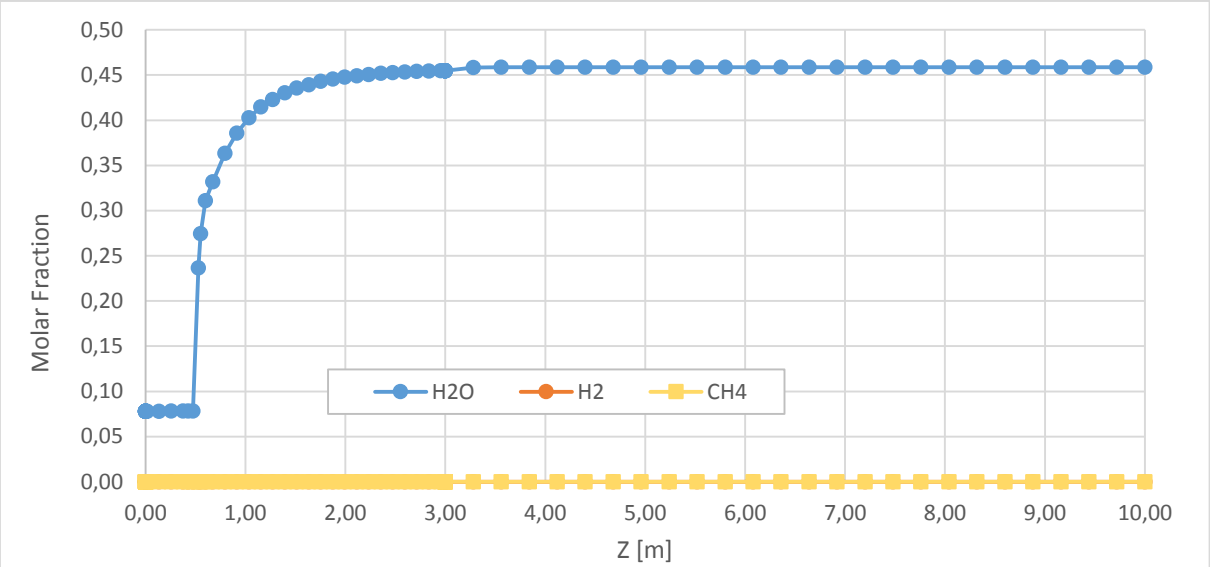

Figure 6.5-3 Concentration profiles of H_2O, H_2, and CH_4 throughout the dryer.

The gas leaving the equipment is composed by the removed moisture from the Fuel-Slurry and an insignificant amount of volatiles. The sudden increase in the water vapour concentration starts near the Fuel-Slurry feeding position at z = 0.5 m. There is no production of hydrogen and hydrocarbons in the drying process; therefore, the fuel is dried without devolatilization taking place.

6.6 Power Generation Processes

6.6.1. Entire power generation process FSIG/GT

The conditions of the parameters at each stream of the process is a product of extensive simulations, analyses and optimizations of the involved systems and sub-systems, with the aim to find the highest power generation efficiency.

The proposed architecture follows the configuration presented in the Figure 6.2-1.

Some of the performance parameters used to evaluate the best configuration and conditions of the overall power generation process are defined below:

- Net power output from the system (P_{out}): is the sum of the liquid power generated by the gas turbine cycle, plus the net power output from the steam Rankine cycles.
- The Efficiency based on the 1st Law is given by

$$\eta_{1^{st}} = \frac{P_{out}}{LHV_{slurry}\dot{m}_{slurry}} \tag{6.1}$$

where the denominator is the product between the lower heating value (LHV) of the MSW slurry [kJ/kg], and its feeding rate [kg/s]. Therefore, the denominator is the energy rate brought by the fuel slurry into the process.

The temperatures, pressures, and mass flows of each stream involved in the process were presented in the Table 6.3-3. More detailed information about the selected FSIG/GT configuration is presented in the Appendix B.

Table 6.6.1-1 presents the overall efficiencies of the entire power generation process. The achieved 1st Law efficiency do not increase in comparison with the values obtained in a prior work (DE SOUZA-SANTOS; CERIBELI, 2013b), where the same level of pressure (2 MPa) was employed.

Table 6.6.1-1 Process overall efficiencies

Main parameters	
Mechanical power input[a]	141.22 MW
Mechanical power output[b]	264.37 MW
Net mechanical power output	123.15 MW
Rate of energy input by fuel slurry[c]	377.82 MW
Efficiency based on 1st Law[d]	32.60 %
Rate of exergy input by fuel slurry	566.70 MW

[a]Due to compressors and pumps. [b]From steam and gas turbines. [c]Based on LHV. [d]Defined as (useful mechanical power)/(rate of energy input by fuel slurry)

6.6.2. Gas Turbine and Rankine cycles

It is possible to split the whole power generation process into three different regions. The first one encompasses the gas process (Figure 6.6.2-1). The second one includes the main Rankine cycle involving equipment 4 to 8 (Figure 6.6.2-2 a), and the third incorporates the secondary Rankine cycle containing equipment 11 to 15 (Figure 6.6.2-2 b).

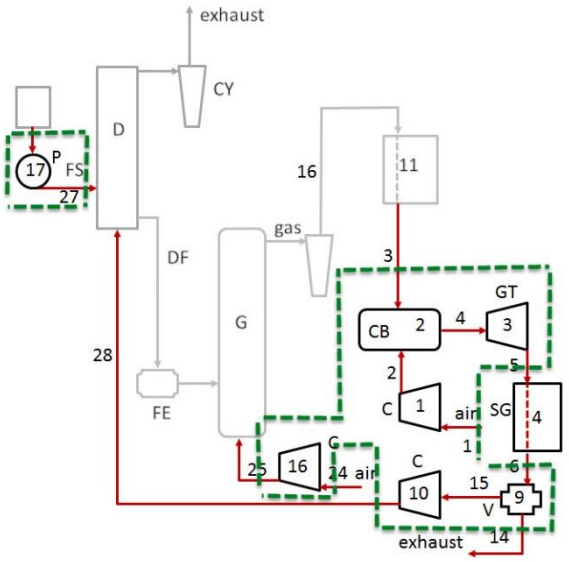

Figure 6.6.2-1 Control volume of the gas process.

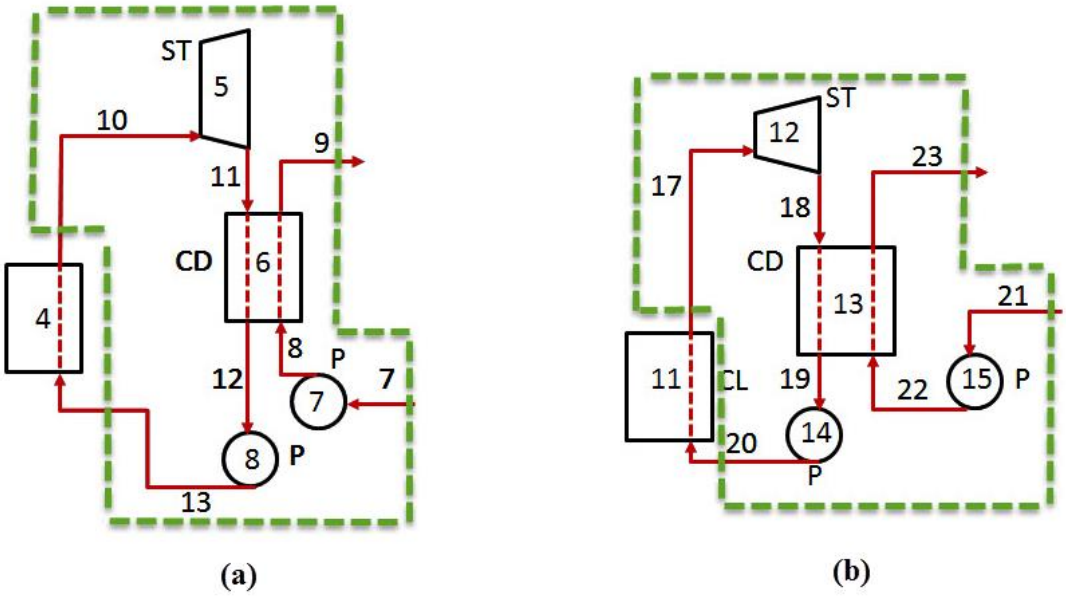

Figure 6.6.2-2 (a) Control volume of the main Rankine cycle involving equipment 4 to 8; (b) Control volume of the secondary Rankine cycle involving equipment 11 to 15

The above figures are based on FSIG/GT configuration C (Figure 2.5-3) and show the studied gas and steam cycles control volumes.

During those studies, the 1st Law efficiency of the gas process is given by:

$$\eta_{1st,gas} = \frac{P_{out}}{LHV_{slurry}\,\dot{m}_{slurry}} \tag{6.2}$$

where P_{out} is the net power of the gas process.

The denominator of equation 6.2 is the product between the Lower Heating Value and the mass flow of the slurry.

- The 1st Law efficiency of the Rankine processes is given by:

$$\eta_{1st,Rankine\ n} = \frac{P_{out,n}}{\dot{Q}_{in,n}} \tag{6.4}$$

where P_{out} is the net power of each of the Rankine cycles.

For the Rankine cycle (I), the inlet heating rate is given by:

$$\dot{Q}_{in,Rankine\ I} = F_{13}(h_{10} - h_{13}) \tag{6.5}$$

For the Rankine cycle (II), the inlet heating rate is given by:

$$\dot{Q}_{in,Rankine\ II} = F_{20}(h_{17} - h_{20}) \tag{6.6}$$

Table 6.6.2-1 Liquid power and First Law Efficiencies of the gas turbine and Rankine cycles.

	$\eta_{1st,}$ [%]	P_{out} [MW]
Gas Cycle	16.6	62.58
Main Rankine Cycle*	33.3	58.26
Secondary Rankine Cycle**	26.3	2.32
FSIG/GT (total)	32.6	123.16

**Composed by equipment 4 to 8; **Composed by equipment 11 to 15*

7 CONCLUSIONS

New studies on optimization of the FSIG/GT (Fuel-Slurry Integrated Gasifier/Gas Turbine) process consuming MSW (Municipal Solid Waste) has been developed. The process uses Fuel-Slurry of MSW dried and gasified in BFB (Bubbling Fluidized Bed) pressurized equipment to provide fuel gas for gas turbines. Variations on the operational pressure of the gasifier, and the mass flow of air injected into the gasifier were tested. This work improves on the developed before by (DE SOUZA-SANTOS; CERIBELI, 2013b) and adopt the configuration validated by (BERNAL, 2014; DE SOUZA-SANTOS; BERNAL; RODRIGUEZ-TORRES, 2015).

Similarly to previous works (BERNAL, 2014; DE SOUZA-SANTOS; BERNAL; RODRIGUEZ-TORRES, 2015; DE SOUZA-SANTOS; CERIBELI, 2013b), steam cycles were integrated to the system to recover energy from the gas process.

Based on the obtained results in the present work, the following conclusions has been determined:

1. Likewise previous studies, the present one indicate that FSIG/GT process is a feasible alternative for thermoelectric power generation consuming MSW.
2. The implementation of the FSIG/GT process at elevated pressures is not possible in a real plant using the configuration shown in Figure 6.2-1, due to the existing limit of 950 K for the temperature of stream leaving axial compressors (BOYCE, [s.d.]).
3. Notwithstanding, it was possible to verify that the exergetic efficiency and cold efficiency of the gasification process increase with the increase on the operational pressure of the equipment.
4. The overall efficiency achieved in the present work is around 33% (Table 6.6.1-1). Such value is near the values achieved in previous works (DE SOUZA-SANTOS; CERIBELI, 2013b) and surpasses the value of 30% obtained in some traditional processes (EUROPEAN COMMISSION, 2006).

7.1 Suggestions for future works

As mentioned in Section 6.2 , the achieved temperature of the gas injected into the dryer, operating at 5.0 MPa, surpasses the limit of the maximum compressor blade working temperatures of 950 K (BOYCE, [s.d.]). According to that, gasifier operations at pressures above 2.0 MPa can only be implemented into FSIG/GT process if intercooling is applied at the compression of the gas injected into the dryer (Stream 15-Figure 6.2-1). A recent work (DE SOUZA-SANTOS, 2015a) evaluates the process operating at elevated pressures, such as 10 MPa. Figure 7.1-1 shows a possible scheme to allow for such alternative.

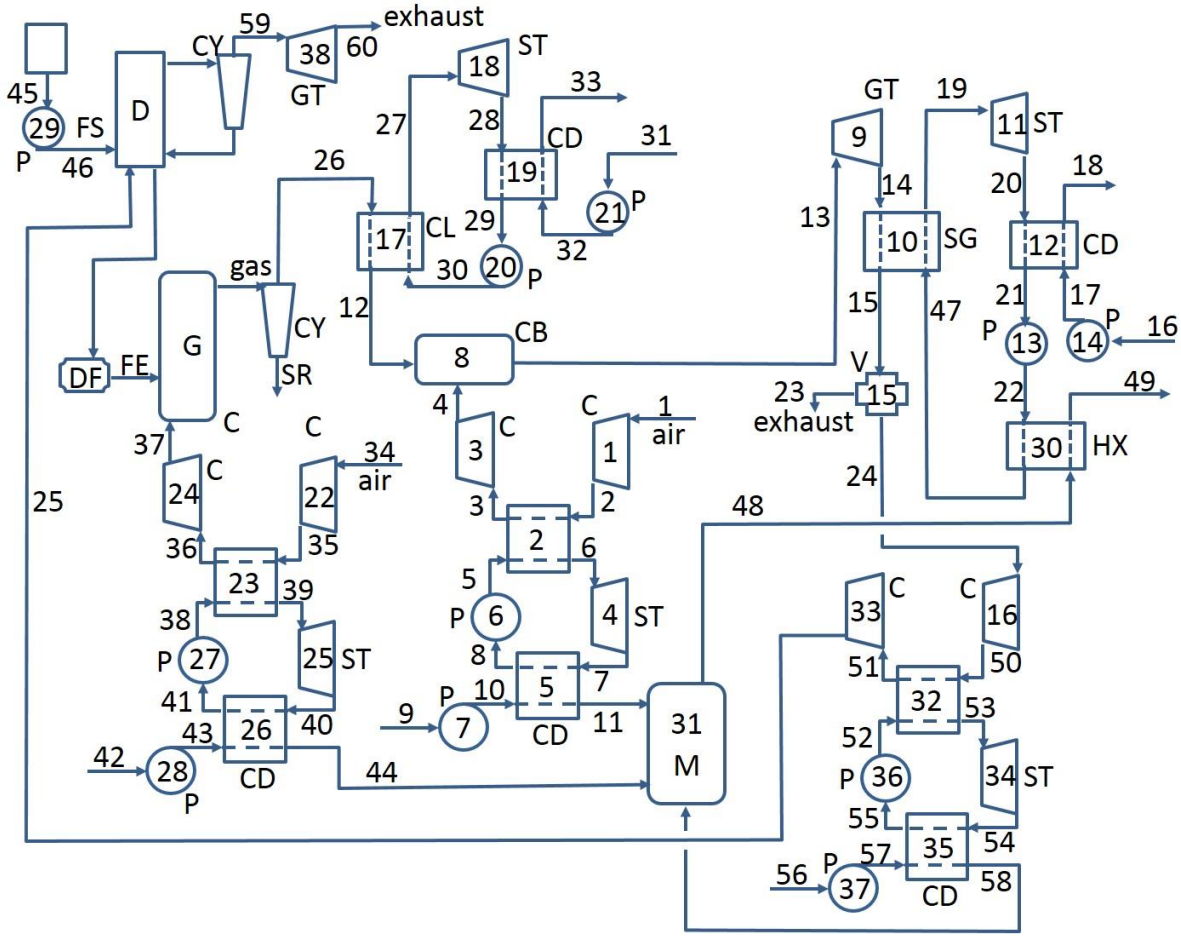

Figure 7.1-1 Scheme of the FSIG/GT process proposed for very high operational pressures.

Notation: C, compressor; CB, combustor; CD, condenser; CL, cleaning system; CY, cyclone; D, dryer; DF, dried fuel; FE, screw feeding; FS, fuel-slurry pumping; G, gasifier; GT, gas turbine; HX, heat exchanger; M, mixer; SG, steam generator; ST, steam turbine; P, water pump; and V, valve or splitter (DE SOUZA-SANTOS, 2015a).

As seen, intercooling is applied at 3 different compression processes at streams 2, 35 and 50. The last intercooling involves equipment 16 and 33 to 37, and allows the compression of the gas used in the drying process until 10.10 MPa. The proposed configuration avoids exceeding the temperature limits of materials composing axial compressor blades (BOYCE, [s.d.]). Moreover, such an alternative uses the energy of the exhausted gas of the dryer. Unfortunately, the time available for the development of the present work did not allow exploring those alternatives. Studies including the application of intercooling and power recovery from the compressing stream leaving the dryer should be left for future developments of processes consuming MSW.

Future studies would also considerate economic evaluations on the proposed alternatives for thermoelectric power generation using MSW.

In addition, incoming investigations may test the influence of fuel particle sizes, dry solid content in the slurry, dryer geometry, as well other parameters, on the overall power generation efficiency. Improvements on the Rankine cycles, such as reheating and others may also be implemented.

Finally, other gasification techniques such as circulating fluidized bed and entrained flow reactor could be analyzed in further investigations.

References

ANTHONY, E. Fluidized bed combustion of alternative solid fuels; status, successes and problems of the technology. **Progress in Energy and Combustion Science**, v. 21, n. 3, p. 239–268, 1995.

ARAFAT, H. A.; JIJAKLI, K. Modeling and comparative assessment of municipal solid waste gasification for energy production. **Waste management (New York, N.Y.)**, v. 33, n. 8, p. 1704–13, ago. 2013.

ARENA, U. Process and technological aspects of municipal solid waste gasification. A review. **Waste management (New York, N.Y.)**, v. 32, n. 4, p. 625–39, abr. 2012.

ASTM-INTERNATIONAL. **ASTM D3176-15 Standard Practice for Ultimate Analysis of Coal and Coke**West Conshohocken, PA, 2015a.

ASTM-INTERNATIONAL. **ASTM D7582-15, Standard Test Methods for Proximate Analysis of Coal and Coke by Macro Thermogravimetric Analysis**West Conshohocken, PA, 2015b.

ASTM-INTERNATIONAL. **ASTM E11-15 Standard Specification for Woven Wire Test Sieve Cloth and Test Sieves**West Conshohocken, PA, 2015c.

BARBA, D.; BRANDANI, F.; CAPOCELLI, M. Process analysis of an industrial waste-to-energy plant: Theory and experiments. **Process Safety and Environmental Protection**, v. 96, p. 61–73, jul. 2015.

BASTOS-NETTO, D.; RIEHL, R.; DE SOUZA-SANTOS, M. L. **Conceptual Design of a Sugar Cane Bagasse Gasifier.ICCEU2010 - 10th International Conference on Combustion and Energy Utilization**. Mugla, Turkey: [s.n.].

BELGIORNO, V. et al. Energy from gasification of solid wastes. **Waste management (New York, N.Y.)**, v. 23, n. 1, p. 1–15, jan. 2003.

BERNAL, A. F. B. **Estudos em geração termelétrica avançada a partir de bagaço de cana utilizando gaseificadores de leito fluidizado borbulhante**. [s.l.] UNICAMP, 2014.

BOYCE, M. P. Axial-Flow Compressors. In: **Gas Turbine Engineering Handbook**. Houston, TX: [s.n.].

BREAULT, R. W. Gasification processes old and new: A basic review of the major technologies. **Energies**, v. 3, n. 2, p. 216–240, 2010.

BROWN, M. G.; BAKER, E. G.; MUDGE, L. K. Evaluation of process for removal of particulates, tars, and oils from biomass gasifier product gases, in Energy from biomass and Wastes. **Elsevier Applied Science**, p. 655–777, 1987.

CENSUS BUREAU. **United States Census Bureau**. Disponível em: <http://www.census.gov/popclock/>.

CHENG, H.; HU, Y. Municipal solid waste (MSW) as a renewable source of energy: current and future practices in China. **Bioresource technology**, v. 101, n. 11, p. 3816–24, jun. 2010.

COHN, A. **Direct coal fired gas turbinesWorkshop Proceedings of Electric Power Research Insstitute**Palo Alto, CA, 1985.

COSTA, A. M. S.; DE SOUZA-SANTOS, M. L. Studies on the mathematical modeling of circulation rates of particles in bubbling fluidized beds. **Powder Technology**, v. 103, n. 2, p. 110–116, jul. 1999.

DE SOUZA-SANTOS, M. L. **Modeling and Simulation of Fluidized-Bed Boilers and gasifiers for Carbonaceous Solids**. [s.l.] Universuty of Sheffield, United Kingdom, 1987.

DE SOUZA-SANTOS, M. L. **Comprehensive modelling and simulation of fluidized bed boilers and gasifiersFuel**, 1989.

DE SOUZA-SANTOS, M. L. Application of Comprehensive Simulation of Fluidized-Bed Reactors to the Pressurized Gasification of Biomass. **Journal of the Brazilian Society of Mechanical Sciences**, v. 16, p. 376–383, 1994a.

DE SOUZA-SANTOS, M. L. Application of comprehensive simulation to pressurized fluidized bed hydroretorting of shale. **Fuel**, v. 73, n. 9, p. 1459–1465, set. 1994b.

DE SOUZA-SANTOS, M. L. A Study on Pressurized Fluidized-Bed Gasification of Biomass through the Use of Comprehensive Simulation. In: **Book on Combustion Technologies for a Clean Environment**. Amsterdam: Gordon and Breach Publishers, 1998.

DE SOUZA-SANTOS, M. L. A Feasibility Study on an Alternative Power Generation

System Based on Biomass Gasification/Gas Turbine Concept. **Fuel**, v. 78, p. 529–538, 1999.

DE SOUZA-SANTOS, M. L. CSFB applied to fluidized-bed gasification of special fuels. **Fuel**, v. 88, n. 5, p. 826–833, maio 2009.

DE SOUZA-SANTOS, M. L. **Solid Fuels Combustion and Gasification: Modeling, Simulation and Equipment Operations**. [s.l.] Taylor & Francis Group, 2010.

DE SOUZA-SANTOS, M. L. Development of Studies on Advanced Power Generation Based on Combined Cycle Using a Single High-Pressure Fluidized Bed Boiler and Consuming Sugar Cane Bagasse. p. 41–47, 2012a.

DE SOUZA-SANTOS, M. L. Development of Studies on Advanced Power Generation Based on Combined Cycle Using a Single High-Pressure Fluidized Bed Boiler and Consuming Sugar Cane Bagasse. 2012b.

DE SOUZA-SANTOS, M. L. Manual for IPES-Industrial Process and Equipment Simulator. 2014.

DE SOUZA-SANTOS, M. L. Very High-Pressure Fuel-Slurry Integrated Gasifier/Gas Turbine (FSIG/GT) Power Generation Applied to Biomass. **Energy & Fuels**, n. stream 26, p. acs.energyfuels.5b02093, 2015a.

DE SOUZA-SANTOS, M. L. **Comprehensive Simulator of Fluidized and Moving Bed equipment, CSFMB©/CeSFaMBTM**. Disponível em: <http://www.csfmb.com/>.

DE SOUZA-SANTOS, M. L.; BENINCA, W. DE A. New Strategy of Fuel-Slurry Integrated Gasifier/Gas Turbine (FSIG/GT) Alternative for Power Generation Applied to Biomass. **Energy & Fuels**, v. 28, n. 4, p. 2697–2707, 17 abr. 2014.

DE SOUZA-SANTOS, M. L.; BERNAL, A. F. B.; RODRIGUEZ-TORRES, A. F. New Developments on Fuel-Slurry Integrated Gasifier/Gas Turbine (FSIG/GT) Alternative for Power Generation Applied to Biomass; Configuration Requiring No Steam for Gasification. **Energy & Fuels**, p. 150526072227002, 2015.

DE SOUZA-SANTOS, M. L.; CERIBELI, K. Technical evaluation of a power generation process consuming municipal solid waste. **Fuel**, v. 108, p. 578–585, jun. 2013a.

DE SOUZA-SANTOS, M. L.; CERIBELI, K. B. Fuel-slurry integrated gasifier/gas turbine (FSIG/GT) alternative for power generation applied to municipal solid waste (MSW). **Energy**

and Fuels, v. 27, n. 12, p. 7696–7713, 2013b.

DE SOUZA-SANTOS, M. L.; CHAVEZ, J. V. Preliminary studies on advanced power generation based on combined cycle using a single high-pressure fluidized bed boiler and consuming sugar-cane bagasse. **Fuel**, v. 95, p. 221–225, maio 2012.

DE SOUZA-SANTOS, M. L.; DE LIMA, E. H. S. Introductory study on Fuel-Slurry Integrated Gasifier/Gas Turbine (FSIG/GT) alternative for power generation applied to high-ash or low-grade coal. **Fuel**, v. 143, p. 275–284, mar. 2015.

DE SOUZA-SANTOS, M. L.; RABI, J. A. Incorporation of a two-flux model for radiative heat transfer in a comprehensive fluidized bed simulator. Part I: Preliminary theoretical investigations. **Thermal Engineering**, v. 3, p. 64–70, 2003.

DE SOUZA-SANTOS, M. L.; RABI, J. A. Incorporation of a two-flux model for radiative heat transfer in a comprehensive fluidized bed simulator. Part II: Numerical results and assessment. **Thermal Engineering**, v. 4, p. 49–54, 2004.

DEDINI, I. **No Title**. Disponível em: <www.dedini.com.br/index.php?lang=en>. Acesso em: 3 mar. 2014.

ENGELBRECHT, A. D. et al. **Fluidised bed gasification of high-ash South African coals: An experimental and modelling study.** Johannesburg, South Africa: [s.n.].

EUROPEAN COMMISSION. **Reference document on the Best Available Techniques for Waste Incineration**. Disponível em: <http://eippcb.jrc.ec.europa.eu/reference/BREF/wi_bref_0806.pdf>. Acesso em: 18 jan. 2016.

EUROPEAN ENVIRONMENT AGENCY. **Diverting waste from landfill: Effectiveness of waste management policies in the European Union**. [s.l: s.n.].

EUROPEAN ENVIRONMENT AGENCY. Waste generation. p. 8–12, 2015.

FINNVEDEN, G. et al. Life cycle assessment of energy from solid waste—part 1: general methodology and results. **Journal of Cleaner Production**, v. 13, n. 3, p. 213–229, fev. 2005.

FODOR, Z.; KLEMEŠ, J. J. Waste as alternative fuel – Minimising emissions and effluents by advanced design. **Process Safety and Environmental Protection**, v. 90, n. 3, p. 263–284, maio 2012.

GASIFICATION TECHNOLOGIES COUNCIL. **Gasification Technologies Council**. Disponível em: <http://www.gasification.org/what-is-gasification/how-does-it-work/the-gasification-process/>.

GIDARAKOS, E.; HAVAS, G.; NTZAMILIS, P. Municipal solid waste composition determination supporting the integrated solid waste management system in the island of Crete. **Waste Management**, v. 26, n. 6, p. 668–679, 2006.

GRESH, M. .; SASSOS, M. J.; WASTON, A. **Axial Air Compressors - Maintaining Peak Efficiency**. Disponível em: <http://turbolab.tamu.edu/proc/turboproc/T21/T21173-181.pdf>. Acesso em: 4 nov. 2015.

HE, W.; PARK, C. S.; NORBECK, J. N. **Rheological Study of Comingled Biomass and Coal Slurries with HydrothermalPretreatment**, 2009. Disponível em: <http://www.escholarship.org/uc/item/62f8t26t>

ISWA, I. S. W. A. **Knowledge Base**. Disponível em: <http://www.iswa.org/media/publications/knowledge-base/>. Acesso em: 7 fev. 2015.

KRZYWANSKI, J. et al. **Experience in Modelling of Oxygen-Enriched Combustion in a CFB Boiler**Turku, Finland22nd International Conference on Fluidized Bed Conversion, , 2015.

LARSON, E. D.; WILLIAMS, R. H.; LEAL, M. R. L. V. A review of biomass integrated-gasifier/gas turbine combined cycle technology and its application in sugarcane industries, with an analysis for Cuba. **Energy for Sustainable Development**, v. 5, n. 1, p. 54–76, mar. 2001.

LOMBARDI, L.; CARNEVALE, E.; CORTI, A. A review of technologies and performances of thermal treatment systems for energy recovery from waste. **Waste Management**, v. 37, p. 26–44, 2014.

MEADOWCROFT, D. .; STRINGER, J. Corrosion in coal-fired gas turbines. **Materials Science and Technology**, p. 562–570, 1987.

MOUTSOGLOU, A. A comparison of prairie cordgrass and switchgrass as a biomass for syngas production. **Fuel**, v. 95, p. 573–577, 2012.

RABI, J. A; DE SOUZA-SANTOS, M. L. Comparison of Two Model Approaches Implemented in a Comprehensive Fluidized-Bed Simulator to Predict Radiative Heat Transfer: Results for a Coal-Fed Boiler. **Computer and Experimental Simulations in Engineering and**

Science, v. 3, p. 87–105, 2008.

RYU, C. Potential of Municipal Solid Waste for Renewable Energy Production and Reduction of Greenhouse Gas Emissions in South Korea. **Journal of the Air & Waste Management Association**, v. 60, n. 2, p. 176–183, 2010.

SILVA ORITZ, P. A.; VENTURINI, O. J.; SILVA LORA, E. E. **Technical and Economic Evaluation of IGCC Systems Using Coal and Petroleum Coke Considering the Brazilian Scenario**Volume 1: Aircraft Engine; Ceramics; Coal, Biomass and Alternative Fuels; Wind Turbine Technology. **Anais**...2011Disponível em: <http://proceedings.asmedigitalcollection.asme.org/proceeding.aspx?articleid=1631384>

TAN, S. T. et al. Energy, economic and environmental (3E) analysis of waste-to-energy (WTE) strategies for municipal solid waste (MSW) management in Malaysia. **Energy Conversion and Management**, 2015.

THE CONFERENCE BOARD OF CANADA. **Municipal Waste Generation.** Disponível em: <http://www.conferenceboard.ca/hcp/details/environment/municipal-waste-generation.aspx>. Acesso em: 20 dez. 2015.

TILLMAN, D. A. **The Combustion of Solid Fuels and Wastes**. [s.l.] Academic Press, Inc., 1991.

U.S. ENVIRONMENTAL PROTECTION AGENCY, E. **Electricty from Municipal Solid Waste**. Disponível em: <http://www.epa.gov/cleanenergy/energy-and-you/affect/municipal-sw.html>. Acesso em: 13 jul. 2015.

U.S. ENVIRONMENTAL PROTECTION AGENCY, E.; COMBINED HEAT PARTNERSHIP, C. Section 4 . Technology Characterization – Steam Turbines. n. March, 2015.

VAN DEN ENDEN, P. J.; LORA, E. S. Design approach for a biomass fed fluidized bed gasifier using the simulation software CSFB. **Biomass and Bioenergy**, v. 26, n. 3, p. 281–287, mar. 2004.

VERES, J. P. Centrifugal and Axial Pump Design and Off-Design Performance Prediction. p. 24, 1994.

VIMALCHAND, P.; PENG, W. W.; LIU, G. **High Pressure Feeder and Method of Operating to Feed Granular or Fine Materials**Google Patents, , 23 jun. 2011. Disponível em: <https://www.google.com/patents/US20110146153>

ZHENG, X. et al. Effect of temperature on the strength of a centrifugal compressor impeller for a turbocharger!!.pdf. v. 227, n. 5, p. 896–904, 2012.

APPENDIX A – Exergy of the solid fuel calculation

The exergy (b) of the solid fuel is computed according the following relations:

$$b = \sum_j w_j b_j$$

$$b_j = h_j - h_{j,0} - T_0(s_j - s_{j,0}) + h_c + d_j$$

where

$$h_j = h_{f,j} + \int_{T_0}^{T} c_{p,j} dT$$

rearranging

$$h_j - h_{j,0} = \int_{T_0}^{T} c_{p,j} dT$$

and

$$s_j - s_{j,0} = \int_{T_0}^{T} \frac{c_{p,j}}{T} dT - \frac{\bar{R}}{M} \ln \frac{p}{p_o}$$

Because is an a solid or liquid (incompressible) fuel:

$$s_j - s_{j,0} = \int_{T_0}^{T} \frac{c_{p,j}}{T} dT$$

Reference

1. Szargut J., Morris D. R., Stewart F. R., Exergy Analysis of Thermal, Chemical, and Metallurgical Processes, Hemisphere, N. Y., 1988

APPENDIX B – Operational conditions and stream characterization

The tables below list the information obtained by simulation of the gasifier at different operational pressures.

The main geometric characteristics, as well the most important input parameters of the gasifier operating at 4.0 MPa are summarized in Table B 1

Table B 1 Gasifier main inputs and operational conditions operating at 4.0 MPa

Main input condition or parameters	Value
Bed internal diameter [m]	2.9
Bed height [m]	4.0
Freeboard internal diameter [m]	2.9
Freeboard height	6.0
Insulation thickness around the bed and freeboard [mm]	100
Number of flutes in the distributor	$2.7x10^4$
Number of orifices per flute	10
Diameter of orifices [mm]	3.0
Fuel feeding position (above the distributor) [m]	2.0
Mass flow of feeding fuel (dry) [kg/s]	18.0
Mass flow of injected air [kg/s]	13
Temperature of injected air [K]	917
Mass flow of injected steam [kg/s]	0.0
Average pressure inside the equipment [MPa]	4.0

The mass flow, the temperature, the composition and the pressure of the gas leaving the gasifier operating at 4.0 MPa were obtained using CeSFaMB©. Such information was used as an input data for the optimization of the entire power generation process in IPES and is presented below.

Table B 2 Mass flow, temperature and composition of gas leaving the gasifier operating at 4.0 MPa

Composition of gas leaving the equipment			
Chemical Species	**Molar percentage**	**Chemical Species**	**Molar percentage**
H2	24.0133	CO	30.0755
H2O	3.6344	CO2	6.9842
H2S	0.0338	HCN	0.0513
NH3	1.0636	CH4	8.1591
NO	0.0000	C2H4	0.1641
NO2	0.0000	C2H6	0.1276
N2	25.6174	C3H6	0.0061
N2O	0.0000	C3H8	0.0058
O2	0.0000	C6H6	0.0590
SO2	0.0047	Tar	0.0000

Output condition or parameter	Value
Mass flow of gas leaving the equipment [kg/s]	29.89
Temperature of gas leaving the equipment [K]	969.91

The FSIG/GT process was simulated and optimized using IPES and the table below presents some of the obtained results.

Table B 3 Description of conditions at each Stream of the FSIG/GT power generation process under gasifier operation at 4.0 MPa

Stream	Fluid nature	Temp. [K]	Pressure [kPa]	Mass Flow [kg/s]	Stream	Fluid nature	Temp. [K]	Pressure [kPa]	Mass Flow [kg/s]
1	Air	298.0	101.3	270.0	**15**	Gas	390.9	108.0	60.0
2	Air	932.4	4000.0	270.0	**16**	Gas[c]	969.9	4010.0	29.9
3	Gas[a]	800.0	4000.0	29.9	**17**	Steam	955.2	10000.0	2.7
4	Gas	1706.1	3990.0	299.9	**18**	Steam	523.2	475.8	2.7
5	Gas	888.4	120.0	299.9	**19**	Water	422.0	465.8	2.7
6	Gas	390.9	110.0	299.9	**20**	Water	422.1	10010.0	2.7
7	Water[b]	298.0	110.0	1000.0	**21**	Water	298.0	110.0	100.0
8	Water	298.0	130.0	1000.0	**22**	Water	298.0	130.0	100.0
9	Water	324.4	110.0	1000.0	**23**	Water	312.8	110.0	100.0
10	Steam	878.0	10000.0	50.0	**24**	Air	298.0	110.0	13.0
11	Steam	347.0	114.0	50.0	**25**	Air	917.4	4100.0	13.0
12	Water	369.0	90.4	50.0	**26**	Slurry	298.0	110.0	40.6
13	Water	369.0	10100.0	50.0	**27**	Slurry	298.0	4100.0	40.6
14	Gas	390.9	108.0	239.9	**28**	Gas	1130.9	4200.0	60.0

[a]After cleaning set alkaline concentration within acceptable levels. [b]Water= liquid water. [c]After cleaning to set particle size and content within acceptable levels.

The results show that the temperature of the gas Stream 28 is above the limit of the maximum compressor blade working temperatures of 950 K (BOYCE, [s.d.]). Therefore, the pressure must be lowered even further.

Table B 4 below shows the conditions and parameters of the gasifier operating at 3.0 MPa.

Table B 4 Gasifier main inputs and operational conditions operating at 3.0 MPa

Main input condition or parameters	Value
Bed internal diameter [m]	3.4
Bed height [m]	4.0
Freeboard internal diameter [m]	3.4
Freeboard height	6.0
Insulation thickness around the bed and freeboard [mm]	100
Number of flutes in the distributor	$3.6x10^4$
Number of orifices per flute	10
Diameter of orifices [mm]	3.0
Fuel feeding position (above the distributor) [m]	2.0
Mass flow of feeding fuel (dry) [kg/s]	18.0
Mass flow of injected air [kg/s]	13
Temperature of injected air [K]	847
Mass flow of injected steam [kg/s]	0.0
Average pressure inside the equipment [MPa]	3.0

The mass flow, temperature, composition and pressure of the gas leaving the gasifier operating at 3.0 MPa were obtained using CeSFaMB©. That information was used as an input data for the optimization of the entire power generation process and is presented below.

Table B 5 Mass flow, temperature and composition of gas leaving the gasifier operating at 3.0 MPa

Composition of gas leaving the equipment			
Chemical Species	**Molar percentage**	**Chemical Species**	**Molar percentage**
H2	25.6745	CO	30.1200
H2O	3.6284	CO2	6.8543
H2S	0.0332	HCN	0.0479
NH3	1.0648	CH4	6.9461
NO	0.0000	C2H4	0.1619
NO2	0.0000	C2H6	0.1259
N2	25.2683	C3H6	0.0060
N2O	0.0000	C3H8	0.0057
O2	0.0000	C6H6	0.0582
SO2	0.0046	Tar	0.0000
Output condition or parameter			**Value**
Mass flow of gas leaving the equipment [kg/s]			29.86
Temperature of gas leaving the equipment [K]			961.6

The table below presents some of the obtained results during the optimization of the FSIG/GT process using IPES.

Table B 6 Description of conditions of each Stream of the FSIG/GT power generation process under gasifier operation at 3.0 MPa

Stream	Fluid nature	Temp. [K]	Pressure [kPa]	Mass Flow [kg/s]	Stream	Fluid nature	Temp. [K]	Pressure [kPa]	Mass Flow [kg/s]
1	Air	298.0	101.3	245.0	**15**	Gas	387.3	108.0	64.0
2	Air	859.0	3000.0	245.0	**16**	Gas[c]	969.9	3010.0	29.9
3	Gas[a]	800.0	3000.0	29.9	**17**	Steam	958.7	10000.0	2.7
4	Gas	1699.4	2990.0	274.9	**18**	Steam	525.5	475.8	2.7
5	Gas	948.3	120.0	274.9	**19**	Water	422.0	465.8	2.7
6	Gas	387.3	110.0	274.9	**20**	Water	422.1	10010.0	2.7
7	Water[b]	298.0	110.0	500.0	**21**	Water	298.0	110.0	100.0
8	Water	298.0	130.0	500.0	**22**	Water	298.0	130.0	100.0
9	Water	352.2	110.0	500.0	**23**	Water	312.7	110.0	100.0
10	Steam	938.0	10000.0	50.0	**24**	Air	298.0	110.0	13.0
11	Steam	377.3	114.0	50.0	**25**	Air	917.4	4100.0	13.0
12	Water	369.0	90.4	50.0	**26**	Slurry	298.0	110.0	40.6
13	Water	369.0	10100.0	50.0	**27**	Slurry	298.0	3100.0	40.6
14	Gas	387.3	108.0	210.9	**28**	Gas	1041.0	3200.0	64.0

[a]After cleaning set alkaline concentration within acceptable levels. [b]Water= liquid water. [c]After cleaning to set particle size and content within acceptable levels.

The obtained results show that the temperature of the gas Stream 28 still above the limit of the maximum compressor blade working temperatures of 950 K (BOYCE, [s.d.]). Therefore, the operational pressure of the gasifier was set at 2.0 MPa. Such value was selected for the optimization of the entire process because the temperature of stream 28 is below the limit of the compressor performance.

Properties of each stream of the FSIG/GT process operating with the BFB gasifier under 2.0 MPa and 15 kg/s of injected air

Table B 7 Mass, molar and volume flow, density and viscosity of each stream of the FSIG/GT with gasifer under 2.0 MPa.

Stream	Mass Flow (kg/s)	Molar Flow (kmol/s)	Volume Flow (m3/s)	Density (kg/m3)	Viscosity (kg/m·s)
1	206.00	7.1404	174.01	1.1838	3.5189E-05
2	206.00	7.1404	22.761	9.0506	7.2637E-05
3	32.06	1.5192	3.7115	8.6380	6.7001E-05
4	238.06	8.2406	49.959	4.7651	1.0646E-04
5	238.06	8.2406	578.32	0.4116	8.7401E-05
6	238.06	8.2406	236.19	1.0079	4.1414E-05
7	500.00	27.7540	0.48654	1027.70	7.6601E-04
8	500.00	27.7540	0.48654	1027.70	7.6601E-04
9	500.00	27.7540	0.51222	976.14	3.4856E-04
10	48.50	2.6922	2.2843	21.2320	7.8575E-05
11	48.50	2.6922	75.22	0.6448	2.9785E-05
12	48.50	2.6922	0.050901	952.820	2.7488E-04
13	48.50	2.6922	0.050904	952.770	2.7488E-04
14	186.36	6.4510	188.3	0.9897	4.1410E-05
15	51.700	1.7896	52.239	0.9897	4.1410E-05
16	32.060	1.5192	4.4622	7.1848	7.6395E-05
17	2.7400	0.1521	0.11711	23.3970	7.1992E-05
18	2.7400	0.1521	1.3658	2.0062	3.6420E-05
19	2.7400	0.1521	0.0030298	904.36	2.7488E-04
20	2.7400	0.1521	0.00303	904.30	2.7488E-04
21	115.00	6.3835	0.1119	1027.70	7.6601E-04
22	115.00	6.3835	0.1119	1027.70	7.6601E-04
23	115.00	6.3835	0.11324	1015.50	6.1737E-04
24	15.000	0.5199	11.672	1.2852	3.5189E-05
25	15.000	0.5199	1.5137	9.9097	7.2857E-05
26	40.636	2.2557	0.039542	1027.70	7.6601E-04
27	40.636	2.2557	0.039543	1027.60	7.6588E-04
28	51.700	1.7896	6.2394	8.2861	8.1796E-05

Table B 8 Enthalpy, entropy, exergy, specific heat and thermal conductivity of each stream of the FSIG/GT with gasifer under 2.0 MPa.

Stream	Enthalpy (kJ/kg)	Entropy (kJ/kg·K)	Exergy (kJ/kg)	Specific Heat (kJ/kg·K)	Thermal Conductivity (W/m·K)
1	-0.21044	6.7402	28.90	1.0127	0.05141
2	488.33	6.8598	481.8	1.1011	0.10748
3	-2744.80	8.7681	9600.0	1.6420	0.16857
4	28.906	7.9951	1401.0	1.2148	0.17308
5	-824.83	8.0880	519.9	1.2287	0.13690
6	-1575.50	7.0011	93.20	1.0604	0.06278
7	-15906.00	2.1844	0.008442	4.1876	1.26400
8	-15906.00	2.1844	0.0279	4.1876	1.26400
9	-15677.00	2.8909	18.77	4.2140	1.38520
10	-11955.00	10.8560	1369.0	2.3003	0.17782
11	-13167.00	11.1020	83.45	1.9299	0.05995
12	-15578.00	3.1623	36.74	4.2289	1.41210
13	-15567.00	3.1629	47.26	4.2289	1.41210
14	-1575.50	7.0063	91.61	1.0604	0.06277
15	-1575.50	7.0063	91.61	1.0604	0.06277
16	-2464.60	9.0839	9786.0	1.7086	0.19332
17	-12157.00	10.6530	1227.0	2.2376	0.16474
18	-13014.00	10.8270	317.60	1.9691	0.07611
19	-15382.00	3.6529	86.47	4.2784	1.43590
20	-15371.00	3.6534	97.09	4.2785	1.43590
21	-15906.00	2.1844	0.008442	4.1876	1.27030
22	-15906.00	2.1844	0.0279	4.1876	1.27030
23	-15851.00	2.3661	1.199	4.1942	1.30660
24	-0.22843	6.7164	35.95	1.0127	0.05141
25	491.69	6.8366	492.1	1.1020	0.10777
26	-15906.00	2.1844	0.008442	4.1876	1.28600
27	-15904.00	2.1846	2.042	4.1876	1.28610
28	-945.71	7.1285	685.0	1.2099	0.12756

Table B 9 Saturation temperature and pressure, critical temperature and pressure of each stream of the FSIG/GT with gasifer under 2.0 MPa.*

Stream	Saturation Temp.* (K)	Saturation Pressure* (kPa)	Critical Temperature (K)	Critical Pressure (kPa)
1	79.635	3660.50	131.48	3672.0
2	119.72	3655.70	131.48	3672.0
3	118.73	3731.10	137.04	3971.7
4	146.40	4520.20	171.80	4753.6
5	105.50	4700.00	171.80	4753.6
6	101.38	586.66	171.80	4753.6
7	375.47	3.1149	647.30	22048.0
8	380.29	3.1149	647.30	22048.0
9	375.47	46.293	647.30	22048.0
10	585.31	22048.00	647.30	22048.0
11	380.29	732.21	647.30	22048.0
12	377.96	112.07	647.30	22048.0
13	586.07	112.26	647.30	22048.0
14	101.20	585.76	171.80	4753.6
15	101.20	585.76	171.80	4753.6
16	118.82	3731.40	137.04	3971.7
17	585.31	22048.00	647.30	22048.0
18	423.05	3830.10	647.30	22048.0
19	422.26	461.74	647.30	22048.0
20	585.38	462.37	647.30	22048.0
21	375.47	3.1149	647.30	22048.0
22	380.29	3.1149	647.30	22048.0
23	375.47	6.6241	647.30	22048.0
24	80.35	3660.40	131.48	3672.0
25	121.74	3655.40	131.48	3672.0
26	375.47	3.1149	647.30	22048.0
27	490.29	3.1168	647.30	22048.0
28	148.58	4511.80	171.80	4753.6

*Saturation temperature and pressure conditions of each stream which does not contain solids

Table B 10 Enthalpy (H), entropy (S), and exergy (B) rate of variation at each equipment of the FSIG/GT process.

Equipment	Type of equipment	ΔH (W)	ΔS (W/K)	ΔB (W)
1	Compressor	1.006E+08	2.465E+04	9.329E+07
2	Combustor	-5.717E+06	2.091E+05	-7.343E+07
3	Gas Turbine	-2.032E+08	2.211E+04	-2.098E+08
4	Steam Generator	-3.504E+06	1.144E+05	-3.750E+07
5	Steam Turbine	-5.879E+07	1.190E+04	-6.233E+07
6	Condenser	-2.293E+06	-3.182E+04	7.105E+06
7	Pump	9.930E+03	6.664E-01	9.731E+03
8	Pump	5.184E+05	2.757E+01	5.102E+05
9	Splitter	-9.656E+03	1.231E+03	-3.767E+05
10	Compressor	3.256E+07	6.321E+03	3.068E+07
11	Cleaning System	-1.761E+05	9.057E+03	-2.870E+06
12	Steam Turbine	-2.349E+06	4.765E+02	-2.491E+06
13	Condenser	-1.272E+05	1.230E+03	-4.986E+05
14	Pump	2.951E+04	1.399E+00	2.910E+04
15	Pump	2.284E+03	1.533E-01	2.238E+03
16	Compressor	7.379E+06	1.802E+03	6.842E+06
17	Pump	8.433E+04	5.660E+00	8.264E+04

Table B 11 Composition in mass fraction of each stream of the FSIG/GT with gasifer under 2.0 MPa.

Composition of each stream of the FSIG/GT process operating with gasifier under 2.0 MPa and 15 kg/s of injected air
Mass fractions

Stream	H2	H2O	H2S	NH3	NO	NO2	N2	N2O	O2	SO2	CO	CO2	HCN	CH4	C2H4	C2H6	C3H6	C3H8	C6H6
1	-	-	-	-	-	-	7.67E-01	-	2.33E-01	-	-	-	-	-	-	-	-	-	-
2	-	-	-	-	-	-	7.67E-01	-	2.33E-01	-	-	-	-	-	-	-	-	-	-
3	2.57E-02	3.60E-02	4.99E-04	7.39E-03	-	-	3.61E-01	-	-	1.40E-04	3.80E-01	1.52E-01	4.23E-04	3.48E-02	2.83E-03	-	-	-	-
4	-	4.85E-02	-	-	1.82E-03	-	7.12E-01	-	1.22E-01	1.45E-04	-	1.15E-01	-	-	-	-	-	-	-
5	-	4.85E-02	-	-	1.82E-03	-	7.12E-01	-	1.22E-01	1.45E-04	-	1.15E-01	-	-	-	-	-	-	-
6	-	4.85E-02	-	-	1.82E-03	-	7.12E-01	-	1.22E-01	1.45E-04	-	1.15E-01	-	-	-	-	-	-	-
7	-	1.00E+00	-	-	-	-	-	-	-	-	-	-	-	-	-	-	-	-	-
8	-	1.00E+00	-	-	-	-	-	-	-	-	-	-	-	-	-	-	-	-	-
9	-	1.00E+00	-	-	-	-	-	-	-	-	-	-	-	-	-	-	-	-	-
10	-	1.00E+00	-	-	-	-	-	-	-	-	-	-	-	-	-	-	-	-	-
11	-	1.00E+00	-	-	-	-	-	-	-	-	-	-	-	-	-	-	-	-	-
12	-	1.00E+00	-	-	-	-	-	-	-	-	-	-	-	-	-	-	-	-	-
13	-	1.00E+00	-	-	-	-	-	-	-	-	-	-	-	-	-	-	-	-	-
14	-	4.85E-02	-	-	1.82E-03	-	7.12E-01	-	1.22E-01	1.45E-04	-	1.15E-01	-	-	-	-	-	-	-
15	-	4.85E-02	-	-	1.82E-03	-	7.12E-01	-	1.22E-01	1.45E-04	-	1.15E-01	-	-	-	-	-	-	-
16	2.57E-02	3.60E-02	4.99E-04	7.39E-03	-	-	3.61E-01	-	-	1.40E-04	3.80E-01	1.52E-01	4.23E-04	3.48E-02	2.83E-03	-	-	-	-
17	-	1.00E+00	-	-	-	-	-	-	-	-	-	-	-	-	-	-	-	-	-
18	-	1.00E+00	-	-	-	-	-	-	-	-	-	-	-	-	-	-	-	-	-
19	-	1.00E+00	-	-	-	-	-	-	-	-	-	-	-	-	-	-	-	-	-
20	-	1.00E+00	-	-	-	-	-	-	-	-	-	-	-	-	-	-	-	-	-
21	-	1.00E+00	-	-	-	-	-	-	-	-	-	-	-	-	-	-	-	-	-
22	-	1.00E+00	-	-	-	-	-	-	-	-	-	-	-	-	-	-	-	-	-
23	-	1.00E+00	-	-	-	-	-	-	-	-	-	-	-	-	-	-	-	-	-
24	-	-	-	-	-	-	7.67E-01	-	2.33E-01	-	-	-	-	-	-	-	-	-	-
25	-	-	-	-	-	-	7.67E-01	-	2.33E-01	-	-	-	-	-	-	-	-	-	-
26	-	1.00E+00	-	-	-	-	-	-	-	-	-	-	-	-	-	-	-	-	-
27	-	1.00E+00	-	-	-	-	-	-	-	-	-	-	-	-	-	-	-	-	-
28	-	4.85E-02	-	-	1.82E-03	-	7.12E-01	-	1.22E-01	1.45E-04	-	1.15E-01	-	-	-	-	-	-	-

Table B 12 Composition in molar fraction of each stream of the FSIG/GT process operating with the BFB gasifier under 2.0 MPa and 15 kg/s of injected air.

Composition of each stream of the FSIG/GT process operating with gasifier under 2.0 MPa and 15 kg/s of injected air Molar fractions																			
Stream	**H2**	**H2O**	**H2S**	**NH3**	**NO**	**NO2**	**N2**	**N2O**	**O2**	**SO2**	**CO**	**CO2**	**HCN**	**CH4**	**C2H4**	**C2H6**	**C3H6**	**C3H8**	**C6H6**
1	-	-	-	-	-	-	7.90E-01	-	2.10E-01	-	-	-	-	-	-	-	-	-	-
2	-	-	-	-	-	-	7.90E-01	-	2.10E-01	-	-	-	-	-	-	-	-	-	-
3	2.70E-01	4.21E-02	3.09E-04	9.16E-03	-	-	2.72E-01	-	-	4.60E-05	2.86E-01	7.27E-02	3.30E-04	4.57E-02	2.13E-03	-	-	-	-
4	-	7.77E-02	-	-	1.75E-03	-	7.35E-01	-	1.10E-01	6.54E-05	-	7.54E-02	-	-	-	-	-	-	-
5	-	7.77E-02	-	-	1.75E-03	-	7.35E-01	-	1.10E-01	6.54E-05	-	7.54E-02	-	-	-	-	-	-	-
6	-	7.77E-02	-	-	1.75E-03	-	7.35E-01	-	1.10E-01	6.54E-05	-	7.54E-02	-	-	-	-	-	-	-
7	-	1.00E+00	-	-	-	-	-	-	-	-	-	-	-	-	-	-	-	-	-
8	-	1.00E+00	-	-	-	-	-	-	-	-	-	-	-	-	-	-	-	-	-
9	-	1.00E+00	-	-	-	-	-	-	-	-	-	-	-	-	-	-	-	-	-
10	-	1.00E+00	-	-	-	-	-	-	-	-	-	-	-	-	-	-	-	-	-
11	-	1.00E+00	-	-	-	-	-	-	-	-	-	-	-	-	-	-	-	-	-
12	-	1.00E+00	-	-	-	-	-	-	-	-	-	-	-	-	-	-	-	-	-
13	-	1.00E+00	-	-	-	-	-	-	-	-	-	-	-	-	-	-	-	-	-
14	-	7.77E-02	-	-	1.75E-03	-	7.35E-01	-	1.10E-01	6.54E-05	-	7.54E-02	-	-	-	-	-	-	-
15	-	7.77E-02	-	-	1.75E-03	-	7.35E-01	-	1.10E-01	6.54E-05	-	7.54E-02	-	-	-	-	-	-	-
16	2.70E-01	4.21E-02	3.09E-04	9.16E-03	-	-	2.72E-01	-	-	4.60E-05	2.86E-01	7.27E-02	3.30E-04	4.57E-02	2.13E-03	-	-	-	-
17	-	1.00E+00	-	-	-	-	-	-	-	-	-	-	-	-	-	-	-	-	-
18	-	1.00E+00	-	-	-	-	-	-	-	-	-	-	-	-	-	-	-	-	-
19	-	1.00E+00	-	-	-	-	-	-	-	-	-	-	-	-	-	-	-	-	-
20	-	1.00E+00	-	-	-	-	-	-	-	-	-	-	-	-	-	-	-	-	-
21	-	1.00E+00	-	-	-	-	-	-	-	-	-	-	-	-	-	-	-	-	-
22	-	1.00E+00	-	-	-	-	-	-	-	-	-	-	-	-	-	-	-	-	-
23	-	1.00E+00	-	-	-	-	-	-	-	-	-	-	-	-	-	-	-	-	-
24	-	-	-	-	-	-	7.90E-01	-	2.10E-01	-	-	-	-	-	-	-	-	-	-
25	-	-	-	-	-	-	7.90E-01	-	2.10E-01	-	-	-	-	-	-	-	-	-	-
26	-	1.00E+00	-	-	-	-	-	-	-	-	-	-	-	-	-	-	-	-	-
27	-	1.00E+00	-	-	-	-	-	-	-	-	-	-	-	-	-	-	-	-	-
28	-	7.77E-02	-	-	1.75E-03	-	7.35E-01	-	1.10E-01	6.54E-05	-	7.54E-02	-	-	-	-	-	-	-

Table B 13 Elemental analysis of each stream of the FSIG/GT with gasifer under 2.0 MPa.

Stream	H	C	N	O	S
1	-	-	7.671E-01	2.329E-01	-
2	-	-	7.671E-01	2.329E-01	-
3	4.026E-02	2.328E-01	3.672E-01	3.591E-01	5.393E-04
4	5.422E-03	3.136E-02	7.132E-01	2.499E-01	7.263E-05
5	5.422E-03	3.136E-02	7.132E-01	2.499E-01	7.263E-05
6	5.422E-03	3.136E-02	7.132E-01	2.499E-01	7.263E-05
7	1.119E-01	-	-	8.881E-01	-
8	1.119E-01	-	-	8.881E-01	-
9	1.119E-01	-	-	8.881E-01	-
10	1.119E-01	-	-	8.881E-01	-
11	1.119E-01	-	-	8.881E-01	-
12	1.119E-01	-	-	8.881E-01	-
13	1.119E-01	-	-	8.881E-01	-
14	5.422E-03	3.136E-02	7.132E-01	2.499E-01	7.263E-05
15	5.422E-03	3.136E-02	7.132E-01	2.499E-01	7.263E-05
16	4.026E-02	2.328E-01	3.672E-01	3.591E-01	5.393E-04
17	1.119E-01	-	-	8.881E-01	-
18	1.119E-01	-	-	8.881E-01	-
19	1.119E-01	-	-	8.881E-01	-
20	1.119E-01	-	-	8.881E-01	-
21	1.119E-01	-	-	8.881E-01	-
22	1.119E-01	-	-	8.881E-01	-
23	1.119E-01	-	-	8.881E-01	-
24	-	-	7.671E-01	2.329E-01	-
25	-	-	7.671E-01	2.329E-01	-
26	1.119E-01	-	-	8.881E-01	-
27	1.119E-01	-	-	8.881E-01	-
28	5.422E-03	3.136E-02	7.132E-01	2.499E-01	7.263E-05